Ministry of Higher Education and Scientific Research
HASSIBA BENBOUALI UNIVERSITY OF CHLEF
FACULTY OF SCIENCE
DEPARTMENT OF PHYSICS

Thesis

A Thesis Submitted For Degree of Doctor in Theoretical physics

Presented By

Atika MEHEDI

Theme

DYNAMICS OF BINARY MIXTURES AT ULTRA COLD TEMPERATURES:

EFFECTS OF INTERSPECIES CORRELATIONS

Examining Committee:

Pr. Chaachoua Sameut Houria	University of Chlef	Chairman
Pr. Bencheikh Kamal	University of Setif	Examiner
Pr .Ladrem Madjid	ENP-EL-Harrach	Examiner
Pr .Balaska Smain	Université of Oran1	Examiner
Dr. Hocine Ahmed	University of Chlef	Co-Supervisor
Pr. Benarous Mohamed	University of Chlef	Supervisor

Acknowledgements

Praise to Allah the most gracious, the most merciful for whom has granted us existence and whom is the source of every success.
There are many people who deserve my gratitude for their role in the completion of my thesis, and it would be impossible to mention them all in a few short paragraphs.
I am grateful to my family particularly to my husband Mohamed and to my children Assil , Razan Tassnim and Mahdi who have given me the force to carry on this thesis. Thank you for supporting me .
I express my sincere gratitude to my supervisor, Pr. Benarous Mohamed at UHBC of Chlef , for His great patience, help and discussions. he was always willing to help and answer to any question. I really appreciated his competence and availability.
I warmly thank my co-supervisor, Dr. Hocine Ahmed, for his guidance and support. I am also thankful for his valuable suggestions.
My heartfelt thanks also go to Pr. Chaachoua Sameut Houria, who honored us by agreeing to chair the jury for this thesis.
I would like to thank Pr. Balaska Smain, Pr.Ladram Madjid and Pr. Bencheikh Kamal for agreeing to be part of the jury for this thesis.
I would also like to thank all members of LPTPM (Laboratory for Theoretical Physics and Material Physics) .
My gratitude goes to all my colleagues of the physics department and the faculty of sciences at university of Chlef.
All thanks and gratitude to the wonderful wonder my mother, otherwise I would not be here at this time, my mother is my second supervisor who contributed to completing this work. My Deepest thanks to my siblings. My thank also to my grand family.

Abstract

This doctoral work intends to take account of dynamical correlations in binary mixtures of Bose-Einstein condensates (BEC), composed of two distinct species. In a preliminary analysis, we consider a purely one-dimensional mixture, where the anomalous (or off-diagonal) correlations are finite and do not require any renormalization.

Their behavior, examined within a variational framework using a gaussian density operator, corroborate a preceding result assessing that the anomalous and noncondensate densities are of the same order and, therefore, any approach considering only non condensate densities can only be viable at very low temperature (or zero temperature) or near the transition. This was demonstrated numerically by solving a set of self-consistent equations. Furthermore, in a binary mixture, a set of unprecedented correlations appears. Indeed, beside the intraspecies correlations, we shed light on interspecies correlations, which depict the entanglement between the species

In the vaste literature, we noticed that these effects are generally omitted owing to the fact that, in many experiments, the entanglement between different species is considered as marginal.

We show however in this work, that it needs not be the case in a general context. These effects are however quite tiny and cannot be observed in situations where the mean field is dominant. Hence, we considered situations where the mean -field is almost zero. This fortunately happens for a binary system when the interspecies interactions are attractive and almost neutralize the interaspecies ones. This leads to self-bound states named droplets which were indeed discovered experimentally.

We therefore focused on droplets in quasi-one dimensional geometries and exhibited the dominant role of interspecies fluctuations. We showed that the droplet states are more stable and therefore more easily observable when one includes interspecies correlations. We also show that these effects add up to the LHY contributions extending the beyond mean-field theory in the Bogoliubov framework. This work was performed in a consistent and methodic way which led to original results published in journal of low temperature physics

Keywords: Mean- field Method, semi-classical approach, Binary BEC, One-body correlations.

Contents

List of abbreviations

BEC Bose-Einstein Condensate

GPE Gross Pitaevskii equation

CGPE coupled Gross Pitaevskii equations

LHY Lee-Hung-Yang.

TDHFB Time Dependent Hartree-Fook Bogoliubov.

HFB Hartree-Fook Bogoliubov.

WT Wigner Transformation.

BV Balian -Véneroni variational principle.

List of Figures

General Introduction

Brief history of Bose-Einstein condensate:

In quantum mechanics, particles lack clearly defined trajectories, and the fact that identical particles are indistinguishable has significant consequences. In classical mechanics, identical particles can be uniquely identified by their position and momentum coordinates at any given time. We must impose specific symmetries on the many-body wave function in order to get acceptable physics. There are two possibilities: wave function may be "symmetric" or "antisymmetric". This is expressed as

$$\Psi\left(\ldots . r_i \ldots, \ldots r_j \ldots\right) = \pm\Psi\left(\ldots\ldots r_j \ldots, \ldots r_i \ldots\right)$$

Particles with symmetric (+) wave functions are known as bosons and follow the Bose Einstein statics, whereas those with antisymmetri (-) wave functions are known as fermions and follow the Fermi-Dirac statistics. One can infer that particles with integer spins are bosons and those with half-integer spins are fermions. A new principle known as the "Pauli exclusion principle" : that fermions cannot share the same quantum state is brought about by this restriction on the symmetry of the wave function. However, Bose-Einstein condensation (BEC) is the term for the tendency of bosons to group together in the same state.

BEC was first described by Albert Einstein in 1925 [2] bassed on the work of Satyendra Nath Bose on the theory of the quantum statistics of photons. Einstein recognized that a macroscopic population of atoms in a single quantum state (the ground state) would be present in an ideal Bose gas that had been cooled to a threshold temperature Tc. In other words, Einstein's prediction is not surprising ; if a perfect Bose gas is cooled at temperatures below a critical value, it makes obvious that a significant ground state occupation will take place.

Stwalley and Nosanow's 1976 publication [3] marked the beginning of efforts to realize BEC in a weakly interacting gas. The authors of this research noted that, except for Helium, all other chemicals change into solid states, whereas Hydrogen stays in its gaseous state up to the temperatures required for BEC. In the early 1980s, the Dutch group Silvera and Walraven and the American group Greytak and Kleppner began conducting experiments to reach BEC in Hydrogen [4]. The first condensates in alkali vapors were discovered three years prior to the American group's 1998 observation of BEC [5].

Soon after laser cooling was developed, it was discovered that, in addition to the hydrogen strategy, this method provided a second potential path to BEC. The Nobel Prize was given to the pioneers of laser cooling in 1997 [6, 7], two years after three groups achieved BEC (in Sodium, Rubidium, and Lithium) almost simultaneously in 1995 [8, 9]. The Nobel Prize for their work on BEC was awarded to Carl E. Wiemann, Eric Cornell, and Wolfgang Ketterle in 2001 [10, 11].

Why two-component?

BEC of mixtures has been recently the subject of an intensive experimental and theoretical research because it shows many interesting phenomena that do not exist in one component due the interplay between intra- and inter-species interactions.

Experimental realization:

It is possible to experimentally produce a mixture of Bose-Einstein Condensates (BEC) by employing different species or trapping atoms in various hyperfine states. With a double condensate of ^{87}Rb in two different hyperfine states $|F, M_F\rangle = |1, -1\rangle$ and $|2, 2\rangle$, the first experimental demonstration of two interacting BECs was accomplished at JILA [12]. The two condensates in this combination somewhat overlapped, which set it apart. Since then, spinor condensates of Sodium in optical traps [13] and double condensates of rubidium [14–16] have been used in a number of further experiments. These systems have also been thoroughly examined from a theoretical perspective. Ho and Shenoy originally studied ground state density profiles in the Thomas–Fermi (TF) approximation in 1996 [17]. A lot of research has been done on the border between interpenetrating BECs [18]. Numerical results have been achieved for metastable states, which do not correlate to the system's lowest energy [19]. Additionally, a lot of research has been done on the stability of two-component systems in both confined and homogeneous scenarios. In fact, stability has been studied when an outside force disturbs the system. Additionally, it has been discovered that the binary BEC displays a collapse when attractive interactions are present, much like a one-species condensate [20, 21]. BEC mixtures have also been studied in non-harmonic trapping potentials, including optical lattices (where the potential has spatially periodic wells) [22], double well magnetic traps [23], and more recently, ring potentials, where it was discovered that the fragility of the system depended on the speed of the persistent currents [24]. A number of other types of ultra-cold atomic mixtures have

been thoroughly studied, including BEC-impurity mixtures [25, 26], spinor condensates [27], and Bose-Fermi mixtures [28–30]

.

Ultracold Bose mixtures are attracting considerable interest due to the unique characteristics arising from the combination of intra - and interspecies interactions. Experimentally, these interactions can be adjusted using a Feshbach resonance, which results in a diverse ground state phase diagram, featuring either mixed or separated phases, and facilitates the formation of structures.

Usually, binary mixtures are studied in the mean-field approximation at zero temperature, therefore adopting the coupled Gross-Pitaevskii equations (CGPE). Finite temperature and beyond mean-field effects are rarely taken into account owing to the dilute ness criterion and to the weak couplings. If the former, such as the appearance of a non-condensate component and the anomalous average are known to be extremely small at low temperatures, the latter are raising greater and greater interest such as the Lee - Huang Yang (LHY) corrections. Indeed, due to the many-body nature of the problem at hand, the correlations need not be so small and especially at finite temperature when their effects may be dramatic.For strongly interacting systems or for high densities, the situation is worse and one has to rely on quite different approaches than the ones usually adopted

One and two body correlations are among the most popular in the literature since they can be directly measured. Higher order correlations are less accessible to experiments and also to calculations.

In multi-species mixtures, the correlations are among atoms of the same species, or among atoms of different species. One may talk about intraspecies and interspecies correlations, exactly as one does for the interactions. In the case of CGPE, both correlations are assumed to vanish.

In some cases, the (one body) correlation between atoms or molecules of the same species have been studied [31]. But, to the best of our knoweledge, up to now, correlations between different species are not considered at all.

Outline of the dissertation

In chapter 1, we begin by general introduction about BEC , where we give a short background of the domain, this includes a discussion of the early experiments. To give the reader an idea of how the Bose-Einstein condensate phase emerges statistically as a function of temperature, we also discuss the phenomenon of BEC in both a uniform and trapped, non-interacting (ideal) gas of bosons in a general d- dimensional form.

In chapter 2, we discuss the Gross Pitaevskii equation which is the fundamental tool in quantum mechanics used to describe the behavior of Bose-Einstein condenstes . It provides mean-field approximation of the system by treating the many-body problem as a single wave function evolution. Then we examine the validity of GPE and its breakdown.

To go beyond the Gross Pitaevskii equation, we use the Balian-Vénéroni variationel principle [32–36] to derive the time-dependent Hartree-Fock-Bogoliubov (TDHFB) equations for single species. These equations govern in a self-consistent way the dynamics of the condensate, the non-condensate and the anomalous average densities. Then we determine analytic expressions for both the anomalous and the non-condensate densities for one, two and three dimensional systems in the case of single species. It is demonstrated that the anomalous density is finite for $d = 1$ and logarithmically and linearly divergent for $d = 2$ and 3, respectively.

In chapter 3 , we derive the TDHFB equations of the binary mixture for a system of trapped bosons with general two-body interaction and examine some of their properties using a Gaussian density operator (see appendix). We obtain a set of eight dynamical equations . Then we discuss the zero temperature static solutions, paying particular attention to the anomalous density because it is crucial to account for many-body effects. Taking into consideration the non-correlated case where $\tilde{n}_{12} = \tilde{m}_{12} = 0$, we derive analytic expressions for both the anomalous and the non-condensate densities in the case of a homogeneous 1D bose mixture. Finally, we solved those equations numerically at zero temperature.

Most importantly, the anomalous and the non-condensate densities, although small at zero temperature, are found to be of the same order of magnitude, leading to the conclusion that it would be very hazardous to omit one of them while keeping the other such as what is performed in the so (wrongly) called Popov approximation [35, 36]

Additionally, we examined the previous behaviors at finite (but low enough) temperature in order to understand the interplay between quantum and thermal fluctuations. Analysis is done on a homogeneous 1D Bose gases by comparing the non-condensate and anomalous densities at various temperatures. This analysis demonstrates the importance of the anomalous density at low temperatures in relation to the non-condensate density [35]

In chapter 4, at zero temperature, we derive the energy density related to a general two-body Hamiltonian for a homogeneous binary Bose mixture. We provide generalized formulas for the chemical potentials and the mixture's stability criteria by reducing the grand canonical energy density. We can obtain more quantitative results using this method..

Then, we compute the intraspecies and interspecies quantum fluctuations for a quasi one-dimensional mixture. For the former, we recover the well-known (negative) LHY terms. We demonstrate that the interspecies fluctuations have the same order of magnitude than the intraspecies ones, confirming that neglecting them is a risky approximation in the general case [37, 38] .

Finally, we discuss the importance of these results and how they affect the stability of quasi-one dimensional droplets.

In chapter 5, we present the theoretical and experimental aspects of quasi-one dimensional droplets.

Finally, we present some concluding remarks and perspectives.

Chapter 1

Background:Theory and Experiment

1.1 What is Bose-Einstein Condensate

BEC is one of the most interesting phenomena predicted by quantum statistical me chanics. The history of Bose-Einstein condensation (BEC) began in 1924, when a yong Indian physist Satyendra Nath Bose sent a short article to Einstein and a letter asking him to publish his derivation of the Planck radiation law by treating the photons as identical particles [39] .

In the next year 1925, Einstein generalized Bose's theory for non interacting bosonic atoms . This behavior at low temperature is due to the particle indistinguishability. Bosons can occupy the same quantum state and , in suitable conditions when the De Broglie waves of the atoms begin to overlap , leading to the phenomenon of Bose-Einstein condensation.

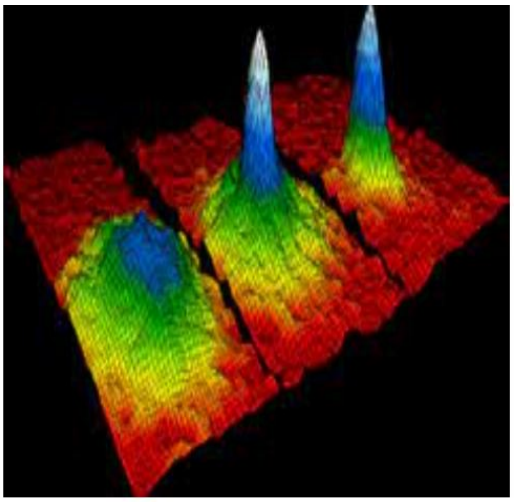

Figure 1.1: Bose-Einstein condensation phenomenon [1]

1.2 How to observe a condensate ?

The condensate is observed by lighting with a brief light pulse, whose absorption or phase shift by the atomic assembly is then measured. We thus have access to the spatial distribution of atoms in the magnetic potential. We can also cut the magnetic trap and let the atomic assembly spread out for a period of a few tens of milliseconds, before sending out the flash of light. From the expansion of the atomic cloud after spreading, we deduce the distribution at initial speed.

It should be noted that this imaging technique for the observation of condensates is the only one available with sufficient resolving power. It nevertheless poses a lot of relevant questions. Indeed after the traps have been extinguished, the gas evolves freely for a certain period of time, before one starts taking "photos". It is therefore implicitly assumed that the state of the gas between times 0 and t remains unchanged. To cheek this hypothesis,it is necessary to solve the dynamical equations with an initial state made up of the two phases (condensed and non-condensed) and , without a trap.

The subject has experienced a resurgence of interest with the advent of trapping and laser cooling of atoms. Thanks to the very low temperatures (and therefore to the large De Broglie wavelengths) reached, the researchers were hopeful that they would finally obtain the Bose-Einstein condensation for densities low enough so that the mutual interactions between atoms do not mask the effects of condensation.

1.2.1 Cooling and trapping techniques

Atoms are slowed and cooled by radiation pressure from laser light and then trapped in a bottle whose "walls" are magnetic fields. First, six laser beams (red) cool atoms, initially at room temperature, while corralling them toward the center of an evacuated glass box. Next, the laser beams are turned off, and the magnetic coils(copper) are energized. The magnetic field created by the current flowing through the coils further limits the majority of the atoms while permitting the energetic ones to escape. Thus, the average energy of the remaining atoms decreases, making the sample colder and even more closely confined to the center of the trap. Ultimately, many of the atoms attain the lowest possible energy state allowed by quantum mechanics and become a single entity known as a Bose- Einstein condensate .

1.2.2 Laser cooling and trapping

Laser cooling of an atom makes use of the pressure, or force, exerted by repeated photon impacts. An atom moving with the same beam is adjusted so that an atom moving into the beam scatters many more photons than an atom moving away from the beam. The net effect is to reduce the speed and thus cool the atom .

Assume that a light of frequency ν is shone on a gas of atoms that is on resonance with one of the atomic transitions. The photons have energy $\hbar\omega$ and a momentum $2\pi\hbar/k$. The atom of mass m absorbing a photon will have a different velocity it had before the

absorption, because of momentum conservation. If the atom has a momentum opposite to the one of the photon, i.e. they move into opposite directions, then after absorption the velocity of the atom will be smaller by $\hbar k/m = \hbar\nu/mc$

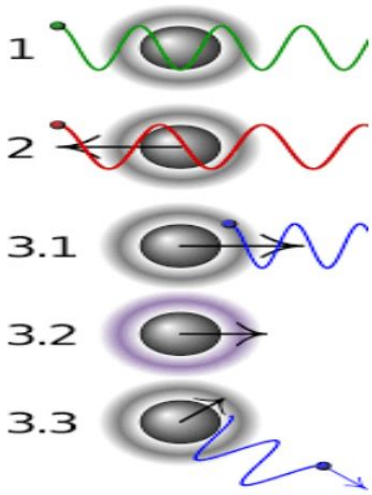

Figure 1.2: The technique of laser cooling

1.2.3 Doppler cooling

The main task is to achieve the low temperature necessary for the formation of a condensate. The first step is optical or Doppler cooling of the atoms with light. The Doppler shift also occurs when an atom moves with respect to a light source. The atom encounters the crests and troughs of the radiation waves at a higher rate, so that the frequency appears to the atom to be shifted up, or higher. Conversely, if the atom moves away from the source, the apparent frequency is shifted down, or lower. The effect of Doppler cooling can be expressed as a velocity dependent friction $= -\alpha v$, the detuning $\delta = \omega - \omega_0$, where ω is the laser frequency and ω_0 is the transition frequency of the atom at rest, and α is proportional to the absorption rate.

1.2.4 Trapping

The role of the magnetic trap in a BEC experiment is to accommodate the pre-cooled atoms and compress them by applying a weak magnetic field which interacts with atomic species with an unpaired electron and therefore with magnetic moment. If the magnetic moment is parallel to the external magnetic field, the atom is attracted to the

local minimum of the field . Magnetic trapping of neutral atoms was first observed in 1985 [40] .

1.2.5 Evaporative cooling

In theory, blowing over the liquid surface is the same method used to cool a hot cup of coffee. Faster atoms leave the cup once steam exits, leaving the slower atoms behind. The method's goal is to rapidly reduce the trap's height so that enough atoms remain in the trap to participate in BEC. This lowers the average kinetic energy, or temperature, of the remaining molecules by removing the fastest molecules in the vaporous phase above the surface. Bose-Einstein condensation may now be observed and temperatures in the nanokelvin range can be reached thanks to the evaporative cooling of trapped neutral atoms.

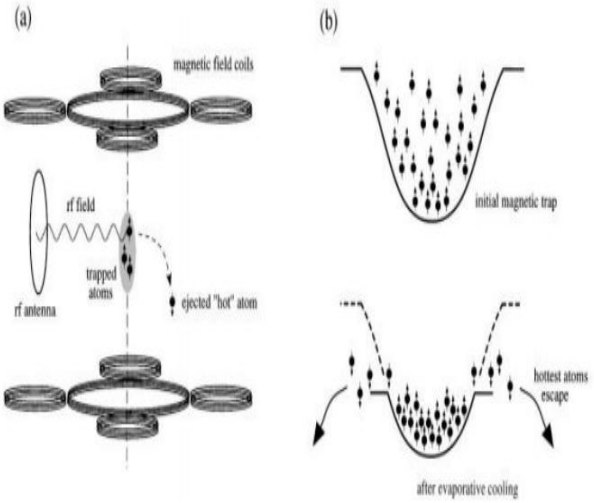

Figure 1.3: Schematics of the evaporative cooling process in a magnetic trap configuration. (a) Cloverleaf configuration of trapping coils. The central (outer) coils provide axial(radial)confinement. The rf field induces spin flips of hot atoms. By adjusting the frequency of the rf field, the effective depth of the trap is altered (b)

1.3 The ideal bose gas in D- dimensions

In the grand canonical ensemble, we will consider an equilibrium gas at temperature T, where the number of particles N fluctuates and the chemical potential μ is fixed. This is equal to the description in the canonical ensemble (constant N and fluctuating μ) in

the thermodynamic limit($N \to \infty$).

According to the Bose-Einstein distribution of occupation, the total number of particles is correlated with temperature and chemical potential.

$$N = \sum_i \frac{1}{e^{\beta(E_i-\mu)} - 1} \tag{1.1}$$

where $\beta = \frac{1}{k_B T}$ and k_B is Boltzmann's constant. Furthermore, E_i is the eigeneenergies of the system.

1.3.1 Uniform gas

In an infinitely large, uniform gas , the particle eigenstates are defined by their momentum k and corresponding eigenenergy $E_k = \frac{\hbar^2 k^2}{2m}$, where m is the mass of the particles.

We can safely suppose that the momentum for k is continuous, danging the sums over k into integrals $\sum_k \to V \int \frac{d^d k}{(2\pi)^d}$. Then eq (1.1) becomes

$$N = N_c + V \int \frac{d^d k}{(2\pi)^d} \frac{1}{e^{\beta(E_k-\mu)} - 1} \tag{1.2}$$

d : the dimension of the system
V : the d-dimensional hyper volume
N_c :the number of condensed particles
We consider the transformation from Cartesian to spherical coordinates

$$\int_{-\infty}^{+\infty} dx_1 ....dx_d = S_d \int_0^{\infty} r^{d-1} dr \tag{1.3}$$

where $S_d = \dfrac{2\pi^{\frac{d}{2}}}{\Gamma(\dfrac{d}{2})}$ is the surface of the d-dimensional unit sphere. We use (1.3) to write the number non condensed of particles

$$\tilde{N} = N - N_c = \frac{V}{\Gamma(d/2)} \left(\frac{m}{2\pi\hbar^2}\right)^{\frac{d}{2}} \int_0^{\infty} dE \frac{E^{\frac{d}{2}-1}}{e^{\beta(E_k-\mu)} - 1} \tag{1.4}$$

Comparing (1.4) with the well known expression

$$\tilde{N} = \int_0^{\infty} dE \frac{g_d(E)}{e^{\beta(E_k-\mu)} - 1} \tag{1.5}$$

we get the density state

$$g_d = \frac{V}{\Gamma(d/2)} \left(\frac{m}{2\pi\hbar^2}\right)^{\frac{d}{2}} E^{\frac{d}{2}-1} \tag{1.6}$$

we will express the thermodynamic quantities in terms of the thermal De-Broglie wavelength $\lambda = \sqrt{\frac{2\pi\hbar^2\beta}{m}}$and the generalized Riemann zeta-function

$$\xi_\alpha = \frac{1}{\Gamma(\alpha)} \int_0^\infty dx \frac{x^{\alpha-1}}{z^{-1}e^x - 1} \tag{1.7}$$

where $z = e^{\beta\mu}$ is the fugacity. Therefore, the total number of particles can be rewritten as

$$N = N_c + \frac{V}{\lambda^d}\zeta_{\frac{d}{2}}(z) \tag{1.8}$$

Varying the temperature, the chemical potential must adjust so that the total number of particles is conserved. On the other hand, since $\mu < 0$ the number of excited atoms in (1.8) reaches its maximum at $\mu = 0$. If the total number of particles N exceeds the available excited energy levels, all excess particles must be accommodated in the ground state E_0 .

To calculate the limit $z \to 1$, we use the series representation of the generalized function for small negative values of the chemical potential :

$$\lim_{\alpha\to 1} \zeta_\alpha(e^{\beta\mu}) = -\ln(-\beta\mu) + \sum_{j=0}^{\infty} \frac{(\beta\mu)^j}{j!}\zeta(1-j) \tag{1.9}$$

In the limit $z \to 1$, the generalized zeta function reduces to the Riemann zeta function

$$\zeta(d/2)_{z\to 1} = \zeta(d/2) \tag{1.10}$$

For $T > T_c$: $\tilde{N} \leq N$ and $\mu < 0$: As the system approaches the critical temperature, the chemical potential increases until it reaches the limit $\mu \to 0$ as $z \to 1$. For $T < T_c$: μ remains zero so that N_c increases while $\tilde{N}$ decreases .

We now calculate the critical temperature at the onset of the phase transition, where the chemical potential vanishes. Using (1.8) and (1.10), the maximum number of particles in the excited states is given by

$$\tilde{N} = N = \frac{V}{\lambda^d}\zeta(d/2) \tag{1.11}$$

We thus arrive at the following expression for the critical temperature

$$k_B T_c = \frac{2\pi\hbar^2}{m}\left(\frac{N}{V\zeta(d/2)}\right)^{2/d} \tag{1.12}$$

The condensed fraction as a function of temperature now follows immediately from (1.8) and (1.12):

$$\frac{N_c}{N} = 1 - \left(\frac{T}{T_c}\right)^{d/2} \tag{1.13}$$

1.3.2 Trapped gas

When an isotropic trap is present, the density of states changes and the thermal behavior is different from that of the free gas. The density of states for the harmonic trapping potential is given by

$$g_d(E) = \frac{E^{d-1}}{\Gamma(d)(\hbar\omega)^d} \tag{1.14}$$

The number of thermal atoms now reads:

$$\tilde{N} = \frac{1}{(\hbar\omega\beta)^d\Gamma(d)}\int_0^\infty dE \frac{E^{d-1}}{e^{\beta(E_k-\mu)-1}} = \frac{\zeta_d(z)}{(\hbar\omega\beta)^d} \tag{1.15}$$

Similar to the free gas, the limit $z \to 1$ can be used to determine the maximum number of particles in the excited levels. so we now find

$$\tilde{N} = N = \frac{\zeta(d)}{(\hbar\omega/k_B T_c)^d} \tag{1.16}$$

and the critical temperature is given by:

$$k_B T_c = \hbar\omega\left(\frac{N}{\zeta(d)}\right)^{1/d} \tag{1.17}$$

Hence, the temperature dependence of the condensate fraction is, in contrast to (1.13), expressed by:

$$\frac{N_c}{N} = 1 - \left(\frac{T}{T_c}\right)^{d} \tag{1.18}$$

1.4 Illustration :Ideal Bose gas in three dimensions

Let us see how the previous results work in 3d.

1.4.1 Homogeneous case

The total particle number becomes (using 1.8)

$$N = N_c + \frac{V}{\lambda^3}\zeta_{3/2}(z) \tag{1.19}$$

The condition for BEC to occur is obtained from (1.11)

$$n\lambda^3 = \zeta(3/2) \tag{1.20}$$

where we have introduced the density $n = N/V$. This means that there exists a critical temperature at that the phase transition. It is obtained from (1.12)

$$T_c = \frac{2\pi\hbar^2}{mk_B}\left(\frac{n}{\zeta(3/2)}\right)^{2/3} \tag{1.21}$$

And finally we get for the condensate fraction

$$\frac{N_c}{N} = 1 - \left(\frac{T}{T_c}\right)^{3/2} \tag{1.22}$$

1.4.2 Trapped case

For the harmonically trapped gas, we get from (1.21) and (1.22)

$$k_B T_c = \hbar\omega\sqrt{N/\zeta(3)} \simeq 0.94\hbar\omega\sqrt{N} \tag{1.23}$$

and we notice that the condensate fraction decreases with the temperature as

$$\frac{N_c}{N} = 1 - \left(\frac{T}{T_c}\right)^{3} \tag{1.24}$$

1.5 Illustration : Bose gas in two dimensions

The function $\mu(T)$ is analytic and has a monotonic increase with decreasing temperature down $T = 0$.

1.5.1 Homogeneous case

In two dimensions, the density of states is independent of the energy and is given by:

$$g_2 = \frac{mA}{2\pi\hbar^2} \tag{1.25}$$

Where A is the area. The number of excited particles is given by

$$\tilde{N} = \frac{A}{\lambda^2}\zeta_1(z) \tag{1.26}$$

But ζ_1 has a pole at $z = 1$. To calculate the limit $z \to 1$, we use Robinson's formula (1.9) for $\alpha \to 1$ [41, 42].

We now substitute this into (1.26) and consider the limit $z \to 1, \mu \to 0$.

$$\tilde{N} = \frac{A}{\lambda^2}\lim_{\mu\to 0}(-\ln(-\beta\mu) + \sum_{j=0}^{\infty}\frac{(\beta\mu)^j}{j!}\zeta(1-j)) = -\frac{A}{\lambda^2}\lim_{\mu\to 0}\ln(-\beta\mu) \tag{1.27}$$

This expression diverges logarithmically . Hence, there is no Bose-Einstein condensation at finite temperatures. This is true even when interactions are included and has been proved in the Hohenberg theorem [43].

1.5.2 Trapped gas

On the other hand , BEC may occur if the gas is trapped. From (1.16) , the number of thermal particles is given by

$$\tilde{N} = \frac{\zeta_2(z)}{(\hbar\omega\beta)^2} \tag{1.28}$$

The critical temperature is given by (1.17):

$$k_B T_c = \frac{\hbar\omega}{\pi}\sqrt{6N} \tag{1.29}$$

where we used $\zeta_2(1) = \pi^2/6$. The temperature dependence of the condensate fraction follows from (1.18):

$$\frac{N_c}{N} = 1 - \left(\frac{T}{T_c}\right)^2 \tag{1.30}$$

The result(1.30) was first obtained by Bagnato and Kleppner [44]. They showed also that BEC can occur in two dimensions for any power law trapping potential $V = r^\eta$. In the vicinity of $\eta = 2$ (parabolic trapping potential), the critical temperature has a broad maximum.

1.6 Bose gas in one dimension

Quasi-one-dimensional systems have been experimentally realized using advanced techniques such as harmonic trapping, where the motion of particles in directions other than the main direction is constrained using magnetic or optical fields. In this context, Bose-Einstein condensation (BEC) in quasi-one-dimensional systems has been achieved by cooling the system to extremely low temperatures, causing bosonic particles to accumulate in a single low-energy state, which is the BEC state. Although Bose-Einstein condensation typically does not occur in low dimensions, such as one-dimensional systems, in the thermodynamic limit, experiments have shown that the system can exhibit BEC at low temperatures when magnetic or optical traps are used to restrict the motion. Through these experiments, researchers can study unique quantum effects that appear in quasi-one-dimensional systems, such as particle interactions or the system's behavior at very low temperatures.

These are some of the techniques used to achieve quasi-one dimensional systems experimentally:

Optical Traps : Quasi-1D BECs can be realized using optical dipole traps that create tight confinement in two directions (usually the radial directions), while leaving the third direction much weaker. This is typically done using laser light to create a potential well that is much stronger in two dimensions than in the third [45].

Evaporative Cooling : To achieve Bose-Einstein condensation in the quasi-1D regime, evaporative cooling techniques are used to lower the temperature of the atoms, making them condense into a single quantum state. This cooling is often performed in

the longitudinal direction, resulting in a condensate that behaves as a quasi-1D system.

Bose Gases in Tubes : In some experiments, BECs are created within narrow, tubular traps that have dimensions on the order of micrometers. These traps can limit the atoms to effectively move in only one dimension, allowing for the study of low-dimensional quantum phenomena.

For a homogeneous Bose gas in 1D, Eq.(1.11) yields:

$$\tilde{N} = \frac{L}{\lambda} g_{1/2}(z) \tag{1.31}$$

but since $g_{1/2}(z)$ diverges for $Z \to 1$, we conclude that here is no macroscopically occupied ground state in 1D .

As the thermal de Broglie wavelength of the particles approaches the average distance between them, quantum effects start to manifest at the degeneracy temperature T_d for homogeneous bosonic systems in a one-dimensional system. the degeneracy temperature T_d is defined using the following expression:

$$T_d = \frac{\hbar^2 n^2}{2mk_\beta} \tag{1.32}$$

where n is the 1D density. This equation shows that the degeneracy temperature depends on the particle density and the particle mass. Below the temperature T_d , quantum effects such as Bose-Einstein condensation start to manifest in the system.

In a trapped one-dimensional ideal Bose gas, the critical temperature T_c is the temperature at which Bose-Einstein condensation (BEC) occurs in the system. For such a system, the critical temperature is determined by the density of states in the trap and the statistical properties of the Bose gas. For a 1D ideal Bose gas in a harmonic trap, the critical temperature T_c is given by

$$k_\beta T_c = \hbar\omega \left(\frac{N}{\zeta(1)} \right)^2 \tag{1.33}$$

where $\zeta(1)$ is the Riemann zeta function evaluated at 1, which is $\zeta(1) \to \infty$ as it diverges at this point. This equation indicates that Bose-Einstein condensation in a one-dimensional system with a harmonic trap can only occur at very low temperatures, as the critical temperature in low dimensions is usually small compared to higher-dimensional systems.

Chapter 2

Interacting Bose-Einstein Condensates

2.1 The Gross-Pitaevskii Equation

When describing a many-particle system, such as the dilute Bose gas in a trap. A defining feature of Bose-Einstein condensation is the formation of a state with macroscopic occupation, which can be represented by a classical wave function. At temperatures far below the critical temperature, where the phase transition to Bose-Einstein condensation occurs, this provides an excellent description of the condensed state. Even at higher temperatures, one can treat the thermal atoms as fluctuations of this classical field with a very good approximation. Important properties of the condensate, such as its shape and momentum distribution, can be described by a non-linear Schrödinger equation. The interactions between the atoms are accounted for by a term proportional to the condensate density $|\Phi(r)|^2$.

Let us consider a system of trapped bosons interacting via a two-body potential. The grand canonical Hamiltonian can be written :

$$H = \int d\vec{r}\hat{\Psi}^{+}\left(\vec{r},t\right)h^{sp}\hat{\Psi}(\vec{r},t) + \frac{1}{2}\iint d\vec{r}d\vec{r}'\hat{\Psi}^{+}\left(\vec{r}',t\right)\hat{\Psi}^{+}\left(\vec{r},t\right)V\left(\vec{r},\vec{r}'\right)\hat{\Psi}\left(\vec{r}',t\right)\hat{\Psi}(\vec{r},t). \tag{2.1}$$

where $h^{sp} = -\frac{\hbar^2}{2m}\Delta + V_{\text{ext}}\left(\vec{r}\right)$ is the single particle Hamiltonian, $V\left(\vec{r},\vec{r}'\right)$ is the two-body interaction potential, and $V_{ext}(\vec{r})$ the external confining field. $\hat{\Psi}(\vec{r})$ and $\hat{\Psi}^{+}(\vec{r})$ are the creation and annihilation operators satisfying the usual commutation relation.

$$\left[\hat{\Psi}(\vec{r}),\hat{\Psi}^{+}\left(\vec{r}'\right)\right] = \delta\left(\vec{r},\vec{r}'\right) \tag{2.2}$$

$$\left[\hat{\Psi}^{+}(\vec{r}),\hat{\Psi}^{+}\left(\vec{r}'\right)\right] = \left[\hat{\Psi}(\vec{r}),\hat{\Psi}\left(\vec{r}'\right)\right] = 0.$$

This Hamiltonian is the starting point for all theoretical treatments of dilute Bose gases [46], and includes quantum fluctuations. All theories appearing in the literature arise from distinct approximations for this Hamiltonian. For dilute gases at very low temperature, the usual procedure is to make a contact interaction (also called pseudo-potential) approximation.

$$V\left(\vec{r},\vec{r}'\right) = g\delta\left(\vec{r}-\vec{r}'\right) \tag{2.3}$$

where δ is the delta Dirac distribution.

The potential (2.3) means that the two atoms undergo perfectly elastic local collisions, like two billiard balls. The strength of the interaction is given by $g = \frac{4\pi\hbar^2 a}{m}$, where a is the s-wave scattering length for a particular atomic species, which can be determined from

experiments. This is a some what idealized scenario, which can nonetheless be put on firm ground by a more careful treatment [47]- the origin and validity of this approximation will be discussed later.
Substitution into the Hamiltonian Eq. (2.2) then gives:

$$H = \int d\vec{r}\hat{\Psi}^{+}(\vec{r},t)h^{sp}\hat{\Psi}(\vec{r},t) + \frac{g}{2}\int d\vec{r}\hat{\Psi}^{+}(\vec{r},t)\hat{\Psi}^{+}(\vec{r},t)\hat{\Psi}(\vec{r},t)\hat{\Psi}(\vec{r},t) \tag{2.4}$$

The starting point for the dynamics of ultra cold gases is to consider the equation governing the evolution of the bosonic field operator $\hat{\Psi}(\vec{r},t)$. The second-quantized form of the appropriate equation can be analyzed in one of two distinct pictures, known as the Schrödinger, and the Heisenberg pictures, depending on whether the state vectors, the operators corresponding to system observables, are time-dependent [48] . In the Schrödinger picture, the solution of the Schrödinger equation at time t , given the initial solution at t_0 , is given by a unitary transformation $|\Psi_s(t)\rangle = \exp\frac{-i\hat{H}(t-t_0)}{\hbar}|\Psi_0(t)\rangle$, where $\hat{H}$ does not contain any explicit time-dependence. In the Heisenberg picture the state vectors can be constructed from the corresponding Schrödinger picture state vectors via $|\Psi_H(t)\rangle = \exp\frac{i\hat{H}t}{\hbar}|\Psi_s(t)\rangle$, are time independent and all time dependence is contained in the operators. While all pictures can be used inter changeably, most subsequent discussion will be given in the Heisenberg picture in which the equation of motion of a general operator $\hat{O}_H$ is

$$\imath\hbar\frac{d\hat{O}_H}{dt} = \left[\hat{O}_H, \hat{H}\right]. \tag{2.5}$$

In studying the system dynamics, we will actually be concerned with the equations of motion of the Bose field operator $\hat{\Psi}$. For the Hamiltonian of Eq. (2.4), this evolves according to the Heisenberg equation of motion

$$\imath\hbar\frac{d\hat{\Psi}(\vec{r},t)}{dt} = [\hat{\Psi}(\vec{r},t),\hat{H}] = h^{sp}\hat{\Psi}(\vec{r},t) + g\hat{\Psi^{+}}(\vec{r},t)\hat{\Psi}(\vec{r},t)\hat{\Psi}(\vec{r},t) \tag{2.6}$$

In order to extract information from this equation, it is convenient to separate the condensate contribution, which corresponds to the macroscopic occupation of a single quantum state, from the remaining part of the Bose field operator. Hence the Bose field operator is divided into two parts [49, 50] .

$$\hat{\Psi}(\vec{r},t) = \Phi(\vec{r},t) + \hat{\tilde{\Psi}}(\vec{r},t) \tag{2.7}$$

corresponding respectively to a classical field for the condensate, and a fluctuating filed

operator for the non-condensed atoms,$\hat{\tilde{\Psi}}$. These could either correspond to thermally excited atoms, quantum mechanical fluctuations, or atoms promoted into higher energy states due to interactions. It is important to notice at this level that the condensate is described by a classical function and not by a field operator. This approximation is well justified since the ground state is macroscopically occupied [49, 50], and is called Bogoliubov approximation.

Then we break down the full system Hamiltonian into various contributions based on the number of condensate and non-condensate factors contained in each of them. In particular, substitution of (2.7) into the system Hamiltonian (2.4) leads to

$$H = H_0 + H_1 + H_2 + H_3 + H_4. \tag{2.8}$$

Where

$$\begin{aligned}
H_0 &= \int d\vec{r} \left[\Phi^\star \hat{h}^{sp} \Phi + \frac{g}{2} |\Phi|^4 \right], \\
H_1 &= \int d\vec{r} \left[\hat{\tilde{\Psi}}^+ \left(\hat{h}^{sp} \Phi + g \left| \Phi^2 \right| \right) \Phi + \Phi^\star \left(\hat{h}^{sp} \Phi + g \left| \Phi^2 \right| \right) \hat{\tilde{\Psi}} \right], \\
H_2 &= \int d\vec{r} \left[\hat{\tilde{\Psi}}^+ \left(\hat{h}^{sp} \Phi + 2g \left| \Phi^2 \right| \right) \hat{\tilde{\Psi}} + \frac{g}{2} \left(\Phi^{\star 2} \hat{\tilde{\Psi}} \hat{\tilde{\Psi}} + \hat{\tilde{\Psi}}^+ + \hat{\tilde{\Psi}}^+ \Phi^2 \right) \right], \\
H_3 &= g \int d\vec{r} \left[\Phi \hat{\tilde{\Psi}}^+ \hat{\tilde{\Psi}}^+ \hat{\tilde{\Psi}} + \Phi^\star \hat{\tilde{\Psi}}^+ \hat{\tilde{\Psi}} \hat{\tilde{\Psi}} \right], \\
H_4 &= \frac{1}{2} \int d\vec{r} \hat{\tilde{\Psi}}^+ \hat{\tilde{\Psi}}^+ \hat{\tilde{\Psi}} \hat{\tilde{\Psi}}
\end{aligned} \tag{2.9}$$

In the $T = 0$ limit, all particles occupy the condensate, and the non-condensate operator can be neglected ($\hat{\tilde{\Psi}} = \hat{\tilde{\Psi}}^+ \simeq 0$). The exact Heisenberg equation of motion (2.6) reduces to the so called Gross-Pitaevskii Equation (GPE) [1, 51].

$$\imath\hbar \frac{d\Phi(\vec{r}, t)}{dt} = \left[\frac{-\hbar^2}{2m} \nabla^2 + V_{ext}(\vec{r}, t) + g|\Phi(\vec{r}, t)|^2 \right] \Phi(\vec{r}, t). \tag{2.10}$$

This equation is a nonlinear Schrödinger equation, corresponding to the zero temperature hydrodynamic description of Bose gases, first introduced to study vortex lines in an imperfect Bose gas. This equation is mathematically analogous to a Ginzburg-Landau-type approach [52], valid near the critical regime although the origin of the various contributions and the physical interpretation here is actually quite distinct. Remarkably, the GPE, which was first numerically implemented for dilute weakly-interacting trapped Bose gases was undertaken by Mark Edwards, Keith Burnett and collaborators [53, 54], provides a good description of the dynamics of a Bose-Einstein condensate for a wide class

of prob lems at temperatures as high as $T \approx \frac{T_c}{2}$. The GPE can be used, at low temperature, to explore the macroscopic behavior of the system, characterized by variations of the order parameter Φ over distances larger than the mean distance between atoms.
One can find static solutions by eliminating the time-dependence via the Madeliing transformation:

$$\Phi(\vec{r}, t) = \Phi(\vec{r}) \exp\left(\frac{-i\mu t}{\hbar}\right) | \tag{2.11}$$

where ,μ is the chemical potential. Substituting Eq. (2.11) into Eq. (2.10), we obtain the time-independent Gross-Pitaevskii equation (GPE):

$$\mu\Phi(\vec{r}) = \left[\frac{-\hbar^2}{2m}\nabla^2 + V_{ext}(\vec{r}) + g|\Phi(\vec{r})|^2\right]\Phi(\vec{r}) \tag{2.12}$$

In the form given above, the wave function is normalized to the total number of particles, i.e $\int |\Phi(\vec{r})|^2 d\vec{r} = N$. Alternatively, the Gross-Pitaevskii equation Eq (2.10) can also be obtained using a variational procedure:

$$\imath\hbar\frac{d\Phi}{dt} = \frac{\delta E}{\delta\phi^\star} \tag{2.13}$$

where the energy functional E is given by

$$E[\Phi] = \int dr \left[-\frac{\hbar^2}{2m}|\nabla\Phi|^2 + V_{ext}(r)|\Phi|^2 + \frac{g}{2}|\Phi|^4\right] = E_{kin} + E_p + E_{int} \tag{2.14}$$

The first term in the integral Eq. (2.14) is the kinetic energy of the condensate E_{kin}, the second is the trapping energy E_p, while the last one is the mean field interaction energyE_{int} .

2.2 Validity of Gross-Pitaevskii Equation

The GPE is used to model the macroscopic wave function of a condensate, and it is particularly important for understanding phenomena like superfluidity and vortices in BECs. It is a mean-field approximation to the many-body quantum problem, where the interactions between particles are considered through an effective potential. The GPE is an approximation that is valid under specific conditions [55–59], typically for dilute, weakly interacting bosonic gases at very low temperatures. Its validity is determined by several assumptions:

Low-Temperature Regime (Quantum Degeneracy)

The GPE is most effective when the system is in the Bose-Einstein condensate phase, which occurs at low temperatures. Bosons condense into the lowest quantum state at these temperatures, and the ground state wave function dominates the system's dynamics [60]. Because thermal fluctuations are negligible and quantum effects predominate in this regime, the mean-field approximation becomes accurate.

Dilute Gas (Weak Interactions)

The GPE assumes that the gas is dilute , meaning the particle density is low enough that interactions between particles can be treated as weak and localized. This ensures that the system can be approximated by a mean-field theory where the interactions are incorporated as a simple non-linear term $g|\psi|^2$. In this regime, the particles are far apart on average, which allows for the treatment of the system's behavior by a single macroscopic wave function .

Weak Interactions

If the interaction strength g is too large, the mean-field breaks down, and more complex models (like many-body theory or perturbative approaches) are required.

Single-Mode Approximation

The GPE assumes that the condensate can be described by a single macroscopic wavefunction that represents the bulk properties of the system. This approximation is valid when the condensate is relatively homogeneous or when the system can be treated as a single collective mode. If the condensate is highly inhomogeneous or consists of multiple components (e.g., in multi-component BECs), more sophisticated treatments are required. The single-mode approximation implies that the condensate is largely in the ground state, and deviations from the ground state are treated as small perturbations. This approximation works well for systems where the condensate is large and the excited states do not significantly affect the overall dynamics.

Stationary Solution

The Gross-Pitaevskii equation frequently results in stationary solutions for the condensate, which allow for the separation of the wavefunction's time dependence and make the equation time-independent. This is particularly useful when describing equilibrium properties of the condensate. However, the equation can also describe dynamical evolution, such as the behavior of solitons or vortex formation in the condensate [61, 62].

2.3 Breakdown of the Gross-Pitaevskii Equation:

The breakdown of the Gross-Pitaevskii Equation (GPE) occurs in the following cases:

Strongly Interacting Regimes:
For very strong interactions, the Gross-Pitaevskii equation may not be accurate because the interactions between particles cannot be treated as a simple mean-field term. In these cases, more sophisticated methods, such as beyond-mean-field corrections (e.g., using the Bogoliubov approximation or the Hartree-Fock method), are required.

Finite-Temperature Effects:
The system's thermal fluctuations are not taken into consideration by the GPE. The GPE is invalid at temperatures well over the critical temperature for BEC creation, and alternative methods such as the BEC-BCS crossover theory or the Boltzmann equation would be more suitable.

Quantum Fluctuations:

The GPE ignores quantum fluctuations and describes the condensate as a coherent state, which works well for systems with a large number of particles [55, 57]. However, at very small particle numbers or in the presence of significant quantum fluctuations, the GPE may not provide an accurate description.

2.4 Beyond the Gross Pitaevskii regime

To go beyond the standard mean-field approximation, one must include both quantum and thermal fluctuations. This can be performed by different methods.

Among the most interesting and consistent ones, we can cite the variational derivation. We choose the Balian-Vénéroni (BV) principle which appears to us more adapted to this kind of problems. Indeed, the BV principle requires selecting a trial space for the density operator [32–36]. We will focus on a Gaussian, time-dependent, density-like operator. This Ansatz, which belongs to the class of generalized coherent states, enables us to carry out the calculation (thanks to the existence of Wick's theorem), while preserving key features, such as the pairing between atoms. Let us first define the quantities:

$$\begin{aligned} \Phi(\mathbf{r},t) &= \langle \hat{\Psi}(\mathbf{r}) \rangle \\ \tilde{n}\left(\mathbf{r},\mathbf{r}',t\right) &= \tilde{n}^{*}\left(\mathbf{r}',\mathbf{r},t\right) = \left\langle \hat{\Psi}^{+}(\mathbf{r})\hat{\Psi}\left(\mathbf{r}'\right)\right\rangle - \Phi^{*}(\mathbf{r})\Phi\left(\mathbf{r}'\right) \\ \tilde{m}\left(\mathbf{r},\mathbf{r}',t\right) &= \tilde{m}\left(\mathbf{r}',\mathbf{r},t\right) = \left\langle \hat{\Psi}(\mathbf{r})\hat{\Psi}\left(\mathbf{r}'\right)\right\rangle - \Phi(\mathbf{r})\Phi\left(\mathbf{r}'\right) \end{aligned} \tag{2.15}$$

where $\hat{\Psi}(\mathbf{r})$ and $\hat{\Psi}^{+}(\mathbf{r})$ are the boson destruction and creation.

The symbole $\langle..\rangle$ means taking expectoration values with respect to the density operator D. For any operator A , $\langle A\rangle = \frac{TrAD}{TrD}$, where Tr is the trace in the many-body Fock space. Moreovor, the line dependence in the quantities (2.15) appears due to the line dependence of D . The quantities (2.15) completely characterize the gaussian density operator and, in our langage, are akin to an order parameter and to one-body correlation functions. The local limit of the latter are just the noncondensate density $\lim_{\mathbf{r}'\to\mathbf{r}} \tilde{n}\left(\mathbf{r},\mathbf{r}',t\right) = \tilde{n}(\mathbf{r},t)$ and the anomalous density $\lim_{\mathbf{r}'\to\mathbf{r}} \tilde{m}\left(\mathbf{r},\mathbf{r}',t\right) = \tilde{m}(\mathbf{r},t)$.

Let us consider the second quantized Hamiltonian (2.1). The stationarity conditions of the BV action-like functional (see appendix) lend to a set of dynamical equations which couple the various densities :(The dots cknote time derivation) [36].

$$\begin{aligned} i\hbar\dot{\Phi}(\mathbf{r}) = h^{\mathrm{sp}}(\mathbf{r})\Phi(\mathbf{r}) + \int_{\mathbf{r}'} V\left(\mathbf{r},\mathbf{r}'\right) \Big[&\left|\Phi\left(\mathbf{r}'\right)\right|^{2}\Phi(\mathbf{r}) \\ &+ \Phi^{*}\left(\mathbf{r}'\right)\tilde{m}\left(\mathbf{r},\mathbf{r}'\right) + \Phi\left(\mathbf{r}'\right)\tilde{n}\left(\mathbf{r},\mathbf{r}'\right) + \Phi(\mathbf{r})\tilde{n}\left(\mathbf{r}',\mathbf{r}'\right)\Big] \end{aligned}$$

$$
\begin{aligned}
i\hbar\dot{\tilde{n}}\left(\mathbf{r},\mathbf{r}'\right) &= \left[h^{\mathrm{sp}}(\mathbf{r}) - h^{\mathrm{sp}}\left(\mathbf{r}'\right)\right]\tilde{n}\left(\mathbf{r},\mathbf{r}'\right) + \int_{\mathbf{r}''} V\left(\mathbf{r}',\mathbf{r}''\right)\left[a\left(\mathbf{r}'',\mathbf{r}'\right)\tilde{n}\left(\mathbf{r},\mathbf{r}''\right)\right. \\
&\quad + a\left(\mathbf{r}'',\mathbf{r}''\right)\tilde{n}\left(\mathbf{r},\mathbf{r}'\right) + b\left(\mathbf{r}',\mathbf{r}''\right)\tilde{m}^{*}\left(\mathbf{r}'',\mathbf{r}\right)\Big] - \int_{\mathbf{r}''} V\left(\mathbf{r},\mathbf{r}''\right)\left[a\left(\mathbf{r},\mathbf{r}''\right)\tilde{n}\left(\mathbf{r}'',\mathbf{r}'\right)\right. \\
&\quad \left. + a\left(\mathbf{r}'',\mathbf{r}''\right)\tilde{n}\left(\mathbf{r},\mathbf{r}'\right) + b^{*}\left(\mathbf{r},\mathbf{r}''\right)\tilde{m}\left(\mathbf{r}'',\mathbf{r}'\right)\right] \\
i\hbar\dot{\tilde{m}}\left(\mathbf{r},\mathbf{r}'\right) &= \left[h^{\mathrm{sp}}(\mathbf{r}) + h^{\mathrm{sp}}\left(\mathbf{r}'\right)\right]\tilde{m}\left(\mathbf{r},\mathbf{r}'\right) + \int_{\mathbf{r}''} V\left(\mathbf{r}',\mathbf{r}''\right)\left[a\left(\mathbf{r}'',\mathbf{r}'\right)\tilde{m}\left(\mathbf{r},\mathbf{r}''\right)\right. \\
&\quad \left. + a\left(\mathbf{r}'',\mathbf{r}''\right)\tilde{m}\left(\mathbf{r},\mathbf{r}'\right) + b\left(\mathbf{r}',\mathbf{r}''\right)\times\left(\tilde{n}^{*}\left(\mathbf{r},\mathbf{r}''\right) + \delta\left(\mathbf{r}-\mathbf{r}''\right)\right)\right] \\
&\quad + \int_{\mathbf{r}''} V\left(\mathbf{r},\mathbf{r}''\right)\left[a\left(\mathbf{r}'',\mathbf{r}\right)\tilde{m}\left(\mathbf{r}',\mathbf{r}''\right) + a\left(\mathbf{r}'',\mathbf{r}''\right)\tilde{m}\left(\mathbf{r},\mathbf{r}'\right) + b\left(\mathbf{r},\mathbf{r}''\right)\tilde{n}\left(\mathbf{r}'',\mathbf{r}'\right)\right]
\end{aligned}
\tag{2.16}
$$

where

$$
a\left(\mathbf{r},\mathbf{r}'\right) = a^{*}\left(\mathbf{r}',\mathbf{r}\right) = \left\langle\psi^{+}(\mathbf{r})\psi\left(\mathbf{r}'\right)\right\rangle = \tilde{n}\left(\mathbf{r},\mathbf{r}'\right) + \Phi^{*}(\mathbf{r})\Phi\left(\mathbf{r}'\right)
$$

and

$$
b\left(\mathbf{r},\mathbf{r}'\right) = b\left(\mathbf{r}',\mathbf{r}\right) = \left\langle\psi(\mathbf{r})\psi\left(\mathbf{r}'\right)\right\rangle = \tilde{m}\left(\mathbf{r},\mathbf{r}'\right) + \Phi(\mathbf{r})\Phi\left(\mathbf{r}'\right)
$$

In the case of a contact potential $V\left(\mathbf{r},\mathbf{r}'\right) = g\delta\left(\mathbf{r}-\mathbf{r}'\right)$, these equations become

$$
i\hbar\dot{\Phi}(\mathbf{r}) = \left[h^{\mathrm{sp}}(\mathbf{r}) + g\left(n_c(\mathbf{r}) + 2\tilde{n}(\mathbf{r})\right)\right]\Phi(\mathbf{r}) + g\tilde{m}(\mathbf{r})\Phi^{*}(\mathbf{r}), \tag{2.17}
$$

$$
\begin{aligned}
i\hbar\dot{\tilde{n}}\left(\mathbf{r},\mathbf{r}'\right) =& \left[\left(h^{\mathrm{sp}}(\mathbf{r}) + 2gn(\mathbf{r})\right) - \left(h^{\mathrm{sp}}\left(\mathbf{r}'\right) + 2gn\left(\mathbf{r}'\right)\right)\right]\tilde{n}\left(\mathbf{r},\mathbf{r}'\right) \\
&+ g\left[b\left(\mathbf{r}',\mathbf{r}'\right)\tilde{m}^{*}\left(\mathbf{r},\mathbf{r}'\right) + b^{*}(\mathbf{r},\mathbf{r})\tilde{m}\left(\mathbf{r},\mathbf{r}'\right)\right]
\end{aligned}
\tag{2.18}
$$

$$
\begin{aligned}
i\hbar\dot{\tilde{m}}\left(\mathbf{r},\mathbf{r}'\right) =& \left[\left(h^{\mathrm{sp}}(\mathbf{r}) + 2gn(\mathbf{r})\right) + \left(h^{\mathrm{sp}}\left(\mathbf{r}'\right) + 2gn\left(\mathbf{r}'\right)\right)\right]\tilde{m}\left(\mathbf{r},\mathbf{r}'\right) \\
&+ g\left[b\left(\mathbf{r}',\mathbf{r}'\right)\left(\delta\left(\mathbf{r}-\mathbf{r}'\right) + \tilde{n}^{*}\left(\mathbf{r},\mathbf{r}'\right)\right) + b(\mathbf{r},\mathbf{r})\tilde{n}\left(\mathbf{r},\mathbf{r}'\right)\right]
\end{aligned}
\tag{2.19}
$$

Where $n_c\left(\mathbf{r}\right) = \left|\Phi\left(\mathbf{r}\right)\right|^2$ is the condensate density and $n\left(\mathbf{r}\right) = n_c\left(\mathbf{r}\right) + \tilde{n}\left(\mathbf{r}\right)$ the total density. For convenience, we have suppressed the time dependence. Notice that upon setting $\tilde{n} = \tilde{m} = 0$,(2.17) yields bach the GPE (2.10) .

This set of equations was also obtained in a local form using a quite different method by [63–66]. However, in the quasi-homogeneous case, these equations can only be connected to the well-known HFB-BdG equations. Indeed, upon setting.

$$
\begin{aligned}
\tilde{m}\left(\mathbf{r},\mathbf{r}'\right) &= -\frac{1}{2}\sum_{k}\left(1+2n_k\right)\left(U_k(\mathbf{r})V_k\left(\mathbf{r}'\right) + U_k\left(\mathbf{r}'\right)V_k(\mathbf{r})\right) \\
\tilde{n}\left(\mathbf{r},\mathbf{r}'\right) &= \sum_{k}\left(n_k U_k^{*}(\mathbf{r})U_k\left(\mathbf{r}'\right) + \left(1+n_k\right)V_k^{*}(\mathbf{r})V_k\left(\mathbf{r}'\right)\right)
\end{aligned}
\tag{2.20}
$$

where U_k and V_k are linearly independent space functions and n_k is the occupation probability of the mode k which is given at equilibrium by the Bose-Einstein distribution function, we readily get from (2.18) and (2.19)

$$\begin{aligned} i\hbar\dot{U}_k(\mathbf{r}) &= \left[h^{\mathrm{sp}}(\mathbf{r}) + 2gn(\mathbf{r})\right] U_k(\mathbf{r}) - gb(\mathbf{r},\mathbf{r})V_k^*(\mathbf{r}) \\ i\hbar\dot{V}_k(\mathbf{r}) &= \left[h^{\mathrm{sp}}(\mathbf{r}) + 2gn(\mathbf{r})\right] V_k(\mathbf{r}) - gb(\mathbf{r},\mathbf{r})U_k^*(\mathbf{r}), \end{aligned} \tag{2.21}$$

which, together with (2.17) form the so-called (generalized) time dependent HFB-BdG equations [63, 66, 67]. Hence, our equations can be considered as a variational extension of the time dependent HFB-BdG equations for non homogeneous situations.
Among the interesting properties of the TDHFB equations, We can quote the conservation of the energy and of the total particle number. Moreevor, the "Heisenberg" parameter is described as

$$\begin{aligned} I\left(\mathbf{r},\mathbf{r}'\right) = &\int_{\mathbf{r}''} \left(\delta\left(\mathbf{r}-\mathbf{r}''\right) + 2\tilde{n}\left(\mathbf{r},\mathbf{r}''\right)\right) \\ &\times \left(\delta\left(\mathbf{r}''-\mathbf{r}'\right) + 2\tilde{n}\left(\mathbf{r}'',\mathbf{r}'\right)\right) \\ &- 4\int_{\mathbf{r}''} \tilde{m}^*\left(\mathbf{r},\mathbf{r}''\right)\tilde{m}\left(\mathbf{r}'',\mathbf{r}'\right) \end{aligned} \tag{2.22}$$

and that can be expressed in a more accessible, condensed format.

$$I\left(\mathbf{r},\mathbf{r}'\right) = \left(\delta\left(\mathbf{r}-\mathbf{r}'\right) + 2\tilde{n}\left(\mathbf{r},\mathbf{r}'\right)\right)^2 - 4\left|\tilde{m}\left(\mathbf{r},\mathbf{r}'\right)\right|^2 \tag{2.23}$$

is also a constant of motion at zero temperature. Indeed, for $T = 0, I\left(\mathbf{r},\mathbf{r}'\right) = \delta\left(\mathbf{r}-\mathbf{r}'\right)$ and $\int_{\mathbf{r}''} \tilde{n}^*\left(\mathbf{r},\mathbf{r}''\right)\tilde{m}\left(\mathbf{r}'',\mathbf{r}'\right) = \int_{\mathbf{r}''} \tilde{m}\left(\mathbf{r},\mathbf{r}''\right)\tilde{n}\left(\mathbf{r}'',\mathbf{r}'\right)$. One can easily check that these properties remain true during the evolution if they are initially fulfilled. This conservation law is not however new since it is intimately related to the unitary evolution of the single particle density matrix [34, 68, 69].

Equation (2.19) involves an explicitly diverging term (for $\mathbf{r} = \mathbf{r}'$) which should be regularized. To this end, one may absorb this diverging expression in a redefinition of the thermal average [66, 70, 71] or, as performed by [72, 73], one may use the pseudo-potential method [74] to renormalize the coupling constant. A more rigorous approach is the Λ-potential method first discussed in references [75, 76] . Neverttheless, these approaches suffer from conceptual difficulties in that they are based on substraction schemes, which

are not compatible with the variational technique. Another way of proceeding, which seems to us much more interesting, since it allows to remain in the variational framework, is to resort to a better representation which would "wash out" these singular terms. One of the best candidates is the Wigner representation [67,77] . To this end, let us define the Wigner transform for any function $A(\mathbf{r},\mathbf{r}')$ as

$$A(\mathbf{r},\mathbf{r}') = \int_{\mathbf{k}} A_W\left(\frac{\mathbf{r}+\mathbf{r}'}{2},\mathbf{k}\right)\exp\left[-i\mathbf{k}\cdot(\mathbf{r}-\mathbf{r}')\right]$$

and its inverse

$$A_W(\mathbf{R},\mathbf{k}) = \int_{\mathbf{r}} A(\mathbf{R}+\mathbf{r}/2,\mathbf{R}-\mathbf{r}/2)\exp(i\mathbf{k}\cdot\mathbf{r})$$

where $\int_{\mathbf{k}} = \frac{1}{(2\pi)^3}\int d^3\mathbf{k}$. In the limit $\mathbf{r}=\mathbf{r}'$, equations (2.20) and (2.21) take the form

$$\begin{aligned} i\hbar\dot{\tilde{n}}_W(\mathbf{r},\mathbf{k}) =& -\frac{i\hbar^2}{m}\mathbf{k}\cdot\nabla_{\mathbf{r}}\tilde{n}_W(\mathbf{r},\mathbf{k}) \\ &+ g\left[\left(\Phi^2(\mathbf{r})+\tilde{m}(\mathbf{r})\right)\tilde{m}^*_W(\mathbf{r},\mathbf{k})\right. \\ &\left.-\left(\Phi^{*2}(\mathbf{r})+\tilde{m}^*(\mathbf{r})\right)\tilde{m}_W(\mathbf{r},\mathbf{k})\right] \end{aligned} \tag{2.24}$$

$$\begin{aligned} i\hbar\dot{\tilde{m}}_W(\mathbf{r},\mathbf{k}) =& 2\left[H^{\mathrm{sp}}+2gn(\mathbf{r})+\frac{\hbar^2k^2}{2m}\right]\tilde{m}_W(\mathbf{r},\mathbf{k}) \\ &+ g\left(\Phi^2(\mathbf{r})+\tilde{m}(\mathbf{r})\right)\left(1+2\tilde{n}_W(\mathbf{r},\mathbf{k})\right) \end{aligned} \tag{2.25}$$

In the static case, and for a neutral gas, one may consider without loss of generality that $\Phi,\tilde{m}$ and $\tilde{n}$ are real space functions. Equation (2.24) translates into

$$\mathbf{k}\cdot\nabla_{\mathbf{r}}\tilde{n}_W(\mathbf{r},\mathbf{k}) = 0 \tag{2.26}$$

which means in particular that there is no current associated with the non condensate and that the condensate current is conservative. On the other hand, equations (2.17) and (2.25) yield

$$0 = \left[h^{\mathrm{sp}}+g\left(n_c+2\tilde{n}+\tilde{m}\right)\right]\Phi(\mathbf{r}) \tag{2.27}$$

$$\begin{aligned} 0 =& 2\left(h^{\mathrm{sp}}+2gn(\mathbf{r})+\frac{\hbar^2k^2}{2m}\right)\tilde{m}_W(\mathbf{r},\mathbf{k}) \\ &+ g\left(n_c+\tilde{m}\right)\left(1+2\tilde{n}_W(\mathbf{r},\mathbf{k})\right) \end{aligned} \tag{2.28}$$

Next, one may use the gradient expansion method [67,77] to show that $\tilde{n}_W$ and $\tilde{m}_W$ write

simply

$$2\tilde{m}_W(\mathbf{r},\mathbf{k}) = -\,(1+2n_k)\sinh\sigma(\mathbf{r},\mathbf{k}),$$

$$1+2\tilde{n}_W(\mathbf{r},\mathbf{k}) = (1+2n_k)\cosh\sigma(\mathbf{r},\mathbf{k}), \tag{2.29}$$

where we recall that n_k is the Bose-Einstein distribution function at equilibrium. The quantity σ is an intermediate variable .
The Wigner transform of the Heisenberg parameter I_W takes the familiar form

$$\sqrt{I_W} = 1+2n_k = \coth\left(\beta\epsilon_k/2\right) \tag{2.30}$$

where $\beta = 1/k_BT, k_B$ being the Boltzmann constant. The quantities ϵ_k are the s.p. energies obtained by solving the stationary Gross-Pitaevskii equation (2.29):

$$\epsilon_k = \frac{\hbar^2k^2}{2m} + V_{\text{ext}} - \mu + g(n+\tilde{n}+\tilde{m}) \tag{2.31}$$

Corrections to the expressions (2.29) and (2.30) will measure how far the gas is from homogeneity [67]. Moreover the spectrum (2.31) is manifestly gapless. Since, in the homogeneous long wavelength limit, the Hugenholtz-Pines theorem [78] is automatically satisfied $\mu = g\,(n+\tilde{n}+\tilde{m})$. In contrast, in the standard HFB framework, one has to slightly modify the equations in order to obtain a gapless spectrum (see e.g. [63,66,70,79]). Similarly, in the Λ-potential approach [75,76], a zero gap condition is imposed in order to render the theory consistent and this leads to the correct equation of state.

In order to analyze the anomalous effects, let us derive workable expressions for $\tilde{n}$ and $\tilde{m}$. To this end, we follow the method depicted in reference [77] . The key point shown there is that, up to order $\hbar^2$, the Wigner transform of the product of two s.p. operators is the product of their Wigner transforms [80]. Equation (2.27) may thus be written formally in a classical form

$$(\mu - H_{cl})\,\Phi = 0 \tag{2.32}$$

with the self-consistent hamiltonian $H_{cl} = p^2/2m + V_{\text{ext}} + g(n+\tilde{n}+\tilde{m})$. The local momentum p must satisfy the on-shell condition $p \equiv p_0(\mathbf{r}) = \sqrt{2m\,(\mu - V_{\text{ext}} - g(n+\tilde{n}+\tilde{m}))}$. Using (2.31), we get the intermediate result

$$\tanh\sigma(\mathbf{r},\mathbf{k}) = \frac{g\,(n_c+\tilde{m})}{\frac{p_0^2}{2m} + V_{\text{ext}} - \mu + 2gn + \frac{\hbar^2k^2}{2m}}, \tag{2.33}$$

which yields the desired expressions for $\tilde{n}$ and $\tilde{m}$ [36] :

$$\tilde{m} = -\frac{1}{2}\int \frac{d^3\mathbf{k}}{(2\pi)^3} \frac{g\left(n_c + \tilde{m}\right)}{\sqrt{\left(\frac{\hbar^2 k^2}{2m} + 2gn_c\right)\left(\frac{\hbar^2 k^2}{2m} - 2g\tilde{m}\right)}} \coth\left(\beta\epsilon_k/2\right) \tag{2.34}$$

$$\tilde{n} = \frac{1}{2}\int \frac{d^3\mathbf{k}}{(2\pi)^3} \left[-1 + \frac{\frac{\hbar^2 k^2}{2m} + g\left(n_c - \tilde{m}\right)}{\sqrt{\left(\frac{\hbar^2 k^2}{2m} + 2gn_c\right)\left(\frac{\hbar^2 k^2}{2m} - 2g\tilde{m}\right)}} \coth\left(\beta\epsilon_k/2\right)\right]. \tag{2.35}$$

What is remarkable on these expressions is that the denominator is clearly not of the Bogoliubov type. This is the price to be paid in order to maintain not only the consistency of our variational approach but also the gapless nature of the spectrum. To recover a Bogoliubov-type spectrum, one may set $\tilde{m} = 0$ in the integrand, which is reminiscent to the so-called Popov approximation. But this will be shown to be highly inconsistent in a variational framework.

Furthermore, since the previous expressions can be generalized to any dimension D by simply making the replacement $\int \frac{d^3\mathbf{k}}{(2\pi)^3} \to \int \frac{d^D\mathbf{k}}{(2\pi)^D}$, one can see that they are both free from IR divergences. On the other hand, while $\tilde{n}$ is finite at high momenta, we can clearly see that $\tilde{m}$ is UV divergent for $D = 2$ and $D = 3$. It is however finite in the one-dimensional case.

Chapter 3

Dynamics of binary mixtures at ultra cold temperatures

3.1 Condensate mixtures

In recent years, the study of two-component quantum fluids has garnered increasing attention. The phase mixing and separation of the two components, determined by the relative strength of inter-species and intra-species interactions, have opened the door to a wide range of research topics, including two-mode entanglement [81], Dynamic phase transitions, the formation of dipolar molecules, and macroscopic quantum self-trapping. The phenomenon of phase separation was first observed in ^3He - ^4He mixtures and was later reported in various BEC systems [82]. The ability to control two-body interactions through Feshbach resonances makes these structures highly appealing for practical applications.

Binary mixtures as compared to single species BEC, possess several interesting properties that cannot be observed otherwise. Indeed, by tuning the intra- and inter-species interactions, one can arrive at original situations never explored before. For instance, one can analyse situations where an unstable condensate may be stabilized by the interactions with a stable one. Mixtures can be made of two species, or two isotopes of a single species, or even a two-component BEC, that is a single gas with atoms in diferent magnetic states.

3.2 Experimental and theoretical studies

Multi-component BECs have been extensively studied over the last few years . These studies have been motivated by experimental work performed by the JILA and MIT groups . Many interesting effects have been predicted theoretically and measured experimentally [83].

In June 1995, Carl Wieman and Eric Cornell's group at JILA conducted the first experimental production of Bose Einstein condensates in a diluted vapor of ^{87}Rb [8] . A sample of ^{87}Rb atoms was cooled in a magneto-optical trap before being put into a magnetic trap and further evaporating to achieve extremely low temperatures. After the trap was removed, the condensate was given time to expand before being photographed and exposed to laser light. Additionally, a BEC in sodium was first detected in Ketterle's group on September 29, 1995 [9]. Exploring the realm of quantum phenomena at macroscopic regimes is now possible because to the advancements made in this subject. The 2001 Nobel Prize in Physics was awarded in recognition of the discovery of BECs [10,11].

The growing cold-atom community has become interested in condensate mixes since

the initial realization of BECs. The first experimental realization of mixes of BECs of two hyperfine states of ^{87}Rb in a magnetic trap , $|2,-2\rangle$, $|1,-1\rangle$, was carried out in JILA in 1997 [12]. Numerous experiments have been conducted using various isotopes [84, 85], different elements [86–88], thermal mixtures of alkaline-earth with alkali metals [89], or different hyperfine states of the same atom [14, 90–93].Shenoy [94] published the first theoretical analysis of binary mixes of BECs shortly after, spurred by the first experimental realization of a mixture of condensate. Following Shenoy's publication, a wide range of theoretical studies using various methodologies emerged. For example, weak and strong phase separation (topological properties of ground and excited states, phase transitions) [18, 95–104], as well as fundamental quantum mechanics or collective excitations [105–107]. One important feature of these systems is that, depending on how strongly the species interact, they can behave in both miscible and immiscible ways. Since the first two-component BEC was realized experimentally, many static and dynamic features in harmonic trapping have been investigated analytically and numerically.

Miscible or immiscible two-component BEC systems can be distinguished by the spatial overlap or separation of the respective wave functions of each component. Their phase separation was observed in spinor BECs of Sodium in all hyperfine states of $F = 1$ [108]. The advances in the experimental investigations with multi component BECs have activated a large amount of theoretical descriptions applied to condensed mixtures having spatially segregated phases, by studying their properties related to static and dynamical stability.

3.3 Dynamical equations for binary mixtures

.

We consider a two component Bose-Einstein condensate with contact interactions described by the general two-body second quantized hamiltonian

$$\begin{aligned} H = &\sum_{i=1}^{2} \int_{\mathbf{r}} \hat{\Psi}_i^+(\mathbf{r}) h_i(\mathbf{r}) \hat{\Psi}_i(\mathbf{r}) + \frac{1}{2} \sum_{i=1}^{2} g_{ii} \int_{\mathbf{r}} \hat{\Psi}_i^+(\mathbf{r}) \hat{\Psi}_i^+(\mathbf{r}) \hat{\Psi}_i(\mathbf{r}) \hat{\Psi}_i(\mathbf{r}) \\ &+ g_{12} \int_{\mathbf{r}} \hat{\Psi}_1^+(\mathbf{r}) \hat{\Psi}_2^+(\mathbf{r}) \hat{\Psi}_2(\mathbf{r}) \hat{\Psi}_1(\mathbf{r}), \end{aligned} \tag{3.1}$$

where $\hat{\Psi}_1^+(\mathbf{r})$ and $\hat{\Psi}_2^+(\mathbf{r})$ are the creation bose field operators corresponding to the two components and satisfying the usual commutation rules $[\hat{\Psi}_i(\mathbf{r}), \hat{\Psi}_j^+(\mathbf{r}')] = \delta_{ij}\delta(\mathbf{r} - \mathbf{r}')$, $[\hat{\Psi}_i(\mathbf{r}), \hat{\Psi}_j(\mathbf{r}')] = [\hat{\Psi}_i^+(\mathbf{r}), \hat{\Psi}_j^+(\mathbf{r}')] = 0$. g_{ii} and g_{12} are respectively the intra and interspecies

coupling constants and $h_i(\mathbf{r})$ the single particle hamiltonians

$$h_i(\mathbf{r}) = -\frac{\hbar^2}{2m_i}\Delta_{\mathbf{r}} + V_i^{\text{trap}}(\mathbf{r}), \tag{3.2}$$

where V_i^{trap} are the trapping fields and m_i are the masses of the particles

In order to generalize our previous formalism to binary mixtures, we choose a gaussian density operator for eachs species. Hence, the total density operator is also gaussian. Using the notations of the appendix and, again Wick's theorem, this leads to the following expression for the energy

$$\begin{aligned}
E = &\sum_i \int_{\mathbf{r}} \left\{ h_i(\mathbf{r})\tilde{n}_{ii}(\mathbf{r},\mathbf{r}')|_{\mathbf{r}'=\mathbf{r}} + \Phi_i^*(\mathbf{r})h_i(\mathbf{r})\Phi_i(\mathbf{r}) \right\} \\
&+ \frac{1}{2}\sum_i g_{ii} \int_{\mathbf{r}} \left\{ n_i(\mathbf{r})n_i(\mathbf{r}) + |\tilde{n}_{ii}(\mathbf{r})|^2 + |\tilde{m}_{ii}(\mathbf{r})|^2 \right\} \\
&+ \frac{1}{2}\sum_i g_{ii} \int_{\mathbf{r}} \left\{ \left(\tilde{n}_{ii}(\mathbf{r},\mathbf{r})\Phi_i^*(\mathbf{r}) + \tilde{n}_{ii}^*(\mathbf{r},\mathbf{r})\Phi_i(\mathbf{r})\right)\Phi_i(\mathbf{r}) + c.c \right\} \\
&+ g_{12} \int_{\mathbf{r}} n_1(\mathbf{r})n_2(\mathbf{r}) \\
&+ g_{12} \int_{\mathbf{r}} \left(|\tilde{n}_{12}(\mathbf{r},\mathbf{r})|^2 + |\tilde{m}_{12}(\mathbf{r},\mathbf{r})|^2 \right) \\
&+ g_{12} \int_{\mathbf{r}} \left(\tilde{n}_{12}(\mathbf{r},\mathbf{r})\Phi_1^*(\mathbf{r}) + \tilde{m}_{12}^*(\mathbf{r},\mathbf{r})\Phi_1(\mathbf{r})\right)\Phi_2(\mathbf{r}) + c.c
\end{aligned} \tag{3.3}$$

where $c.c$ stands for complex conjugate. In the previous expression, the quantities

$$\begin{aligned}
\Phi_i(\mathbf{r},t) &= \langle\hat{\Psi}_i\rangle(\mathbf{r},t), \\
\tilde{n}_{ij}(\mathbf{r},\mathbf{r}',t) &= \tilde{n}_{ji}^*(\mathbf{r}',\mathbf{r},t) = \langle\bar{\hat{\Psi}}_j^+(\mathbf{r}',t)\bar{\hat{\Psi}}_i(\mathbf{r},t)\rangle, \\
\tilde{m}_{ij}(\mathbf{r},\mathbf{r}',t) &= \tilde{m}_{ji}(\mathbf{r}',\mathbf{r},t) = \langle\bar{\hat{\Psi}}_j(\mathbf{r}',t)\bar{\hat{\Psi}}_i(\mathbf{r},t)\rangle,
\end{aligned} \tag{3.4}$$

are generalizations of (2.15) and are respectively the order parameters and the one-body correlation functions for the two species. Obviously, $n_i(\mathbf{r}) = n_{c_i}(\mathbf{r}) + \tilde{n}_{ii}(\mathbf{r},\mathbf{r})$ is the total density of the species "i" and $n_{c_i}(\mathbf{r}) = |\Phi_i(\mathbf{r})|^2$ its condensate density. Notice, in particular, the appearance of the interspecies correlations $\tilde{n}_{12}$ and $\tilde{m}_{12}$ which contribute to the energy on the same footing as the various correlations in the system, but are associated with the interspecies interactions. Hence, interspecies interactions are a necessary condition for interspecies correlations [109, 110]. Their appearance is essentially due to the correlated gaussian discussed above. Indeed, imagine that our starting point was a

product of two gaussian operators, one for each species. Then, the subsequent dynamics would no longer include any interspecies correlations, even if the interspecies coupling is present. The two last lines in (3.3) would have been absent.

Using the Balian–Vénéroni variational principle [32–36], one obtains a set of eight dynamical equations ($i, j = 1, 2$) which couple the various densities (3.4):
The first one, a generalized Gross-Pitaevskii equation reads:

$$i\hbar\dot{\Phi}_i(\mathbf{r}) = h_i(\mathbf{r})\Phi_i(\mathbf{r}) + \sum_j \int_{\mathbf{r}'} V_{ij}(\mathbf{r},\mathbf{r}') \left[n_j(\mathbf{r}')\Phi_i(\mathbf{r}) + \tilde{n}_{ij}(\mathbf{r},\mathbf{r}')\Phi_j(\mathbf{r}') + \tilde{m}_{ij}(\mathbf{r},\mathbf{r}')\Phi_j^*(\mathbf{r}') \right], \tag{3.5}$$

where one already notices a new set of terms coupling the two species and depending on both the diagonal and the non diagonal correlations $\tilde{n}_{i\neq j}$ and $\tilde{m}_{i\neq j}$. The dynamics of the correlations is now given by:

$$\begin{aligned} i\hbar\dot{\tilde{n}}_{ii}(\mathbf{r},\mathbf{r}') = & \left[h_i(\mathbf{r}) + \int_{\mathbf{r}''} \Big(V_{ii}(\mathbf{r},\mathbf{r}'')n_i(\mathbf{r}'') + V_{ij}(\mathbf{r},\mathbf{r}'')n_j(\mathbf{r}'') \Big) \right] \tilde{n}_{ii}(\mathbf{r},\mathbf{r}') \\ & + \int_{\mathbf{r}''} V_{ii}(\mathbf{r},\mathbf{r}'') \left[\eta_{ii}(\mathbf{r},\mathbf{r}'')\tilde{n}_{ii}(\mathbf{r}'',\mathbf{r}') + \kappa_{ii}(\mathbf{r},\mathbf{r}'')\tilde{m}_{ii}^*(\mathbf{r}'',\mathbf{r}') \right] \\ & + \int_{\mathbf{r}''} V_{ij}(\mathbf{r},\mathbf{r}'') \left[\eta_{ij}(\mathbf{r},\mathbf{r}'')\tilde{n}_{ij}^*(\mathbf{r}',\mathbf{r}'') + \kappa_{ij}(\mathbf{r},\mathbf{r}'')\tilde{m}_{ij}^*(\mathbf{r}',\mathbf{r}'') \right] \\ & - (\mathbf{r} \leftrightarrow \mathbf{r}')^*, \end{aligned} \tag{3.6}$$

$$\begin{aligned} i\hbar\dot{\tilde{m}}_{ii}(\mathbf{r},\mathbf{r}') = & \left[h_i(\mathbf{r}) + \int_{\mathbf{r}''} \Big(V_{ii}(\mathbf{r},\mathbf{r}'')n_1(\mathbf{r}'') + V_{ij}(\mathbf{r},\mathbf{r}'')n_j(\mathbf{r}'') \Big) \right] \tilde{m}_{ii}(\mathbf{r},\mathbf{r}') \\ & + \int_{\mathbf{r}''} V_{ii}(\mathbf{r},\mathbf{r}'') \left[\eta_{ii}(\mathbf{r},\mathbf{r}'')\tilde{m}_{ii}(\mathbf{r}'',\mathbf{r}') + \kappa_{ii}(\mathbf{r},\mathbf{r}'')\tilde{n}_{ii}^*(\mathbf{r}'',\mathbf{r}') \right] \\ & + \int_{\mathbf{r}''} V_{ij}(\mathbf{r},\mathbf{r}'') \left[\eta_{ij}(\mathbf{r},\mathbf{r}'')\tilde{m}_{ij}^*(\mathbf{r}',\mathbf{r}'') + \kappa_{ij}(\mathbf{r},\mathbf{r}'')\tilde{n}_{ij}(\mathbf{r}',\mathbf{r}'') \right] \\ & + (\mathbf{r} \leftrightarrow \mathbf{r}') \\ & + V_{ii}(\mathbf{r},\mathbf{r}')\kappa_{ii}(\mathbf{r},\mathbf{r}'), \end{aligned} \tag{3.7}$$

$$\begin{aligned} i\hbar\dot{\tilde{n}}_{12}(\mathbf{r},\mathbf{r}') = & \left[h_1(\mathbf{r}) + \int_{\mathbf{r}''} \Big(V_{11}(\mathbf{r},\mathbf{r}'')n_1(\mathbf{r}'') + V_{12}(\mathbf{r},\mathbf{r}'')n_2(\mathbf{r}'') \Big) \right] \tilde{n}_{12}(\mathbf{r},\mathbf{r}') \\ & + \int_{\mathbf{r}''} V_{11}(\mathbf{r},\mathbf{r}'') \left[\eta_{11}(\mathbf{r},\mathbf{r}'')\tilde{n}_{12}(\mathbf{r}'',\mathbf{r}') + \kappa_{11}(\mathbf{r},\mathbf{r}'')\tilde{m}_{12}^*(\mathbf{r}'',\mathbf{r}') \right] \\ & + \int_{\mathbf{r}''} V_{12}(\mathbf{r},\mathbf{r}'') \left[\eta_{12}(\mathbf{r},\mathbf{r}'')\tilde{n}_{22}^*(\mathbf{r}',\mathbf{r}'') + \kappa_{12}(\mathbf{r},\mathbf{r}'')\tilde{m}_{22}^*(\mathbf{r}',\mathbf{r}'') \right] \\ & - (1 \leftrightarrow 2, \mathbf{r} \leftrightarrow \mathbf{r}')^*, \end{aligned} \tag{3.8}$$

$$
\begin{aligned}
i\hbar\dot{\tilde{m}}_{12}(\mathbf{r},\mathbf{r}') = &\left[h_1(\mathbf{r}) + \int_{\mathbf{r}''}\Big(V_{11}(\mathbf{r},\mathbf{r}'')n_1(\mathbf{r}'') + V_{12}(\mathbf{r},\mathbf{r}'')n_2(\mathbf{r}'')\Big)\right]\tilde{m}_{12}(\mathbf{r},\mathbf{r}') \\
&+ \int_{\mathbf{r}''} V_{11}(\mathbf{r},\mathbf{r}'')\left[\eta_{11}(\mathbf{r},\mathbf{r}'')\tilde{m}_{12}(\mathbf{r}'',\mathbf{r}') + \kappa_{11}(\mathbf{r},\mathbf{r}'')\tilde{n}^*_{12}(\mathbf{r}'',\mathbf{r}')\right] \\
&+ \int_{\mathbf{r}''} V_{12}(\mathbf{r},\mathbf{r}'')\left[\eta_{12}(\mathbf{r},\mathbf{r}'')\tilde{m}_{22}(\mathbf{r}'',\mathbf{r}') + \kappa_{12}(\mathbf{r},\mathbf{r}'')\tilde{n}^*_{22}(\mathbf{r}'',\mathbf{r}')\right] \\
&+ (1 \leftrightarrow 2, \mathbf{r} \leftrightarrow \mathbf{r}') \\
&+ V_{12}(\mathbf{r},\mathbf{r}')\kappa_{12}(\mathbf{r},\mathbf{r}'),
\end{aligned}
\tag{3.9}
$$

where $\eta_{ij}(\mathbf{r},\mathbf{r}') = \langle\hat{\Psi}^+_j(\mathbf{r}')\hat{\Psi}_i(\mathbf{r})\rangle = \tilde{n}_{ij}(\mathbf{r},\mathbf{r}') + \hat{\Psi}_i(\mathbf{r})\hat{\Psi}^*_j(\mathbf{r}')$
and $\kappa_{ij}(\mathbf{r},\mathbf{r}') = \langle\hat{\Psi}_j(\mathbf{r}')\hat{\Psi}_i(\mathbf{r})\rangle = \tilde{m}_{ij}(\mathbf{r},\mathbf{r}') + \Phi_i(\mathbf{r})\Phi_j(\mathbf{r}')$. We have evidently $\eta_{ij}(\mathbf{r},\mathbf{r}') = \eta^*_{ji}(\mathbf{r}',\mathbf{r})$ and $\kappa_{ij}(\mathbf{r},\mathbf{r}') = \kappa_{ji}(\mathbf{r}',\mathbf{r})$.

In the case of contact potentials $V_{ij}(\mathbf{r},\mathbf{r}') = g_{ij}\delta(\mathbf{r}-\mathbf{r}')$, the equations (3.7-3.9) read

$$
\begin{aligned}
i\hbar\dot{\Phi}_i(\mathbf{r}) &= \mathcal{H}_i(\mathbf{r})\Phi_i(\mathbf{r}) + \sum_k g_{ik}\left[\tilde{n}_{ik}(\mathbf{r})\Phi_k(\mathbf{r}) + \tilde{m}_{ik}(\mathbf{r})\Phi^*_k(\mathbf{r})\right], \\
i\hbar\dot{\tilde{n}}_{ij}(\mathbf{r}) &= \mathcal{H}_i(\mathbf{r})\tilde{n}_{ij}(\mathbf{r}) + \sum_k g_{ik}\left[\eta_{ik}(\mathbf{r})\tilde{n}_{kj}(\mathbf{r}) + \kappa_{ik}(\mathbf{r})\tilde{m}^*_{kj}(\mathbf{r})\right] \\
&\quad - (i \leftrightarrow j)^*, \\
i\hbar\dot{\tilde{m}}_{ij}(\mathbf{r}) &= \mathcal{H}_i(\mathbf{r})\tilde{m}_{ij}(\mathbf{r}) + \sum_k g_{ik}\left[\eta_{ik}(\mathbf{r})\tilde{m}_{kj}(\mathbf{r}) + \kappa_{ik}(\mathbf{r})\tilde{n}^*_{kj}(\mathbf{r})\right] \\
&\quad + (i \leftrightarrow j) \\
&\quad + g_{ij}\kappa_{ij}(\mathbf{r}),
\end{aligned}
\tag{3.10}
$$

where $\mathcal{H}_i(\mathbf{r}) = h_i(\mathbf{r}) + \sum_j g_{ij}n_j(\mathbf{r})$ is the self-consistent one-body hamiltonian.

The first equation consists of two coupled generalized Gross-Pitaevskii equations, where the standard coupling between the two species (density coupling) is already visible on the first term. The second term (with $k = i$) depicts the coupling of one species to its noncondensate and anomalous correlations. In its local form, it is a well known generalization of the Gross-Pitaevskii equation [63, 66, 111–113] at finite temperature. At zero temperature, it appears as a non perturbative coupling between the condensate and the quantum depletion [36] (which one may also call "non perturbative" LHY correction).

Most importantly, the new set of terms (with $k \neq i$), couple the two species and depend directly on the interspecies correlations ($\tilde{n}_{ik}$, $\tilde{m}_{ik}$). Regarding the way they appear, there is no a priori argument to omit them in the presence of mutual coupling. To the best of our knowledge, this kind of term has never appeared in the literature.

The second and third equations depict not only the dynamics of the intraspecies (or diagonal) correlations (for $i = j$) but also that of the interspecies (or off diagonal) correlations (for $i \neq j$). This is the real novelty of our Ansatz. It is clearly visible that the coupling with interspecies correlations is merely due to the interspecies interactions. Indeed, setting $g_{12} = 0$ yields not only a decoupling between the two species but also the vanishing of the interspecies correlations if they are not present in the initial state. In this case, we recover nicely the TDHFB equations already obtained in [35,36]. Moreover, in the presence of g_{12}, $\tilde{n}_{12}$ and $\tilde{m}_{12}$ will evolve toward non trivial values (determined essentially by the noncondensate and anomalous correlations) even if they are initially set to zero.

3.4 Hydrodynamic picture of a binary mixture

In order to get a different picture for the dynamics of the mixture, let us neglect for a while the interspecies fluctuations and focus only on the intraspecies ones.

The dynamical equations (3.10) become

$$\begin{aligned}
i\hbar\dot{\Phi}_i(\mathbf{r}) &= \left[h_i(\mathbf{r}) + g_{ii}\left(n_i(\mathbf{r}) + \tilde{n}_i(\mathbf{r})\right) + g_{12}n_{3-i}(\mathbf{r})\right]\Phi_i(\mathbf{r}) + g_{ii}\tilde{m}_i(\mathbf{r})\Phi_i^*(\mathbf{r}) \\
i\hbar\dot{\tilde{n}}_i\left(\mathbf{r},\mathbf{r}'\right) &= \left[h_i(\mathbf{r}) - h_i\left(\mathbf{r}'\right) + 2g_{ii}\left(n_i(\mathbf{r}) - n_i(\mathbf{r})\right) + 2g_{12}\left(n_{3-i}(\mathbf{r}) - n_{3-i}\left(\mathbf{r}'\right)\right)\right]\tilde{n}_i\left(\mathbf{r},\mathbf{r}'\right) \\
&\quad + g_{ii}\left[\kappa_1^*(\mathbf{r})\tilde{m}_i\left(\mathbf{r},\mathbf{r}'\right) - \kappa_i\left(\mathbf{r}'\right)\tilde{m}_i^*\left(\mathbf{r},\mathbf{r}'\right)\right] \\
i\hbar\dot{\tilde{m}}_i\left(\mathbf{r},\mathbf{r}'\right) &= \left[h_i(\mathbf{r}) + h_i\left(\mathbf{r}'\right) + 2g_{ii}\left(n_i(\mathbf{r}) + n_i\left(\mathbf{r}'\right)\right) + 2g_{12}\left(n_{3-i}(\mathbf{r}) + n_{3-i}\left(\mathbf{r}'\right)\right)\right]\tilde{m}_i\left(\mathbf{r},\mathbf{r}'\right) \\
&\quad + g_{ii}\left[\kappa_i(\mathbf{r})\left(\tilde{n}_i\left(\mathbf{r},\mathbf{r}'\right) + \frac{1}{2}\delta\left(\mathbf{r}-\mathbf{r}'\right)\right) + \kappa_i\left(\mathbf{r}'\right)\left(\tilde{n}_i^*\left(\mathbf{r},\mathbf{r}'\right) + \frac{1}{2}\delta\left(\mathbf{r}-\mathbf{r}'\right)\right)\right]
\end{aligned} \tag{3.11}$$

The equations for the local densities are readily obtained to get

$$\begin{aligned}
i\hbar\dot{\tilde{n}}_i(\mathbf{r}) &= \lim_{\mathbf{r}'\to\mathbf{r}}\left(\left[h_i(\mathbf{r}) - h_i(\mathbf{r}')\right]\tilde{n}_i(\mathbf{r},\mathbf{r}')\right) + g_{ii}\left[\kappa_i^*(\mathbf{r})\tilde{m}_i(\mathbf{r}) - \kappa_i(\mathbf{r})\tilde{m}_i^*(\mathbf{r})\right], \\
i\hbar\dot{\tilde{m}}_i(\mathbf{r}) &= 2\left[h_i(\mathbf{r}) + 2g_{ii}n_i(\mathbf{r}) + 2g_{ij}n_j(\mathbf{r})\right]\tilde{m}_i(\mathbf{r}) + g_{ii}\left[2\tilde{n}_i(\mathbf{r}) + \delta_\epsilon(\mathbf{0})\right]\kappa_i(\mathbf{r}),
\end{aligned} \tag{3.12}$$

Where $\delta_\epsilon(\mathbf{0})$ is a regularized delta function : $\delta(\mathbf{r}) = \lim_{\epsilon\to 0}\delta_\epsilon(\mathbf{r})$.

Let us Wigner transform both sides of Eq (3.12)

$$\begin{aligned} i\hbar\dot{\tilde{n}}_{W_i}(\mathbf{r},k) =& \frac{i\hbar^2}{m_i}\mathbf{k}.\nabla_{\mathbf{r}}\tilde{n}_{W_i}(\mathbf{r},k) + g_{ii}\left[\kappa_i(\mathbf{r})\tilde{m}^*_{W_i}(\mathbf{r},-k) - \kappa^*_i(\mathbf{r})\tilde{m}_{W_i}(\mathbf{r},k)\right], \\ i\hbar\dot{\tilde{m}}_{W_i}(\mathbf{r},k) =& 2\left[-\frac{\hbar^2}{8m_i}\Delta_{\mathbf{r}} + \frac{\hbar^2\mathbf{k}^2}{2m_i} + U(\mathbf{r}) + 2g_{ii}n_i(\mathbf{r}) + 2g_{12}n_{3-i}(\mathbf{r})\right]\tilde{m}_{W_i}(\mathbf{r},k) \\ &+ g_{ii}(1+\tilde{n}_{W_i}(\mathbf{r},k) + \tilde{n}_{W_i}(\mathbf{r},-k))\kappa_i(\mathbf{r}) \end{aligned} \tag{3.13}$$

It is also an easy task to show now that the total density obeys the continuity equation

$$\frac{\partial n_i(\mathbf{r})}{\partial t} + \nabla.\mathbf{J_i}(\mathbf{r}) = 0, \tag{3.14}$$

where the total current density is given by

$$\mathbf{J_i} = \frac{-i\hbar}{2m_i}\left[\Phi^*_i\nabla\Phi_i - \Phi_i\nabla\Phi^*_i\right] + \int \frac{d^3k}{(2\pi)^3}\frac{2\hbar k}{m_i}\,\tilde{n}_{iW}(\mathbf{r},k), \tag{3.15}$$

and, as expected has two contributions coming from the condensate $\mathbf{J_{c}}_i$ and the noncondensate $\mathbf{J_{nc}}_i$ respectively.

$$\begin{cases} \mathbf{J_{c}}_i = \dfrac{-i\hbar}{2m_i}\left[\Phi^*_i\nabla\Phi_i - \Phi_i\nabla\Phi^*_i\right] \\ \mathbf{J_{nc}}_i = \displaystyle\int \frac{d^3k}{(2\pi)^3}\frac{2\hbar k}{m_i}\,\tilde{n}_{iW}(\mathbf{r},k), \end{cases} \tag{3.16}$$

From a hydrodynamical point of view, upon introducing the condensate or superfluid velocity $\mathbf{v_{c}}_i$ and the non condensate velocity $\mathbf{v_{nc}}_i$, one comes up with a quite natural expression for the current density at finite temperature. The currents (3.15) can also be written

$$\mathbf{J}_i = n_{ci}\mathbf{v_{c}}_i + \tilde{n}_i\mathbf{v_{nc}}_i. \tag{3.17}$$

Where $\mathbf{v_{c}}_i = \hbar/m_i\,\nabla\theta_i$ is the condensate (or superfluid) density and θ_i is the phase of the condensate field Φ_i. Moreover, $\mathbf{v_{nc}}_i$ is the non -condensate velocity defined by $(\hbar k/m_i)$. It is also interesting to observe that these veocities are irrotational. Moreover, $\mathbf{v_{nc}}_i$ is a superposition of free particle velocities which are locally irrotational and conservatives. This witnesses a profound difference between the condensate and the non condensate components of the gas.

One may also notice that the conservation of the Heisenberg parameters (2.24) can be

better visualized here. Indeed, the Wigner transform

$$I_{Wi}(\mathbf{r},k) = \left(1+2\tilde{n}_{Wi}(\mathbf{r},k)\right)^2 - 4\left|\tilde{m}_{Wi}(\mathbf{r},k)\right|^2, \tag{3.18}$$

satisfies the continuity equation

$$\frac{\partial I_{Wi}}{\partial t} + \nabla.\mathbf{J}_{Ii} = 0, \tag{3.19}$$

where the current density

$$\mathbf{J}_{Ii} = \frac{\hbar k}{m_i} I_{Wi} + \frac{\hbar}{m_i}\left[4k|\tilde{m}_{Wi}|^2 + \frac{\tilde{m}^*_{Wi}\nabla\tilde{m}_{Wi} - \tilde{m}_{Wi}\nabla\tilde{m}^*_{Wi}}{i}\right], \tag{3.20}$$

is also made of two pieces which represent respectively the normal current $\mathbf{J}_{\mathbf{n}i} = (1 + 2\tilde{n}_{Wi})^2\,\hbar k/m_i$ and the anomalous current $\mathbf{J}_{\mathbf{an}i} = |\tilde{m}_{Wi}|^2\mathbf{v}_{\mathbf{an}i}$, where the anomalous velocity is irrotational and thus proportional to the gradient of the anomalous density's phase. In this form, this conservation equation reveals the importance of the anomalous density which, if neglected, would inevitably lead to inconsistencies.

3.5 Bogoliubov approximation

One may notice that the quasi-homogeneous case allows for a kind of separability of the spatial arguments. Hence, decomposing the shifted operators $\tilde{\hat{\Psi}}$ according to Bogoliubov's prescription and using (3.4), we may write

$$\begin{aligned}
\tilde{n}_{ij}(\mathbf{r},\mathbf{r}') &= \sum_k \left[f_k U_k^{(i)}(\mathbf{r})U_k^{(j)*}(\mathbf{r}') + (1+f_k)V_k^{(i)*}(\mathbf{r})V_k^{(j)}(\mathbf{r}')\right] \\
\tilde{m}_{ij}(\mathbf{r},\mathbf{r}') &= -\sum_k \left[f_k V_k^{(i)*}(\mathbf{r})U_k^{(j)}(\mathbf{r}') + (1+f_k)U_k^{(i)}(\mathbf{r})V_k^{(j)*}(\mathbf{r}')\right]
\end{aligned} \tag{3.21}$$

where $U_k^{(i)}$ and $V_k^{(i)}$ are the Bogoliubov quasi-particles amplitudes satisfying

$$\begin{aligned}
\sum_k \left(U_k^{(i)}(\mathbf{r})U_k^{(j)*}(\mathbf{r}') - V_k^{(i)*}(\mathbf{r})V_k^{(j)}(\mathbf{r}')\right) &= \delta_{ij}\delta(\mathbf{r}-\mathbf{r}') \\
\sum_k \left(U_k^{(i)}(\mathbf{r})V_k^{(j)*}(\mathbf{r}') - V_k^{(i)*}(\mathbf{r})U_k^{(j)}(\mathbf{r}')\right) &= 0
\end{aligned} \tag{3.22}$$

and $f_k = (e^{\beta E_k} - 1)^{-1}$ is the Bose-Einstein distribution function, with $\beta = 1/k_B T$ is the Boltzmann factor. E_k is the excitation energy for the mode k. Now, injecting (3.21) in

(3.10) and using the properties (3.22), we easily get

$$\begin{aligned} i\hbar\dot{U}_k^{(i)}(\mathbf{r}) = &\quad \mathcal{H}_i(\mathbf{r})U_k^{(i)}(\mathbf{r}) + \sum_j g_{ij}\left(\eta_{ij}(\mathbf{r})U_k^{(j)}(\mathbf{r}) - \kappa_{ij}(\mathbf{r})V_k^{(j)}(\mathbf{r})\right) \\ i\hbar\dot{V}_k^{(i)}(\mathbf{r}) = &-\mathcal{H}_i(\mathbf{r})V_k^{(i)}(\mathbf{r}) - \sum_j g_{ij}\left(\eta_{ij}^*(\mathbf{r})V_k^{(j)}(\mathbf{r}) - \kappa_{ij}^*(\mathbf{r})U_k^{(j)}(\mathbf{r})\right) \end{aligned} \tag{3.23}$$

From their structure, they can be recognized as the generalized time dependent Hartree-Fock-Bogoliubov-De Gennes equations (G)HFBdG [63, 66, 67] . It is worth recalling that, since our derivation is variational, no assumption of small fluctuations is required. Thus, the (G)HFBdG equations do not come from the linearization of the Gross-Pitaevskii equations. Moreover, as their parent equations (3.5-3.9), they contain both the intra and interspecies correlations.

3.6 The static equations

In static thermal equilibrium (or local thermodynamic equilibrium), the stationary solutions are obtained by setting

$$\begin{cases} \Phi_i(\mathbf{r}, t = \exp\left(-i\mu_i t/\hbar\right)\Phi_i(\mathbf{r}) \\ \tilde{n}_{ij}(\mathbf{r}, \mathbf{r}', t) = \exp\left(-i\mu_{ij}^{(1)} t/\hbar\right)\tilde{n}_{ij}(\mathbf{r}, \mathbf{r}') \\ \tilde{m}_{ij}(\mathbf{r}, \mathbf{r}', t) = \exp\left(-i\mu_{ij}^{(2)} t/\hbar\right)\tilde{m}_{ij}(\mathbf{r}, \mathbf{r}'). \end{cases} \tag{3.24}$$

Replacing in (3.23), we see that $\mu_{ij}^{(1)} = \mu_i - \mu_j$ and $\mu_{ij}^{(2)} = \mu_i + \mu_j$ (phase locking conditions [114–116]. The "chemical potentials" associated with $\tilde{n}$ and $\tilde{m}$ are not equal and indeed have no reason to be equal (as assumed, for instance, in [117]) nor to each other, neither to the individual species chemical potentials. Most importantly, the noticeable result $\mu_{ii}^{(1)} = 0$ shows that the stationary solutions are compatible with the static thermal cloud approximation [63, 118, 119].

For a completely symmetric (and balanced) mixture ($g_{11} = g_{22} = g$, $m_1 = m_2 = m$, $n_1 = n_2 = n$), the order parameters, the non condensate and the anomalous densities as well as the chemical potentials of the two species are equal (we therefore suppress the indices). This leads us to the equation of state (EOS) $\mu = g(n+\tilde{n}+\tilde{m}) + g_{12}(n+\tilde{n}_{12}+\tilde{m}_{12})$

and to the generalized HFB equations

$$\begin{aligned}
\hbar\omega_k U_k^{(1)} &= \quad \epsilon_k U_k^{(1)} - g\kappa V_k^{(1)} + g_{12}\left(\eta_{12} U_k^{(2)} - \kappa_{12} V_k^{(2)}\right) \\
\hbar\omega_k V_k^{(1)} &= -\epsilon_k V_k^{(1)} + g\kappa U_k^{(1)} - g_{12}\left(\eta_{12} V_k^{(2)} - \kappa_{12} U_k^{(2)}\right) \\
\hbar\omega_k U_k^{(2)} &= \quad \epsilon_k U_k^{(2)} - g\kappa V_k^{(2)} + g_{12}\left(\eta_{12} U_k^{(1)} - \kappa_{12} V_k^{(1)}\right) \\
\hbar\omega_k V_k^{(2)} &= -\epsilon_k V_k^{(2)} + g\kappa U_k^{(2)} - g_{12}\left(\eta_{12} V_k^{(1)} - \kappa_{12} U_k^{(1)}\right)
\end{aligned} \tag{3.25}$$

where $\epsilon_k = \hbar^2 k^2/2m + (2g + g_{12})n - \mu$ and $\kappa = n_c + \tilde{m}$. It is interesting to notice that the coupling between the two species disappears from the local non-condensate densities but does not disappear from the local anomalous densities. We will solve these equations in the next chapter in the droplet regime.

3.7 Numerical illustrations on 1D homogeneous bose mixtures : zero temperature case

To get a better insight into the dynamics of the mixture , we will numerically solve the equations (3.10) in the case of a homogeneous 1D or quasi -1D mixture. In this context, the quantities n_{ii}, n_{ci}, $\tilde{n}_{ii}$ and $\tilde{m}_{ii}$ are space independent.

Moreover, we will consider the non -correlated case where $\tilde{n}_{12} = \tilde{m}_{12} = 0$. Upon Fourier transforming, we obtain the self-consisten solutions:

$$\begin{aligned} \tilde{m}_{ii}(k) &= -\frac{1}{2}\frac{g_{ii}\left(n_{ci}+\tilde{m}_{ii}\right)}{\sqrt{\left(\epsilon_{ki}+2g_{ii}n_{ci}\right)\left(\epsilon_{ki}-2g_{ii}\tilde{m}_{ii}\right)}} \\ \tilde{n}_{ii}(k) &= \frac{1}{2}\left\{-1+\frac{\epsilon_{ki}+g_{ii}\left(n_{ci}-\tilde{m}_{ii}\right)}{2\sqrt{\left(\epsilon_{ki}+2g_{ii}n_{ci}\right)\left(\epsilon_{ki}-2g_{ii}\tilde{m}_{ii}\right)}}\right\} \end{aligned} \tag{3.26}$$

where $\epsilon_{ki} = \frac{\hbar^2 k^2}{2m_i} + g_{ij}n_j$.

Since the system is uncorrelated, we will from simplicity , use a single index "i" for each species. Notice that, even in this simple case, the various densities are still coupled. The numerical resolution proceeds as follows.

One first begins by an initial guess for $\tilde{m}_i$, $\tilde{n}_i$ which are generally set to 0. Since $n_i = n_{ci} + \tilde{n}_i$ and n_i is given, this sets up n_{ci} . Then, compute (3.26) and the inverse Fourier transforms $\tilde{m}_i = \int \tilde{m}_i(k)\frac{dk}{2\pi}, \tilde{n}_i = \int \tilde{n}_i(k)\frac{dk}{2\pi}$

These results are compared to the initial guess and the process is iterated until convergence. The illustrations is performed on a known mixture, namely the Potassium - Rubidium gas.

The atoms of ^{41}K are labeled by 1, with the intraspecies scattering length $a_1 = 65a_0$ (a_0 the Bohr radius), the trap frequency $\omega_1 = 0.83$ Hz and the total density $n_1 = 3.58 \times 10^6 m^{-1}$. For ^{87}Rb (2), $a_2 = 100.4a_0$, $\omega_2 = 0.6$ Hz and the total density $n_2 = 5 \times 10^6 m^{-1}$. We use the equilibrium ratio $n_1/n_2 = \sqrt{g_{22}/g_{11}}$ [120].

In figure (3.1-3.6), We plot the non-condensate $\tilde{n}_i(k)$ and the absolute value of anomalous densities $|\tilde{m}_i(k)|$ for the two species (left panel ^{41}K , right panel ^{87}Rb) as function of k (units of a_0^{-1}) in different values of the interspaces scattering length a_{12} : $a_{12} = 0.1a_1$, $a_{12} = 3a_1$, $a_{12} = 4a_1$, $a_{12} = 5a_1$, $a_{12} = 6a_1$ and $a_{12} = 15a_1$.

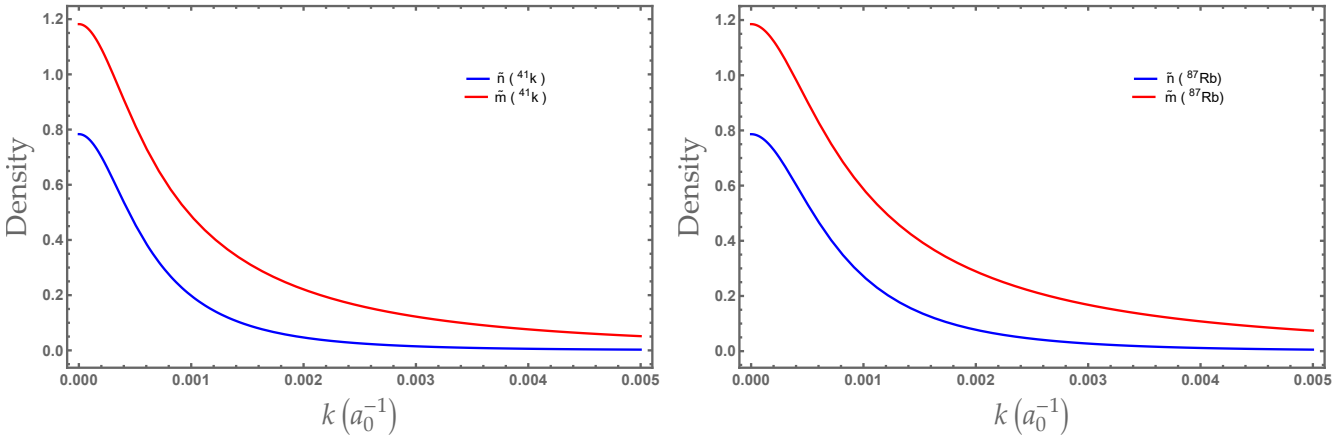

Figure 3.1: Anomalous density$|\tilde{m}_i(k)|$ (red) and the non-condensate density $\tilde{n}_i(k)$ (blue) for the two species $^{41}K -^{87} Rb$ as function of k (units of a_0^{-1}) with $a_{12} = 0.1a_1$.

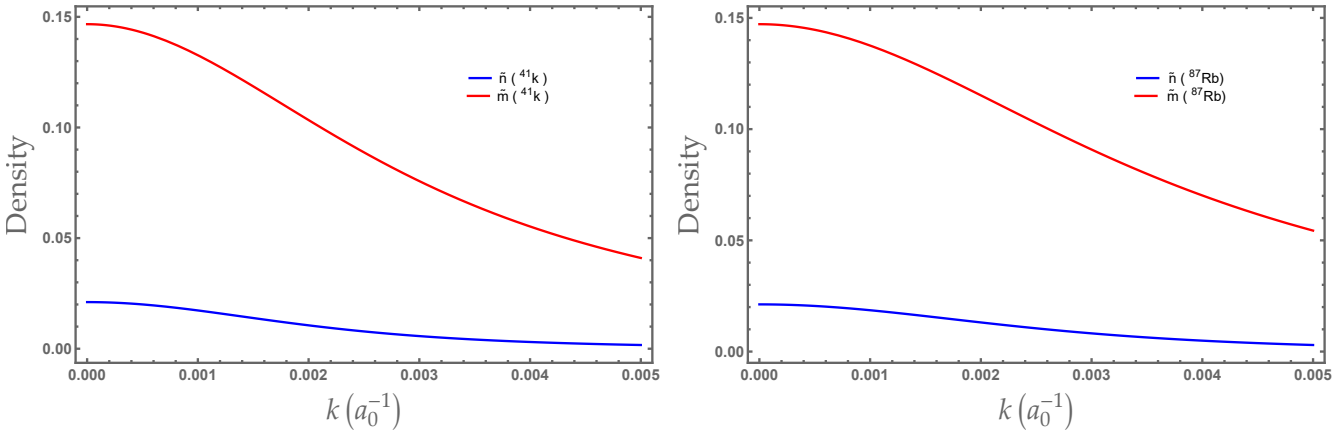

Figure 3.2: Anomalous density$|\tilde{m}_i(k)|$ (red) and the non-condensate density $\tilde{n}_i(k)$ (blue) for the two species $^{41}K -^{87} Rb$ as function of k (units of a_0^{-1}) with $a_{12} = 3a_1$.

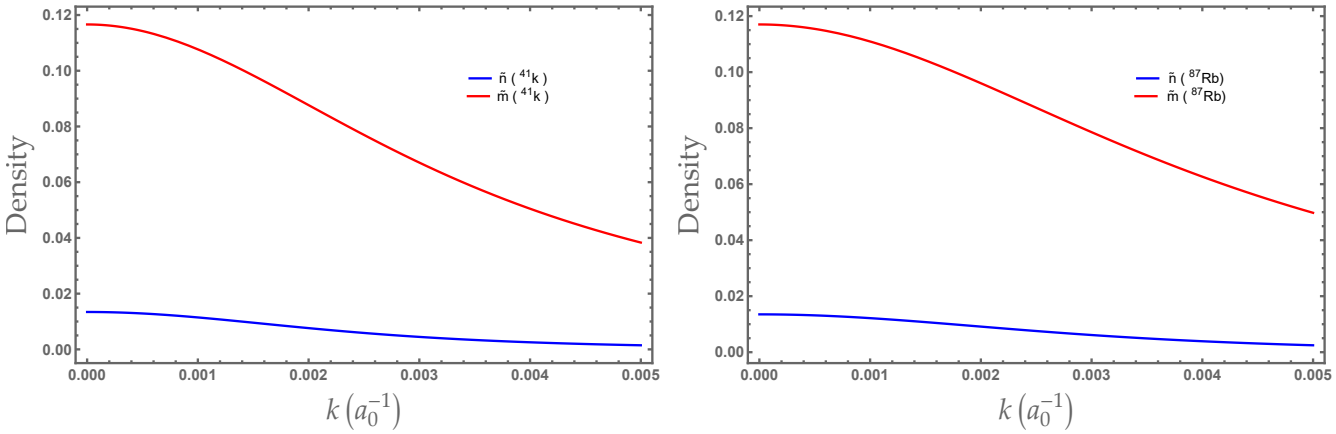

Figure 3.3: Anomalous density$|\tilde{m}_i(k)|$ (red) and the non-condensate density $\tilde{n}_i(k)$ (blue) for the two species $^{41}K -^{87} Rb$ as function of k (units of a_0^{-1}) with $a_{12} = 4a_1$.

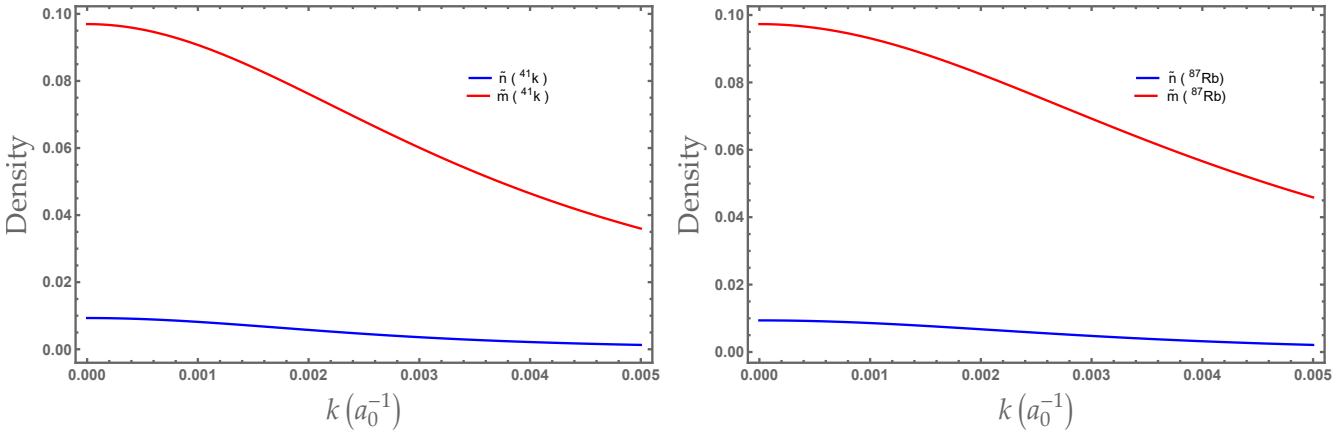

Figure 3.4: Anomalous density$|\tilde{m}_i(k)|$ (red) and the non-condensate density $\tilde{n}_i(k)$ (blue) for the two species $^{41}K -^{87} Rb$ as function of k (units of a_0^{-1}) with $a_{12} = 5a_1$.

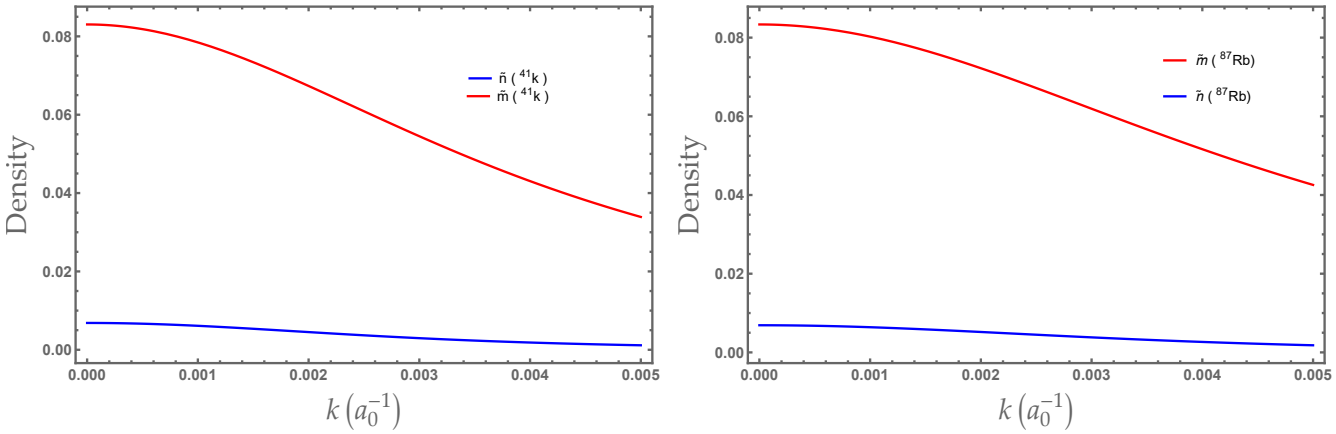

Figure 3.5: Anomalous density$|\tilde{m}_i(k)|$ (red) and the non-condensate density $\tilde{n}_i(k)$ (blue) for the two species $^{41}K -^{87} Rb$ as function of k (units of a_0^{-1}) with $a_{12} = 6a_1$.

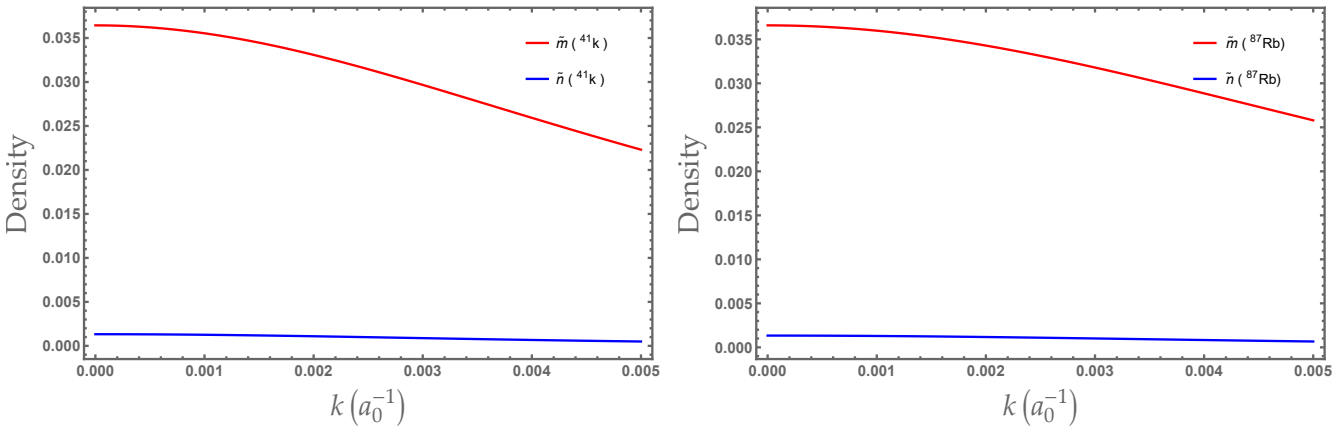

Figure 3.6: Anomalous density$|\tilde{m}_i(k)|$ (red) and the non-condensate density $\tilde{n}_i(k)$ (blue) for the two species$^{41}K -^{87} Rb$ as function of k (units of a_0^{-1}) with $a_{12} = 15a_1$.

From the left panel ^{41}K, we show that at zero temperature $|\tilde{m}_i(k)| > \tilde{n}_i(k)$. We notice further that $\frac{|\tilde{m}|}{n_c} \ll 1$, $n_c \simeq n$. So the non-condensate and the anomalous densities are very small for 0 at $T = 0$. Moreover, their overall behavior shows a decrease toward o at high momenta. the same observations are seen on the right panel ^{87}Rb.

We observe that the anomalous and non-condensate densities for both species decrease when we increase the interspecies scattering length. The last figure (3.6) is however to be taken with great care as one is entering the strong interacting regime.

At low momenta, they reach maximum values, witnessing a great impact of low momentum fluctuations. This phenomenon is will known in 1D systems. On the other hand, comparing the fluctuations of the two species, we note that they are of same order and

show analogous behaviors.

At around $4a_1$ figures(3.2-3.5), there is a change in their shape. This is probably due to the strong repulsion between the atoms of different species.

In order to explain the similarities existing between the densities of different species, we plot in figure(3.7-3.12) a comparison between $\tilde{m}_1(k)$, $\tilde{m}_2(k)$ and $\tilde{n}_1(k)$, $\tilde{n}_2(k)$.

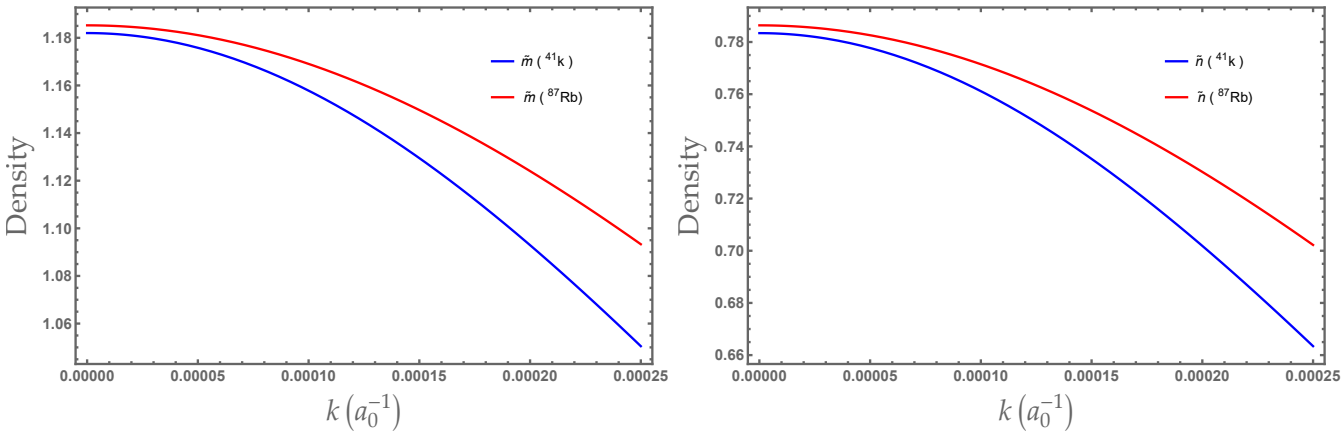

Figure 3.7: Anomalous densities (left panel $|\tilde{m}_i(k)|$) and non-condensate densities (right panel $\tilde{n}_i(k)$) for a mixture ^{41}K (blue) and ^{87}Rb (red) as function of k (units of a_0^{-1}) with $a_{12} = 0.1a_1$.

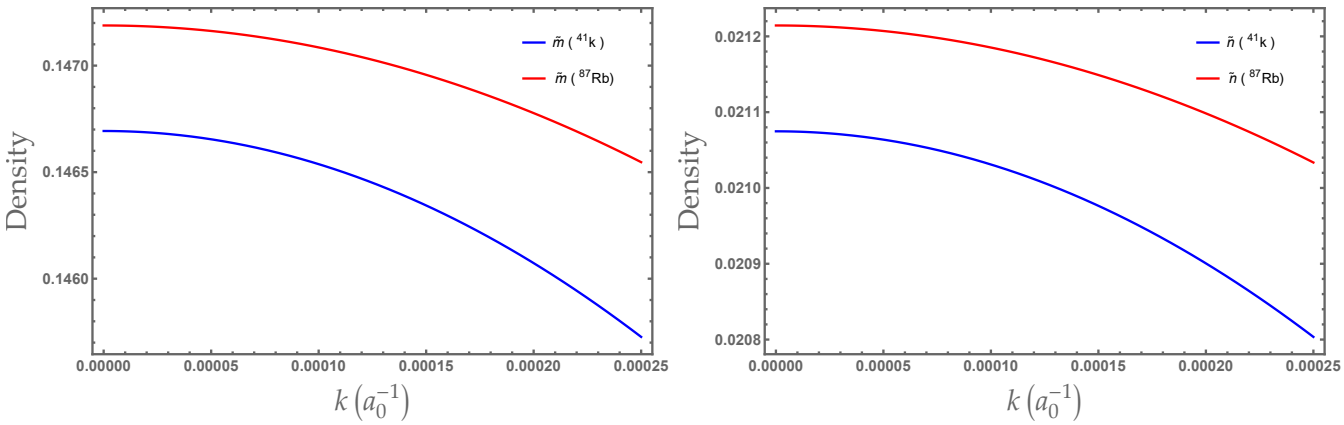

Figure 3.8: Anomalous densities (left panel $|\tilde{m}_i(k)|$) and non-condensate densities (right panel $\tilde{n}_i(k)$) for a mixture ^{41}K (blue) and ^{87}Rb (red) as function of k (units of a_0^{-1}) with $a_{12} = 3a_1$.

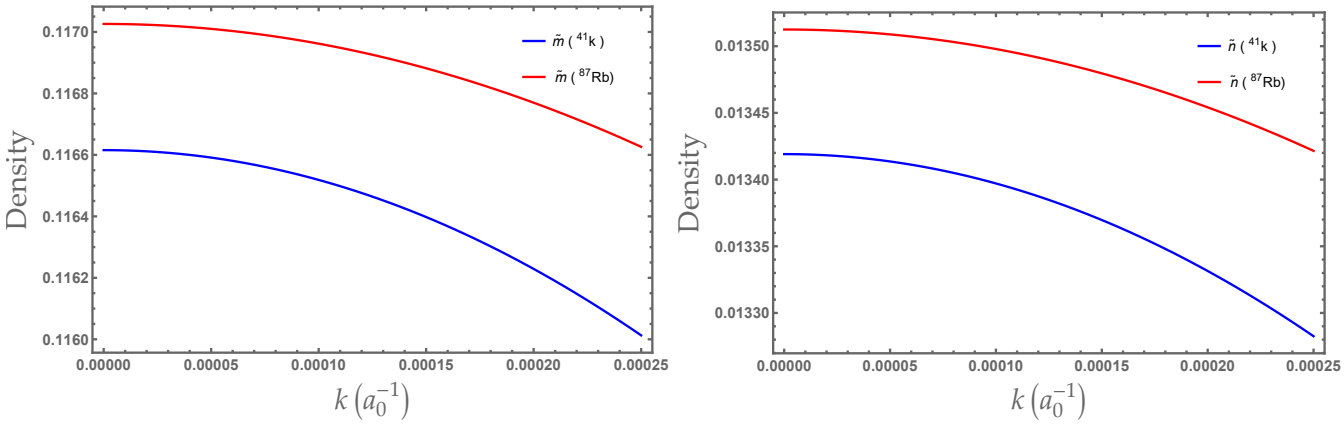

Figure 3.9: Anomalous densities (left panel $|\tilde{m}_i(k)|$) and non-condensate densities (right panel $\tilde{n}_i(k)$) for a mixture ^{41}K (blue) and ^{87}Rb (red) as function of k (units of a_0^{-1}) with $a_{12} = 4a_1$.

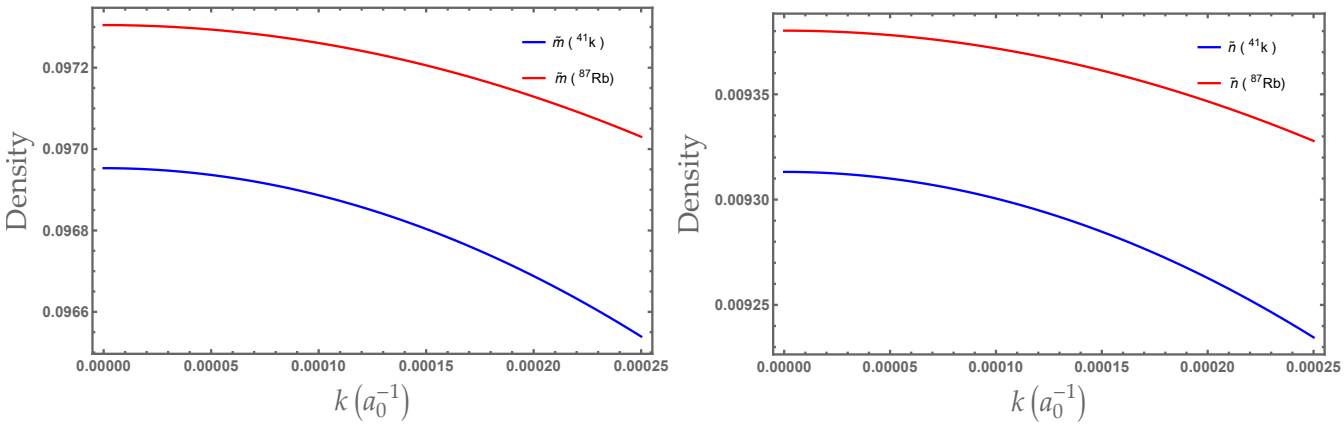

Figure 3.10: Anomalous densities (left panel $|\tilde{m}_i(k)|$) and non-condensate densities (right panel $\tilde{n}_i(k)$) for a mixture ^{41}K (blue) and ^{87}Rb (red) as function of k (units of a_0^{-1}) with $a_{12} = 5a_1$.

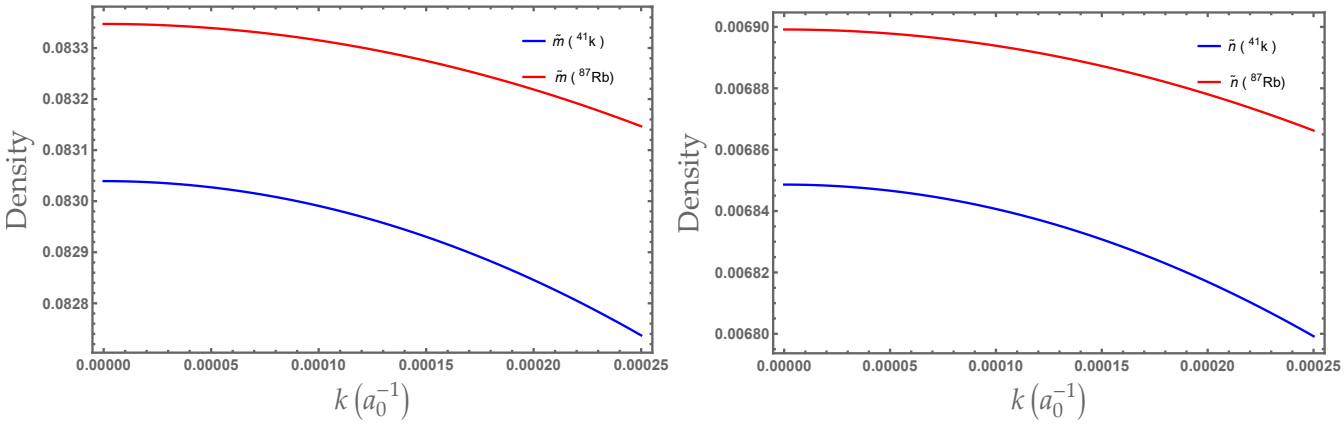

Figure 3.11: Anomalous densities (left panel $|\tilde{m}_i(k)|$) and non-condensate densities (right panel $\tilde{n}_i(k)$) for a mixture ^{41}K (blue) and ^{87}Rb (red) as function of k (units of a_0^{-1}) with $a_{12} = 6a_1$.

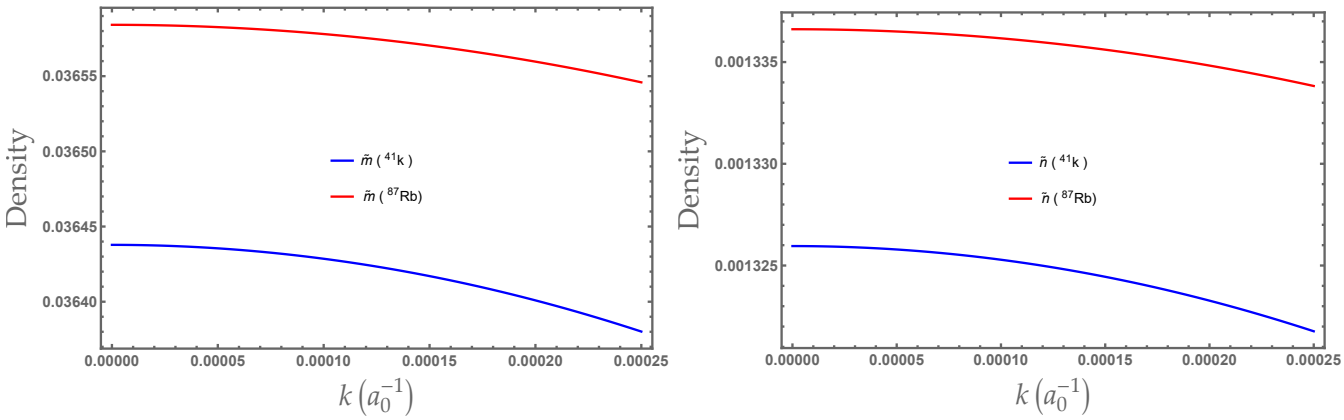

Figure 3.12: Anomalous densities (left panel $|\tilde{m}_i(k)|$) and non-condensate densities (right panel $\tilde{n}_i(k)$) for a mixture ^{41}K (blue) and ^{87}Rb (red) as function of k (units of a_0^{-1}) with $a_{12} = 15a_1$.

We observe that, beginning with $a_{12} = 0.1a_1$ (figure 3.7), $a_{12} = 3a_1$ (figure 3.8), $a_{12} = 4a_1$ (figure 3.9), $a_{12} = 5a_1$ (figure 3.10), $a_{12} = 6a_1$ (figure 3.11), and ending with $a_{12} = 15a_1$ (figure 3.12) , the discrepancies between $\tilde{m}_1(k)$ and $\tilde{m}_2(k)$, on the hand, and $\tilde{n}_1(k)$ and $\tilde{n}_2(k)$ on the other, grow as the interspecies interactions increase. We will see that this is a pure quantum effect when we introduce the effects of temperature.

Most importantly, the anomalous and the non condensate densities, although small at zero temperature, are found to be of the same order of magnitude, leading to the conclusion that it would be very hazardous to omit one of them while keeping the other such as what is performed in the so (wrongly) called Popov approximation

3.8 Numerical illustrations on 1D homogeneous bose mixtures : finite temperature case

It is important to examine the previous behaviors at finite (but low enough) temperature in order to understand the interplay between quantum and thermal fluctuations. At finite temperature the solutions (3.26)become

$$\begin{aligned}\tilde{m}_{ii}(k) &= -\frac{1}{2}\frac{g_{ii}\left(n_{ci}+\tilde{m}_{ii}\right)}{\sqrt{\left(\epsilon_{ki}+2g_{ii}n_{ci}\right)\left(\epsilon_{ki}-2g_{ii}\tilde{m}_{ii}\right)}}\coth\left(\beta\epsilon_k/2\right)\\ \tilde{n}_{ii}(k) &= \frac{1}{2}\left\{-1+\frac{\epsilon_{ki}+g_{ii}\left(n_{ci}-\tilde{m}_{ii}\right)}{2\sqrt{\left(\epsilon_{ki}+2g_{ii}n_{ci}\right)\left(\epsilon_{ki}-2g_{ii}\tilde{m}_{ii}\right)}}\coth\left(\beta\epsilon_k/2\right)\right\}\end{aligned} \tag{3.27}$$

Where we have used the conversation of Heisenberg parameter $(1+2\tilde{n}_i(k))^2-(2\tilde{m}_i(k))^2 = I_{ki} = \left(\coth\left(\beta\epsilon_k/2\right)\right)^2$ and $\epsilon_{ki} = \frac{\hbar^2k^2}{2m_i}+g_{ij}n_j, (i,j=1,2)$.

We consider the same mixture as before namely ${}^{41}K-{}^{87}Rb$ .The transition temperature T_c for these gases are al most the same (500 nK for ${}^{41}K$ and 480 nK for ${}^{87}Rb$). We choose the same experimental situations as before namely $a_1 = 65a_0$, $\omega_1 = 0.83$ Hz and the total density $n_1 = 3.58\times10^6m^{-1}$. For ${}^{87}Rb$ (2), $a_2 = 100.4a_0$, $\omega_2 = 0.6$ Hz and the total density $n_2 = 5\times10^6m^{-1}$ [120]. Moreever, we select four typical regimes: $T=\frac{T_c}{4}$, $T=\frac{T_c}{2}$, $T=0.6T_c$ and $T=\frac{3T_c}{4}$.

We start by plotting the non-condensate $\tilde{n}_i(k)$ and the absolute value of anomalous densities $|\tilde{m}_i(k)|$ for the two species (left panel ${}^{41}K$, right panel ${}^{87}Rb$) as function of k (units of a_0^{-1}) with $a_{12}=5a_1$ at temperatures ($T=0.25T_c$, $T=0.5T_c$, $T=0.6T_c$, and $T=0.75T_c$).

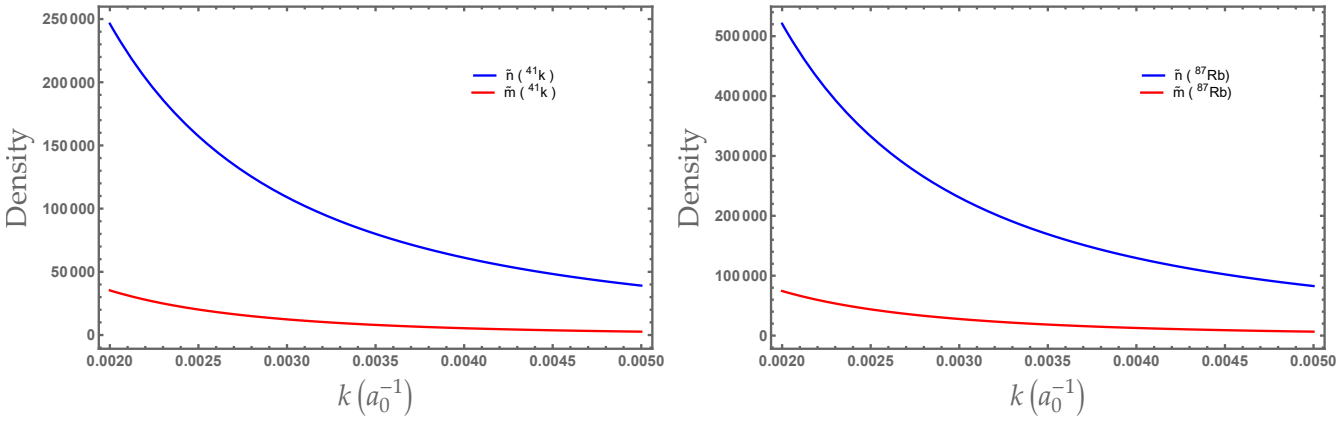

Figure 3.13: Anomalous density$|\tilde{m}_i(k)|$ (red) and the non-condensate density $\tilde{n}_i(k)$ (blue) for the two species^{41}K $-^{87}$ Rb as function of k (units of a_0^{-1}) with $a_{12} = 5a_1$. for $T = 0.25T_c$

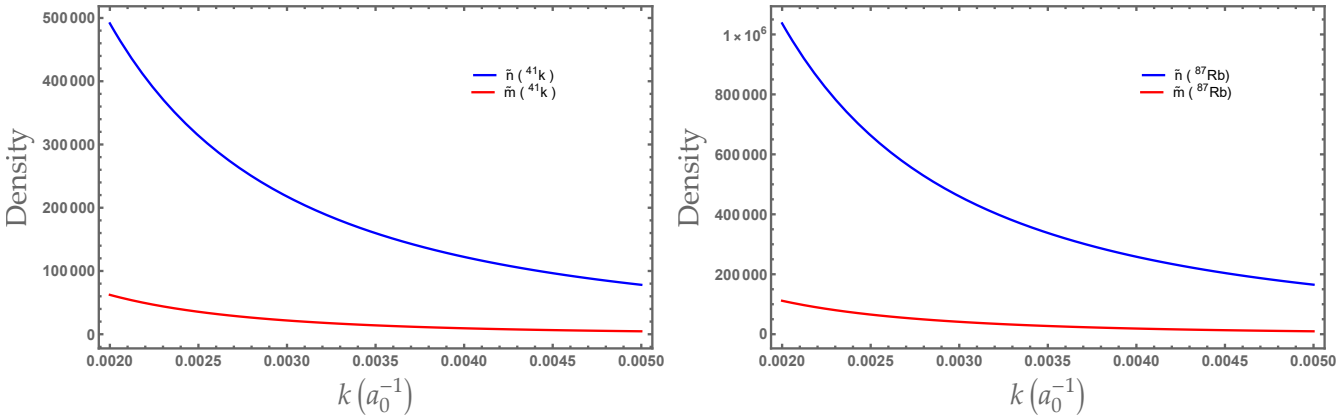

Figure 3.14: Anomalous density$|\tilde{m}_i(k)|$ (red) and the non-condensate density $\tilde{n}_i(k)$ (blue) for the two species^{41}K $-^{87}$ Rb as function of k (units of a_0^{-1}) with $a_{12} = 5a_1$. for $T = 0.5T_c$

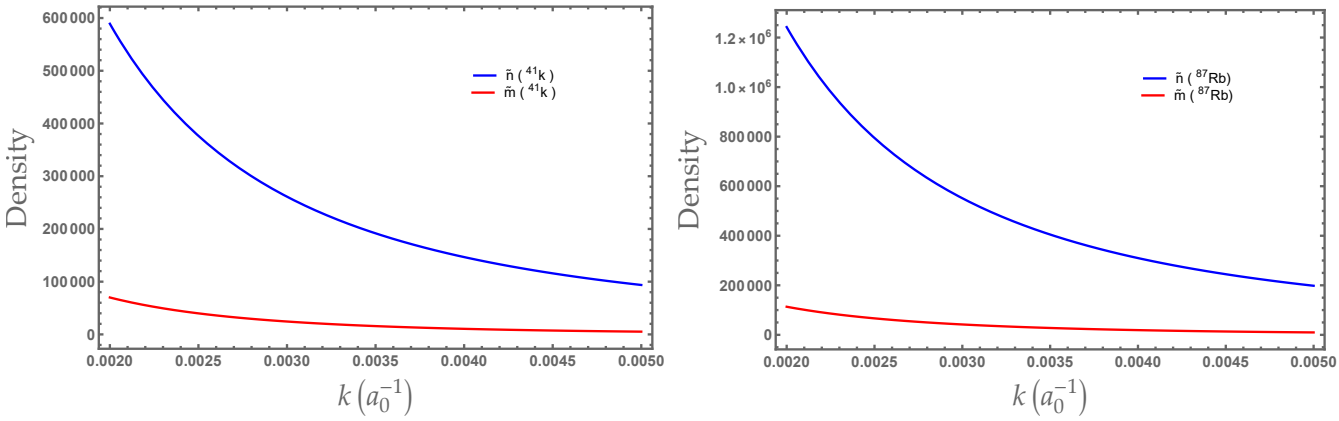

Figure 3.15: Anomalous density$|\tilde{m}_i(k)|$ (red) and the non-condensate density $\tilde{n}_i(k)$ (blue) for the two species$^{41}K -^{87} Rb$ as function of k (units of a_0^{-1}) with $a_{12} = 5a_1$. for $T = 0.6T_c$

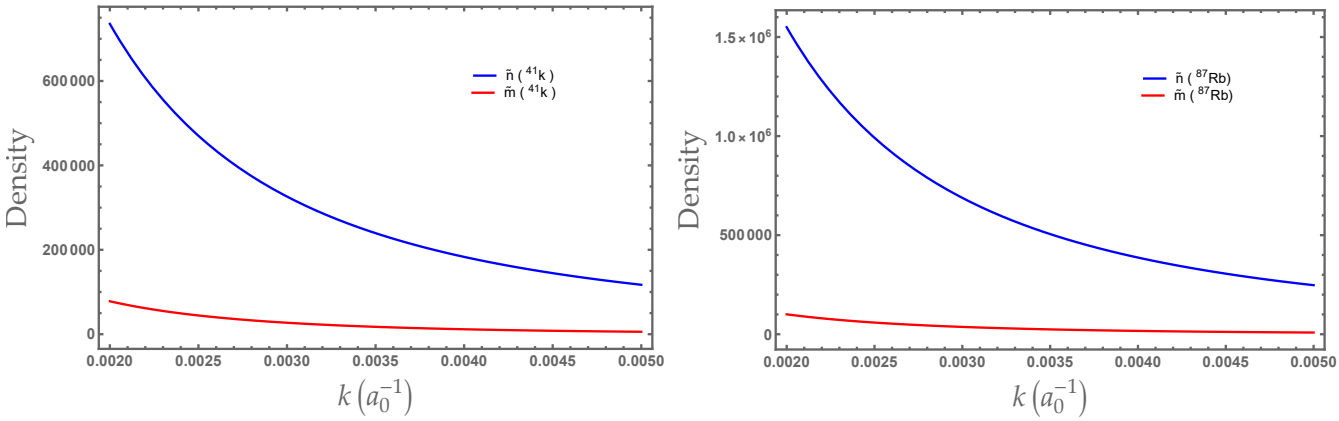

Figure 3.16: Anomalous density$|\tilde{m}_i(k)|$ (red) and the non-condensate density $\tilde{n}_i(k)$ (blue) for the two species$^{41}K -^{87} Rb$ as function of k (units of a_0^{-1}) with $a_{12} = 5a_1$. for $T = 0.75T_c$

The curves (3.13-3.16) for (left panel :Potassium) show that the non-condensate density is greater than the anomalous density. We also notice that the non- condensate density increases with increasing temperature. The same observation appears on the right panal (Rubidium).

We found previously that at zero temperature , the anomalous density and the non condensate density have the same order of magnitude, while these curves indicate that when the temperature is introduced, the non-condensate density becomes greater than the anomalous density .

We observe that at finite temperature the non-condensate density of the Rubidium gas is greater than the non-condensate density of Potassium gas. The same thing happens

with the anomalous density , This due to the mass radio $\frac{m_2}{m_1} \sim 2$.

Finally in the presence of temperature, we note that the swelling tend to disappear and this is due to the dominant thermal effects at finite temperature which clearly confirms that the observed shape at $T = 0$ figure(3.4) is a quantum effect.

In figure(3.17-3.18), we plot the non-condensate $\frac{\tilde{n}_i}{n_i}$ and the anomalous densities $\frac{|\tilde{m}_i|}{n_i}$ for the two species (left panel ^{41}K , right panel ^{87}Rb) as function of the reduce temperature $\frac{T}{T_{ci}}$ in $a_{12} = 5a_1$. It can be seen that $\frac{\tilde{n}_i}{n_i}$ is increasing significantly with increasing temperature. Furthermore, it is quite interesting to observe that the anomalous $\frac{|\tilde{m}_i|}{n_i}$ becomes small as the temperature approaches zero or T_c. It reaches a maximum at intermediate temperatures ($T \sim 0.6Tc$) and then decreases toward 0 . This effect has also been observed in [71] in 3D using HFB-BDG equation.

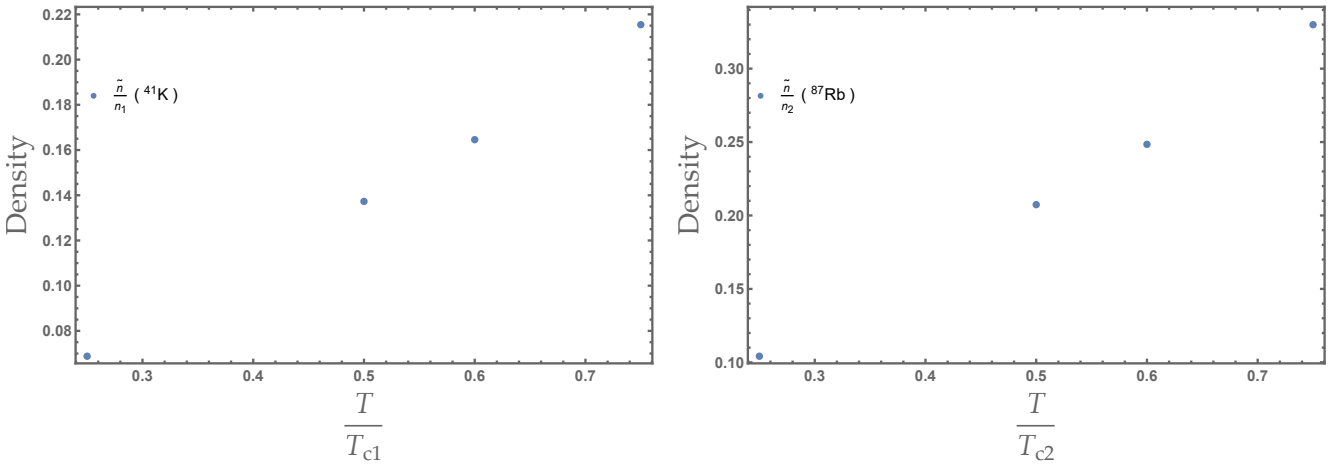

Figure 3.17: The non-condensate density $\frac{\tilde{n}_i}{n_i}$ for the two species $^{41}K -^{87} Rb$ as function of $\frac{T}{T_{ci}}$ with $a_{12} = 5a_1$.

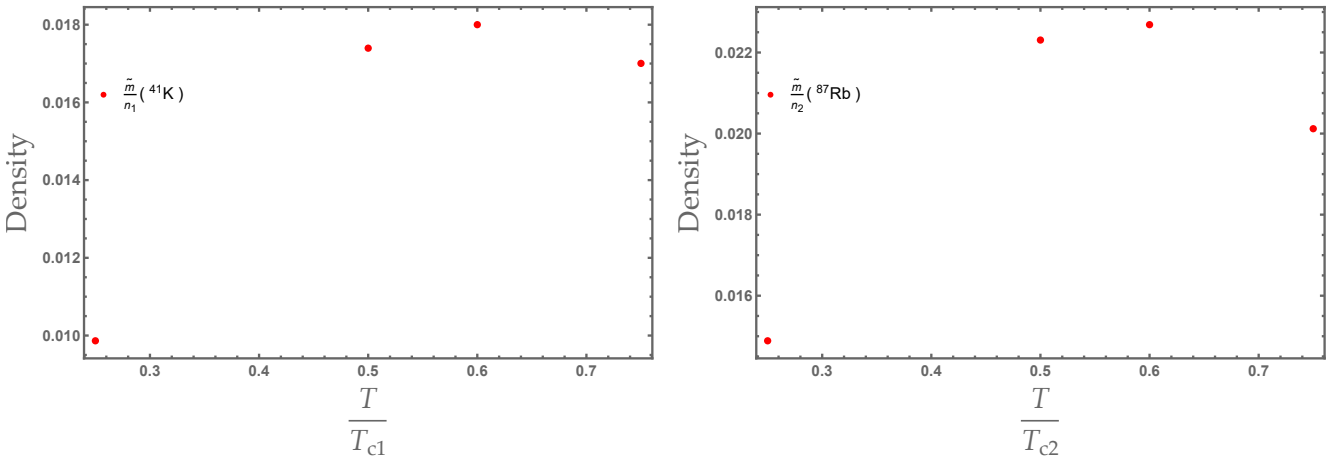

Figure 3.18: Anomalous density $\frac{|\tilde{m}_i|}{n_i}$ for the two species $^{41}K -^{87} Rb$ as function of $\frac{T}{T_{ci}}$ with $a_{12} = 5a_1$.

Chapter 4

Effects of interspecies correlations

4.1 Introduction

In the previous chapters we have examined binary mixtures in the extended mean-field framework, taking into account quantum and thermal fluctuations.

For the two- body Hamiltonien eq (3.1), we have written the expression for the energy eq (3.3) as well as the dynamical equations. For the whole set of correlations in the full TDHFB eqs (3.5-3.9) as well as in the Bogoliubov approximations eq(3.25).

Nevertheless, when solving the static eqs for a homogeneous mixtures, both at zero eq (3.26) and finite temperature eq (3.27), we deliberately omitted the interspecies fluctuations in order to better visualize the known (intraspecies) fluctuations.

In this chapter, we will reintroduce these fluctuations and focus on their role for quasi-1D homogeneous mixtures. Furthermore, we will consider the $T = 0$ case since thermal fluctuations will tend to suppress quantum ones. The following is reported in our paper [37, 38]

4.2 Stability of the mixture

Let us consider the Hmiltonien (3.1) with the same definitions as in section (3-3). The energy density corresponding to eq (3.3) then simplifies to

$$\begin{aligned}\mathcal{E} = &\frac{1}{2}g_{11}n_1^2 + \frac{1}{2}g_{22}n_2^2 + g_{12}n_1n_2 \\ &+ \frac{1}{2}g_{11}n_{c_1}^2\left(2(\tilde{N}_{11}+\tilde{M}_{11}) + \tilde{N}_{11}^2 + \tilde{M}_{11}^2\right) + \left(1\to 2\right) \\ &+ g_{12}n_{c_1}n_{c_2}\left(2(\tilde{N}_{12}+\tilde{M}_{12}) + \tilde{N}_{12}^2 + \tilde{M}_{12}^2\right)\end{aligned} \tag{4.1}$$

where the condensate densities are denoted by n_{c_i} and the total densities by n_i . We have introduced the dimensionless "densities" $\tilde{N}_{ij} = \tilde{n}_{ij}/\sqrt{n_{c_i}n_{c_j}}$ and $\tilde{M}_{ij} = \tilde{m}_{ij}/\sqrt{n_{c_i}n_{c_j}}$. Naturally, $\tilde{n}_{ii}$ and $\tilde{m}_{ii}$ stand for the noncondensate and anomalous densities, respectively. The first line in (4.1) is the usual mean-field contributions. The second line is the so called LHY contributions because it merely contains quantum fluctuations.It was generally omitted for single-species systems until Petrov [121] showed how it may play a dominant role in certain special situations.

Most importanlly, to our knowledge, the third line of the energy (4.1) was never con-

sidered before. Two notable exceptions are [121, 122], where these kind of expressions were written by never considered seriously.

As it stands, this new contributions to the energy is manifestly due to the quantum interspecies fluctuations. It depicts entnglement between the two species. We notice further that interspecies interactions g_{12} are a prerequisite for interspecies correltions [109, 110].

Moreover, we observe on eq (4.1) that the contributions of the interaspecies (second line) and interspecies(third line) fluctuations are of the same form and, as we will see later of the same order. They are however mysteriously absent from literature [38, 121, 123–126]. We can imagine that it was believed that, since the species are not correlated (initially in current experiments), there is no reason that interspecies fluctuations appear in subsequent dynamical evolution. But, recall the general eqs (3.5-3.9). It is clearly visible there that, even of $\tilde{n}_{12}(t=0) = \tilde{m}_{12}(t=0) = 0$, it needs not be the case later.

The previous omissions are well justified when the mean-field (that is, the first line in (4.1) dominates. Thanks to Feshbach resonances, one can tune the coupling constants to make the mean-field energy vanishingly small. This can be performed by setting $g_{12} \sim -\sqrt{g_{11}g_{22}}$ and $n_1 = n_2 = n$ we then easily see that $\mathcal{E}_{MF} = (\sqrt{g_{11}} - \sqrt{g_{22}})^2 \frac{n^2}{2}$ and hence can be made as small as we wish by also tuning g_{11} and g_{22}. This regime leads to the collapse of the mixtures if only the mean-field was present based in the second line contributions, Petrov [121] showed that quantum fluctuations can make the energy nonzero and hence, a stabilization of the condensate. This situation leads to the formation of stable states, knows as droplets.

However, looking back at (4.1), we see that there is another contributions, coming from interspecies entanglement, and not considered by Petrov. We will show later on that, this contributions enhance the stability of the droplets, making them easier to observe . These presumptions are supported when the mean field energy is dominant. Conversely, these presumptions totally collapse when the latter occurs to be vanishingly small, as would be the case when one approaches the droplet zone. In fact, given that the new terms might significantly impact the stability of the droplets, Petrov's [121] conclusion that quantum fluctuations could stabilize a collapsing mixture ($g_{12} + \sqrt{g_{11}g_{22}} \to 0$) is called into doubt.

One of the goals of this work is to demonstrate that, even at zero temperature, the contributions of quantum interspecies fluctuations are numerically and qualitatively equivalent to those of intraspecies fluctuations. In order to do this, we will use the Bogoliubov

technique to calculate $\tilde{N}_{12}$ and $\tilde{M}_{12}$. It should be noted that Larsen [127] was the first to compute these quantities in 3D.

Let us begin by analyzing the stability of the mixture under general contributions. When the grand canonical energy density $\mathcal{E} - \mu_1 n_1 - \mu_2 n_2$ has a minimum, that is

$$\frac{\partial \mathcal{E}}{\partial n_{c_i}} = 0 \tag{4.2}$$

and the Hessian matrix

$$A_{ij} = \frac{\partial^2 \mathcal{E}}{\partial n_{c_i} \partial n_{c_j}}$$

is positive definite, which means $\mathrm{Tr}\, A > 0$, and $\mathrm{Det}\, A > 0$ then, the system is stable. The first condition leads to generalized expressions for the chemical potentials .

$$\begin{aligned} \mu_1 &= g_{11} n_1 + g_{12} n_2 + g_{11} n_{c_1} \left(\tilde{N}_{11} + \tilde{M}_{11} \right) + g_{12} n_{c_2} \left(\tilde{N}_{12} + \tilde{M}_{12} \right) \\ \mu_2 &= g_{22} n_2 + g_{12} n_1 + g_{22} n_{c_2} \left(\tilde{N}_{22} + \tilde{M}_{22} \right) + g_{12} n_{c_1} \left(\tilde{N}_{12} + \tilde{M}_{12} \right) \end{aligned} \tag{4.3}$$

The second requirement leads to generalized stability criteria against phase separation $G_1 G_2 - G_{12}^2 > 0$ and against collapse $G_1 + G_2 > 0$ [37,38] , where the generalized coupling constants are

$$\begin{aligned} G_1 &= g_{11} - g_{12} \frac{\tilde{N}_{12} + \tilde{M}_{12}}{2} \frac{n_{c_2}}{n_{c_1}} \\ G_2 &= g_{22} - g_{12} \frac{\tilde{N}_{12} + \tilde{M}_{12}}{2} \frac{n_{c_1}}{n_{c_2}} \\ G_{12} &= g_{12} \left(1 + \frac{\tilde{N}_{12} + \tilde{M}_{12}}{2} \right). \end{aligned} \tag{4.4}$$

The well-known stability conditions $g_{ii} > 0$ and $g_{11} g_{22} - g_{12}^2 > 0$ for a non-correlated homogeneous bose mixture are obviously naturally generalized by the aforementioned conditions [128].

In order to make these remarks more quantitative, we will compute in the next section the fluctuations $\tilde{N}_{ij}$ and $\tilde{M}_{ij}$ using the Bogoliubov approximation.

4.3 Single Particle Excitations and Droplet Stability in Quasi-One Dimension

Using eq (3.21) in the homogeneous case , we may write

$$\begin{aligned}\tilde{n}_{ij} &= \sum_k \left[f_k U_k^{(i)} U_k^{(j)} + (1+f_k) V_k^{(i)} V_k^{(j)} \right] \\ \tilde{m}_{ij} &= -\sum_k \left[(1+2f_k) U_k^{(i)} V_k^{(j)} \right]\end{aligned} \tag{4.5}$$

where $U_k^{(i)}$ and $V_k^{(i)}$ are the quasi-particles amplitudes, and $f_k = (e^{\hbar\omega_k/k_BT} - 1)^{-1}$ is the Bose-Einstein distribution , which is taken to be 0 at zero temperature.

The Hartree-Fock-Bogoliubov-De Gennes (HFB-BdG) equations (3.25) simplify to

$$\begin{aligned}\hbar\omega_k U_k^{(i)} &= e_{k_i} U_k^{(i)} - g_{ii}\kappa_{ii} V_k^{(i)} + g_{12}\left(\eta_{12} U_k^{(3-i)} - \kappa_{12} V_k^{(3-i)}\right) \\ \hbar\omega_k V_k^{(i)} &= -e_{k_i} V_k^{(i)} + g_{ii}\kappa_{ii} U_k^{(i)} - g_{12}\left(\eta_{12} V_k^{(3-i)} - \kappa_{12} U_k^{(3-i)}\right)\end{aligned} \tag{4.6}$$

where $e_{k_i} = \hbar^2k^2/2m_i + g_{ii}n_{c_i}\left[1 - \tilde{M}_{ii} - \lambda_i \frac{n_{c_{3-i}}}{n_{c_i}}\left(\tilde{N}_{12} + \tilde{M}_{12}\right)\right]$, $\lambda_i = g_{12}/g_{ii}$, $\eta_{ij} = \sqrt{n_{c_i} n_{c_j}}$ $(1 + \tilde{N}_{ij})$ and $\kappa_{ij} = \sqrt{n_{c_i} n_{c_j}}(1 + \tilde{M}_{ij})$, $i, j = 1, 2$. We will consider from now on a two-component balanced system, for which $m_1 = m_2 = m$, $g_{11} = g_{22} = g$ and $n_1 = n_2 = n$. Then, $n_{c_1} = n_{c_2} = n_c$, $\tilde{N}_{11} = \tilde{N}_{22} = \tilde{N}$, $\tilde{M}_{11} = \tilde{M}_{22} = \tilde{M}$ and $\lambda_1 = \lambda_2 = \lambda$.

In order to simplify the eqs as much as possible, the system (4.6) is a simple eigenvalue problem $(4 * 4)$ which yields two branches ($\tilde{\omega} = \hbar\omega_k/gn_c$):

$$\begin{aligned}\tilde{\omega}_- &= \sqrt{\epsilon_k\left(\epsilon_k + 2(1-\lambda) - 2\lambda(\tilde{N}_{12} + \tilde{M}_{12})\right)} \\ \tilde{\omega}_+ &= \sqrt{\epsilon_k\left(\epsilon_k + 2(1+\lambda)\right)}\end{aligned} \tag{4.7}$$

with $\epsilon_k = \frac{\hbar^2k^2}{2mgn_c}$. and two sets of eigenvectors. The $\tilde{\omega}_-$ branch has eigenvectors$(U_k^{(1)}, -U_k^{(1)}, V_k^{(1)}, -V_k^{(1)})$ and the $\tilde{\omega}_+$ branch $(U_k^{(1)}, U_k^{(1)}, V_k^{(1)}, V_k^{(1)})$. This yields the following remarkable solutions:

$$\tilde{\omega}_- : \begin{cases} \tilde{N}_{12} = -\tilde{N} \\ \tilde{M}_{12} = -\tilde{M} \end{cases} \tag{4.8}$$

$$\tilde{\omega}_+ : \begin{cases} \tilde{N}_{12} = +\tilde{N} \\ \tilde{M}_{12} = +\tilde{M} \end{cases} \tag{4.9}$$

These results nicely reproduce the general expressions obtained in [127] upon using their 1D reduction . Most importantly, they confirm the fact that interspecies fluctuations are equal(in absolute value)to the intraspecies one. Hence, neglecting them may head to hazardous conclusions.

The ground state energy density(4.1) writes, up to first order in the fluctuations

$$\frac{\mathcal{E}}{gn^2} = 1 + \lambda + \sum_{\pm} (1 \pm \lambda) \left(\tilde{N} + \tilde{M} \right)_{\pm}, \tag{4.10}$$

which is to be compared to the usually considered case of uncorrelated species ($\tilde{N}_{12} = \tilde{M}_{12} = 0$)

$$\frac{\mathcal{E}_0}{gn^2} = 1 + \lambda + \sum_{\pm} \left(\tilde{N} + \tilde{M} \right)_{\pm}. \tag{4.11}$$

Evidently, the corrections to the mean field energy taking into account quantum fluctuations, are the so-called LHY contributions. Notice that they are different for the correlated and uncorrelated situations. Since in quasi-1D geometries, the LHY terms are negative [123, 125, 126], an uncorrelated mixture may undergo instability as soon as the mean field energy vanishes. It may not be the case for an uncorrelated mixture as the LHY contribution is λ-dependent.

Let us see this more concretely by computing the various fluctuating terms in quasi-1D. Plugging the solutions of eq (4.8-4.9) into eq (4.6), we get

$$\begin{aligned} \tilde{N}_{\pm} &= \alpha \gamma_{1D} \sqrt{1 \pm \lambda} \\ \tilde{M}_{\pm} &= \beta \gamma_{1D} \sqrt{1 \pm \lambda} \end{aligned} \tag{4.12}$$

Where $\gamma_{1D} = \sqrt{mg/\hbar^2 n}$ is the Lieb-Liniger gas parameter and $\alpha = \frac{1}{2\pi}\left(1 - \frac{\text{arcsinh}(1)}{\sqrt{2}}\right) \simeq 0.06$, $\beta = -\frac{\sqrt{2}}{8} \simeq -0.177$. Hence, as mentioned above, the LHY term $\tilde{N}_{\pm} + \tilde{M}_{\pm} = -0.117\gamma_{1D}\sqrt{1 \pm \lambda}$ is effectively negative and falls in the stability region defined in section(4.2). The energy densities eqs (4.10 - 4.11) write

$$\begin{aligned} \frac{\mathcal{E}}{gn^2} &= 1 + \lambda + (\alpha + \beta)\gamma_{1D} \left((1 + \Lambda)^{3/2} + (1 - \lambda)^{3/2} \right) \\ \frac{\mathcal{E}_0}{gn^2} &= 1 + \lambda + (\alpha + \beta)\gamma_{1D} \left((1 + \lambda)^{1/2} + (1 - \lambda)^{1/2} \right) \end{aligned} \tag{4.13}$$

The droplet regime shows up when $g_{12} \to -\sqrt{g_{11}g_{22}}$. In our symmetric case, this means $\lambda \sim -1$, hence $1+\lambda \sim 0$. Setting $1+\lambda = \delta g/g << 1$, the energy densities (4.13) write

$$\begin{aligned} \mathcal{E} &\simeq \delta g n^2 - \gamma (gn)^{3/2} \\ \mathcal{E}_0 &\simeq \delta g n^2 - \gamma_0 (gn)^{3/2} \end{aligned} \tag{4.14}$$

where

$$\begin{aligned} \gamma &= -(\alpha+\beta)\sqrt{m/\hbar^2}\left(2\sqrt{2} - \frac{3}{\sqrt{2}}\delta g/g + (\delta g/g)^{3/2}\right) \\ \gamma_0 &= -(\alpha+\beta)\sqrt{m/\hbar^2}\left(\sqrt{2} - \frac{}{2\sqrt{2}}\delta g/g + (\delta g/g)^{1/2}\right). \end{aligned} \tag{4.15}$$

Hence, although the two expressions have the same functional form in the density characterizing the existence of a stable self-bound state [123, 125, 126], they differ by their dependence on the coupling constant. For the correlated case, the minimum energy is

$$\mathcal{E}_{min} = -\frac{27}{256}\gamma^4 \left(\frac{g^2}{\delta g}\right)^3, \tag{4.16}$$

which can easily be shown to be larger in absolute value by a factor of $(\gamma/\gamma_0)^4 \simeq 16$ than the uncorrelated case. Furthermore, the density at minimum

$$n_{min} = \frac{9\gamma^2}{16}\frac{g^3}{\delta g^2}, \tag{4.17}$$

is also larger by an amount of $(\gamma/\gamma_0)^2 \simeq 4$ than the uncorrelated value. We may conclude that interspecies fluctuations shift upward the equilibrium density and downward the minimum energy leading to a more stable self-bound droplet state in the liquid phase.

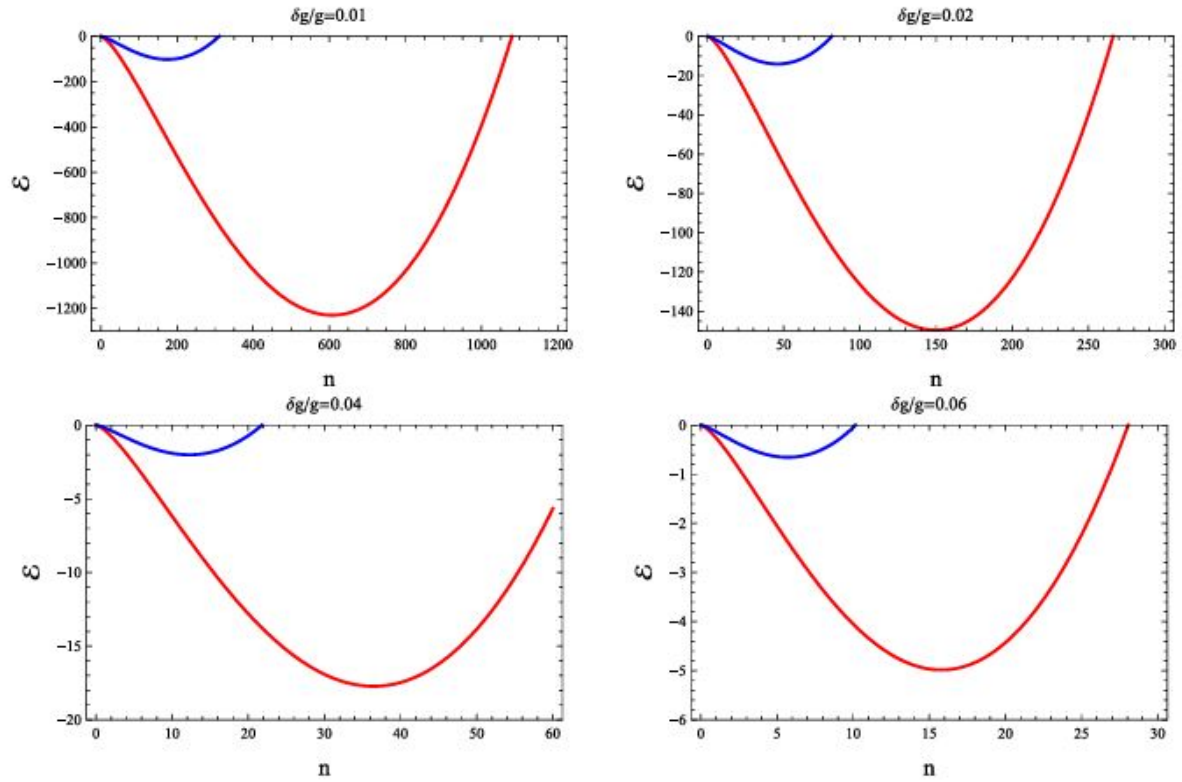

Figure 4.1: Energy (arbitrary units) vs. density for the correlated (red) and uncorrelated (blue) case. Notice the rapid change of scales for both axes as $\delta g/g$ increases

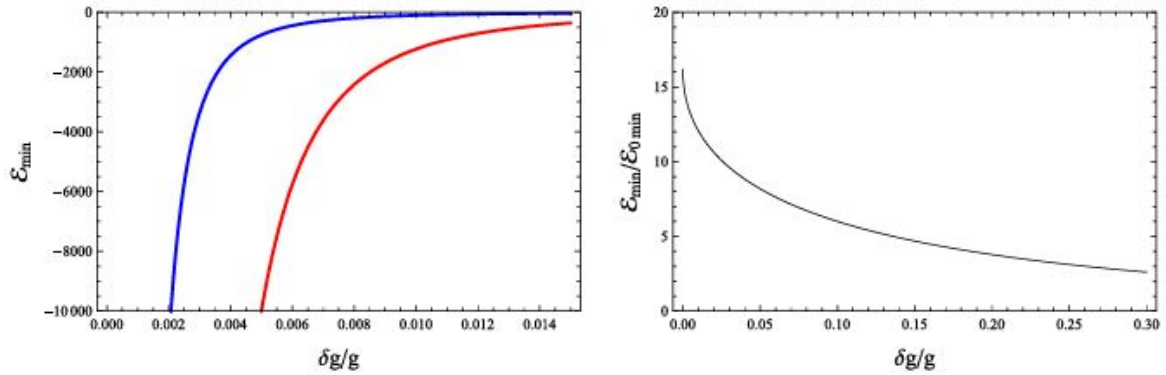

Figure 4.2: Left: Minimum energy (arbitrary units) vs. $\delta g/g$ for the correlated ($\mathcal{E}_{min}$, red) and uncorrelated ($\mathcal{E}_{0min}$, blue) case. Right: Ratio $\mathcal{E}_{min}/\mathcal{E}_{0min}$. $m = \hbar = g = 1$.

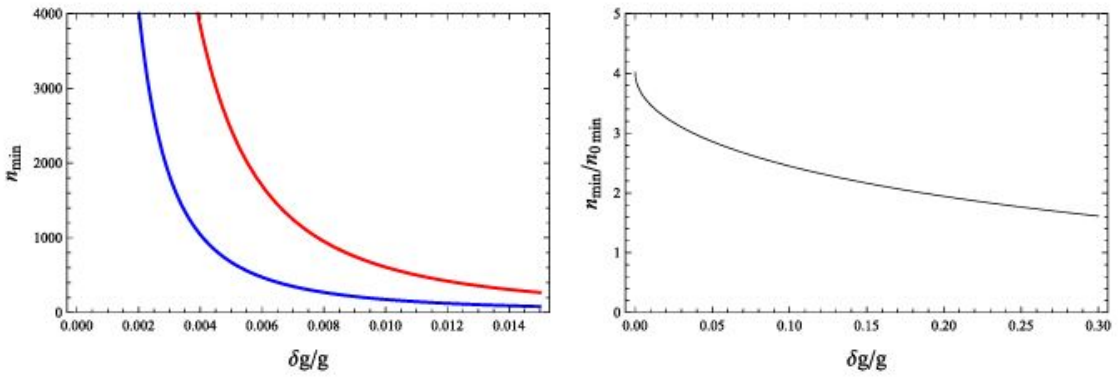

Figure 4.3: Left: Density at minimum vs. $\delta g/g$ for the correlated (n_{min}, red) and uncorrelated (n_{0min}, blue) case. Right: Ratio n_{min}/n_{0min}. $m = \hbar = g = 1$.

This is clearly depicted on figure (4.1), where one also notices the rapid change of scales as $\delta g/g$ varies witnessing a strong sensitivity of the minima to $\delta g/g$. Moreover, one observes on figures (4.2) and (4.3) that, as $\delta g/g$ becomes smaller, that is approaching further the droplet regime, $|\mathcal{E}_{min}|$ and n_{min} become larger meaning a more stable state. On the contrary, when one moves away from the droplet state, the minimum energy and density get close to zero meaning that the sole remaining minimum is at $n = 0$.

Lastly, one can question the significance of the nonlinear fluctuations that are left out of the energy expression (4.1). The fact that they only contribute a relatively modest λ-independent term of the order γ_{1D}^2 may really be validated with ease. As a result, our findings remain unchanged.

4.4 Conclusions

In conclusion, contrary to the extensive scientific literature on binary Bose mixtures, which often assumes uncorrelated species and attributes beyond-mean-field effects solely to intraspecies quantum fluctuations (the so-called LHY corrections), we demonstrate in this chapter a fundamentally different perspective.

First, we derive generalized stability conditions to address collapse and phase separation, incorporating interspecies fluctuations. These conditions extend and refine the well-established stability criteria. Within the framework of Bogoliubov's approach, interspecies fluctuations are found to be of the same order of magnitude as the LHY terms, challenging the common assumption that they can be neglected. Most significantly, near

the droplet regime, interspecies fluctuations enhance the traditional LHY effects, contributing to the formation of more stable self-bound droplets.

To gain a clearer understanding of the impact of these novel behaviors, the previous calculations will be extended in an upcoming work to address the unbalanced, non-symmetric case, where the effects of unequal populations and interactions are expected to emerge. Additionally, the role of the system's geometry will be carefully studied, as the LHY corrections are strongly influenced by the spatial dimension and the presence of traps.

Finally, since all these effects occur within very narrow energy and density ranges, experimentally verifying them is quite challenging. Specialized setups could be designed to precisely tailor the measurements to these specific conditions.

Chapter 5

Quasi-One Dimension Quantum Droplets: experimental and theoretical

Since we obtained droplets in the previous chapter . We will present the theoretical and experimental aspects of quasi-one dimensional droplets in this chapter .

5.1 Introduction

The experimental realization of Bose–Einstein condensates (BECs) in diluted atomic gases was one of the major breakthroughs in condensed matter physics at the close of the previous century [8, 9] [39, 60].The existence, stability, and dynamics of BEC have been demonstrated to be satisfactorily explained by mean-field theory, which is based on the Gross–Pitaevskii equation (GPE) [39, 60] [129].Beyond mean-field effects research has recently drawn interest in the field of atomic Condensate physics of Bose-Einstein [130].

The discovery of quantum droplets (QDs), which have attracted the interest of many scholars, is one particularly significant outcome of this study. According to Lee–Huang–Yang (LHY) corrections [131], quantum droplets are self-bound states of BEC that arise in three-dimensional free space as a result of a balancing process that stems from the competition between the attractive mean-field energy and the repulsive beyond mean-field energy . For two-component Bose gas, Petrov [121]was the first to theoretically anticipate the formation of the quantum droplet. In two and three dimensions, the BEC of attracting atoms is known to be unstable against collapse in mean-field theory [39, 60]. When dispersion compensates for atom-to-atom attractive forces due to quantum pressure mixtures, stable BEC exists in one dimension [132]. A primary driving force behind the study of quantum droplets was the pursuit of stable BEC states in two and three dimensions [133].

The effect of the quantum corrections on the ground state energy of the one component Bose gas, as represented by the LHY term, is negligible when compared to the contribution of mean field terms in the governing Gross–Pitaevskii equation. Nevertheless, as shown by Petrov [121], the repulsive LHY component and the attractive mean-field term can both be included in the final single modified GPE by controlling the interspecies and intraspecies interactions in symmetric binary BECs. Crucially, the attracting term's strength can be separately adjusted, enabling the creation of diluted liquid droplet states that are stabilised by quantum fluctuation.Stable quantum droplets in BEC were successfully described using the modified three-dimensional GPE equation [125], which has repulsive quartic nonlinearity that causes LHY corrections. In single component

Bose–Einstein condensates (BEC) with dipolar atomic interactions, QD was first experimentally realised [134, 135] Later, it was realised in binary Bose gas mixtures [136–138] .Additional experimental investigations involving quantum fluctuations include collisions of the droplets [139] and QD in a heteronuclear bosonic mixture [120]. It was also explained that quantum droplets exist in lower dimensions. Specifically, it was demonstrated that the spectrum of zero-point excitations is significantly altered in one dimension by the tight external potential. The LHY term is changed from quartic to quadratic and its sign is altered as a result [140, 141] [142]. In those conditions, the two-body mean-field interaction should be repulsive in order to provide the presence of quantum droplets. It was discussed in [143, 144] [145, 146] that quantum droplets for 1D GPE exist, are stable, and have dynamics.However, in the case of a loose external potential, the LHY corrections are identical to those found in the 3D case [140].In this context, the quasi-1D GPE and quantum droplets are examined in the papers [147, 148]. While the paper [149] examines the surface tension of QD in 1D and quasi-1D ultra-cold atomic Bose gases, [150] focusses on the interaction of quasi-1D QD with impurities [136–138].

The study of quantum droplets has emerged as one of the most exciting developments in the field of ultracold atomic physics. These droplets are small, self-bound clusters of atoms that result from the delicate balance between attractive interactions and repulsive quantum fluctuations. While the concept of quantum droplets has been established for 3D systems, their study in lower-dimensional systems, especially quasi-one-dimensional (quasi-1D) systems, has been a subject of intensive research. Quasi-1D systems are those where atoms are confined in two spatial directions, but free to move in a single direction, typically due to tight external trapping.

In quasi-1D systems, the interplay between mean-field interactions and quantum fluctuations becomes more pronounced due to reduced dimensionality, and the stabilization mechanisms of quantum droplets differ from those in higher-dimensional systems. The formation, dynamics, and stability of quantum droplets in such systems offer new insights into the behavior of quantum gases and have led to the prediction and experimental realization of novel states of matter.

5.2 Theoretical Background of Quasi-1D Quantum Droplets

5.2.1 Gross-Pitaevskii Equation in Quasi-1D Systems

The Gross-Pitaevskii equation (GPE) is the cornerstone of theoretical models for Bose-Einstein condensates (BECs), including quantum droplets. For quasi-1D systems, the GPE takes the following form, considering tight transverse confinement and free motion along the longitudinal direction:

$$i\hbar\frac{\partial\psi(z,t)}{\partial t} = \left[-\frac{\hbar^2}{2m}\frac{\partial^2}{\partial z^2} + \frac{g_1}{2}|\psi(z,t)|^2 + \frac{g_2}{2}|\psi(z,t)|^4 + \cdots\right]\psi(z,t) \tag{5.1}$$

Where the condensate's wave function along the longitudinal direction is represented by $\psi(z,t)$,the atomic mass by m , the strength of the contact interaction in the longitudinal direction is represented by g_1 and g_2 includes higher-order terms (e.g, from beyond-mean-field corrections like the Lee-Huang-Yang (LHY) term, which is particularly important in quasi-1D systems).
The transverse directions are typically confined, leading to a quasi-1D regime where the motion is significantly constrained in two directions.

The mean-field interactions are represented by the $g_1|\psi(z,t)|^2$ term, while the higher-order quantum fluctuations modify this picture, especially in low-dimensional systems, through terms like the $g_2|\psi(z,t)|^4$ term. These terms are crucial for the stability of quantum droplets, where the attractive contact interaction g_1 is balanced by the repulsive effects arising from quantum fluctuations.

5.2.2 Lee-Huang-Yang (LHY) Corrections and Stabilization

In low-dimensional systems such as quasi-1D, quantum fluctuations play a dominant role. The LHY correction modifies the mean-field interaction and introduces a repulsive quantum pressure that stabilizes the condensate. The LHY correction is more significant in lower-dimensional systems due to the enhanced role of quantum fluctuations. The correction in a quasi-1D system can be written as:

$$E_{\mathrm{LHY}} \sim \hbar\omega_\perp n^{1/2} \tag{5.2}$$

where n represents the condensate's density in the longitudinal direction and $\omega_\perp$ is the transverse trapping frequency, which controls the confinement in the transverse direction.

In quasi-1D systems, the quantum pressure becomes more pronounced, and its effects are felt more strongly, acting as an effective repulsive force that counteracts the attractive contact interactions.

For quantum droplets to form, the attractive interactions (mean-field term) must be precisely balanced by the repulsive quantum fluctuations (LHY term). If the mean-field interaction is too strong, the condensate would collapse; if too weak, the condensate would be unable to form stable droplets. Hence, the formation of quantum droplets is a delicate process, requiring the right interplay between these terms.

5.2.3 Quantum Droplet Formation in Quasi-1D Systems

The formation of quantum droplets in quasi-1D systems involves the delicate balance between attractive interactions and repulsive quantum fluctuations. To achieve stable droplets, one must tune the interactions in such a way that the attractive part of the interaction is just compensated by the repulsive quantum fluctuations.

In quasi-1D systems, the longitudinal mean-field interaction and transverse confinement are correlated with the effective 1D interaction strength. The interaction strength in a quasi-1D gas is highly sensitive to the transverse trapping potential, and by adjusting this potential, the system can be tuned into a regime where quantum droplets form spontaneously.

Theoretical models have demonstrated that in quasi-1D systems, quantum droplets can be formed when the longitudinal density is sufficiently high, and the transverse confinement is tight enough to suppress the motion in the transverse directions. As the interaction strength reaches a critical value, quantum droplets emerge as self-bound structures that are stabilized by quantum fluctuations, rather than by external confinement.

5.2.4 Stability and Dynamics of Quasi-1D Quantum Droplets

Once quantum droplets are formed, their stability depends on the competition between the attractive contact interaction and the repulsive LHY correction. In the quasi-1D regime, these droplets are not necessarily stable under all conditions. Stability can be analyzed by examining the Bogoliubov excitations around the ground state. When these excitations have real frequencies, the droplet is stable; if any imaginary frequencies are found, the droplet is unstable and may undergo fragmentation or collapse.

In quasi-1D systems, the stability of quantum droplets can also be influenced by external perturbations, including changes in the transverse trapping potential or the introduction of impurities in the system. Numerical simulations using the GPE with LHY corrections can predict the dynamical behavior of these droplets, such as their oscillations, fragmentation, or merging, when subjected to small perturbations.

5.3 Experimental Realization of Quasi-1D Quantum Droplets

5.3.1 Experimental Setup for Quasi-1D Systems

To experimentally realize quantum droplets in quasi-1D systems, experimentalists typically use optical lattices or tight waveguides to confine atoms in the transverse directions. These setups create a quasi-1D regime by strongly confining the atoms in two directions while allowing free motion in the third dimension (along the longitudinal direction).

One of the main challenges in creating quasi-1D quantum droplets is to achieve the necessary transverse confinement while maintaining a sufficiently high density in the longitudinal direction to allow for droplet formation. This often involves fine-tuning parameters like the transverse trapping frequency $\omega_\perp$, which governs the quantum fluctuations and LHY effects.

5.3.2 First Experimental Observation of Quantum Droplets

The first experimental realization of quantum droplets in a quasi-1D system was achieved in dipolar Bose gases. Researchers used dysprosium atoms—which have a large magnetic dipole moment and exhibit strong dipole-dipole interactions—to create a quasi-1D condensate. By adjusting the magnetic field, the interaction strength was controlled, leading to the formation of stable quantum droplets.

In 2016, a breakthrough experiment led by Kadau et al. [134] demonstrated the creation of quantum droplets in dipolar Bose-Einstein condensates (BECs). The interaction between the dipolar and contact interactions caused the droplets to develop in the system. This experiment gave the first direct observation of these persistent self-bound structures in a low-dimensional system and validated the theoretical predictions of quantum droplet production.

5.3.3 Experimental Observations in Quasi-1D Dipolar Gases

Experiments on quasi-1D dipolar gases have shown that quantum droplets can form in quasi-1D systems under the right conditions. By using tight optical lattices or waveguides to confine the atoms in two dimensions and allowing free motion along the longitudinal direction, experimentalists have been able to tune the interaction strength and observe the formation of self-bound quantum droplets. These droplets were found to be stabilized by the combination of contact interactions and dipolar interactions, along with quantum fluctuations.

Recent experimental advances have provided more precise control over the parameters that affect the formation of quantum droplets, enabling researchers to study their dynamics, including oscillations, merging, and fragmentation.

5.4 Dynamics of Quasi-1D Quantum Droplets

Once quantum droplets form in quasi-1D systems, they exhibit unique dynamics governed by attractive and repulsive interactions. These interactions are largely dependent on the strength of contact interactions, which can typically be tuned via Feshbach resonances, and on dipolar interactions, if present, which provide an additional long-range repulsive force.

Contact interactions in quasi-1D systems are usually density-dependent and short-range, indicating that the strength of the connection varies with the system's longitudinal density. In contrast, dipolar interactions are long-range and anisotropic, meaning they decay as $1/r^3$and have different effects depending on the relative orientation of the dipoles.

When quantum droplets are close enough, their interactions can lead to a variety of fascinating phenomena, such as:

Merging: If two droplets are placed close to each other, their interactions can cause them to merge into a single, larger droplet.The relative sizes of the droplets and the type of contacts determine the dynamics of this process. Dipolar connections can alter this process by adding a repulsive force that slows the merging, whereas in the absence of dipolar interactions, merging is mostly driven by attractive contact interactions.

In a recent experiment, merging of droplets formed in a dipolar Bose-Einstein condensate (BEC) was observed when they were brought closely together. The dipolar in-

teractions lead to complex behavior that can stabilize the droplets at larger distances, preventing them from merging too quickly.

Oscillations and Breathing Modes: Quantum droplets can also exhibit breathing modes—oscillatory motions where the droplets expand and contract in response to changes in interaction strength or external perturbations. These oscillations are similar to collective modes observed in classical droplets, but in the quantum system, they are influenced by quantum fluctuations and nonlinearities caused by mean-field interactions.

The breathing frequencies of droplets are affected by the longitudinal density and transverse confinement. These oscillations are a signature of the droplet's stability and the competition between attractive and repulsive forces. In recent experiments, researchers excited these modes by introducing small perturbations into the system, and the resulting oscillations provided additional insights into the stability of quantum droplets in quasi-1D systems.

Fragmentation: Under certain conditions, quantum droplets in quasi-1D systems may fragment into multiple smaller droplets, especially when subjected to external perturbations or when interactions change. Fragmentation occurs when attractive mean-field interactions dominate and the quantum pressure from Lee-Huang-Yang (LHY) corrections is insufficient to stabilize the condensate. This causes the droplet to break apart into several smaller stable clusters.

The fragmentation process is highly sensitive to the system's density and interaction strength. Studies have shown that higher densities favor droplet formation, while lower densities may lead to the collapse or fragmentation of droplets into smaller clusters.

These dynamic behaviors provide important insights into the role of interactions and quantum fluctuations in stabilizing or destabilizing quasi-1D quantum droplets.

5.5 Conclusion

Quasi-one-dimensional quantum droplets represent an exciting area of research at the intersection of quantum mechanics, condensed matter physics, and ultracold atomic gases. The interplay between quantum fluctuations, mean-field interactions, and dimensionality

leads to the formation of stable, self-bound droplets, offering potential applications in fundamental physics and technological innovations.

Theoretical work, based on the Gross-Pitaevskii equation and beyond-mean-field effects such as Lee-Huang-Yang (LHY) corrections, has provided a robust framework for understanding these droplets. Experimental validations in dipolar gases, binary Bose mixtures, and quasi-one-dimensional traps have confirmed theoretical predictions and opened new avenues for deeper exploration.

As research in this field continues, we can anticipate further exciting discoveries that will deepen our understanding of quantum matter in low dimensions and potentially lead to new applications in quantum technologies.

General Conclusion

In the first part, we discussed the general properties of the condensate as well as the techniques used for cooling and trapping.

In the second part of this thesis, we began by deriving the Gross-Pitaevskii equation (GPE) that describes the behavior of Bose-Einstein Condensates, and then examined its validity and limitations. This led us to explore what lies beyond the GPE, prompting us to derive the time-dependent Hartree-Fock-Bogoliubov (TDHFB) equations for a single component Bose-Einstein Condensates using the time-dependent variational principle of Balian and Vénéroni.

In the third part of our thesis, we analyzed the equilibrium properties of a binary mixture. Utilizing a Gaussian density operator, we derived a set of eight coupled equations of motion for a self-interacting trapped Bose gas using the time-dependent variational principle of Balian and Vénéroni. These equations self-consistently govern the dynamics of the condensate, the non-condensate, the anomalous average and interspeices fluctuation. As a result, we obtained the TDHFB equations for the binary 1D homogeneous mixture .

Next, when we neglected quantitative fluctuations, we derive analytic expressions for both the anomalous and non-condensate densities in one-dimensional system. Numerical computations of the anomalous averages and non-condensate densities for a 1D homogeneous Bose mixture at zero temperature reveal that Popov's theory is incorrect regarding the anomalous density, showing it retains a non-zero value at T=0.

Additionally, we examined the TDHFB equation solutions at finite temperature and discussed about how the anomalous and non-condensate densities behaved. More significantly, we found that when temperature is included, the anomalous densities do not have the same order of magnitude as the non-condensate.

In the fourth part, we derive generalized stability conditions to address collapse and phase separation, incorporating the effects of interspecies fluctuations. These conditions extend and refine the well-known stability criteria.

Furthermore, within the framework of Bogoliubov's approach, interspecies fluctuations are found to be of the same order of magnitude as the LHY terms. Therefore, their omission, as is commonly assumed, is no longer justified in the general case.

Notably, near the droplet regime, interspecies fluctuations are shown to reinforce the traditional LHY effects, resulting in more stable self-bound droplets.

In the last chapter, we present the theoretical and experimental aspects of quasi-one dimensional droplets.

Bibliography

[1] L. P. Pitaevskii, "Vortex lines in an imperfect bose gas," *Sov. Phys. JETP*, vol. 13, no. 2, pp. 451–454, 1961.

[2] A. Einstein, "Zur quantentheorie des idealen gases," *Albert Einstein: Akademie-Vorträge: Sitzungsberichte der Preußischen Akademie der Wissenschaften 1914–1932*, pp. 258–266, 2005.

[3] W. C. Stwalley and L. Nosanow, "Possible" new" quantum systems," *Physical Review Letters*, vol. 36, no. 15, p. 910, 1976.

[4] T. J. Greytak and D. Kleppner, "Lectures on spin-polarized hydrogen," in *New trends in atomic physics*, 1984.

[5] D. G. Fried, T. C. Killian, L. Willmann, D. Landhuis, S. C. Moss, D. Kleppner, and T. J. Greytak, "Bose-einstein condensation of atomic hydrogen," *Physical Review Letters*, vol. 81, no. 18, p. 3811, 1998.

[6] S. Chu, "Nobel lecture: The manipulation of neutral particles," *Reviews of Modern Physics*, vol. 70, no. 3, p. 685, 1998.

[7] C. N. Cohen-Tannoudji, "Nobel lecture: Manipulating atoms with photons," *Reviews of Modern Physics*, vol. 70, no. 3, p. 707, 1998.

[8] M. H. Anderson, J. R. Ensher, M. R. Matthews, C. E. Wieman, and E. A. Cornell, "Observation of bose-einstein condensation in a dilute atomic vapor," *science*, vol. 269, no. 5221, pp. 198–201, 1995.

[9] K. B. Davis, M.-O. Mewes, M. R. Andrews, N. J. van Druten, D. S. Durfee, D. Kurn, and W. Ketterle, "Bose-einstein condensation in a gas of sodium atoms," *Physical review letters*, vol. 75, no. 22, p. 3969, 1995.

[10] E. A. Cornell and C. E. Wieman, "Nobel lecture: Bose-einstein condensation in a dilute gas, the first 70 years and some recent experiments," *Reviews of Modern Physics*, vol. 74, no. 3, p. 875, 2002.

[11] W. Ketterle, "Nobel lecture: When atoms behave as waves: Bose-einstein condensation and the atom laser," *Reviews of Modern Physics*, vol. 74, no. 4, p. 1131, 2002.

[12] C. Myatt, E. Burt, R. Ghrist, E. A. Cornell, and C. Wieman, "Production of two overlapping bose-einstein condensates by sympathetic cooling," *Physical Review Letters*, vol. 78, no. 4, p. 586, 1997.

[13] D. Stamper-Kurn, M. Andrews, A. Chikkatur, S. Inouye, H.-J. Miesner, J. Stenger, and W. Ketterle, "Optical confinement of a bose-einstein condensate," *Physical Review Letters*, vol. 80, no. 10, p. 2027, 1998.

[14] D. Hall, M. Matthews, J. Ensher, C. Wieman, and E. A. Cornell, "Dynamics of component separation in a binary mixture of bose-einstein condensates," *Physical Review Letters*, vol. 81, no. 8, p. 1539, 1998.

[15] J. Martin, C. McKenzie, N. Thomas, J. Sharpe, D. Warrington, P. Manson, W. Sandle, and A. Wilson, "Output coupling of a bose-einstein condensate formed in a top trap," *Journal of Physics B: Atomic, Molecular and Optical Physics*, vol. 32, no. 12, p. 3065, 1999.

[16] P. Maddaloni, M. Modugno, C. Fort, F. Minardi, and M. Inguscio, "Collective oscillations of two colliding bose-einstein condensates," *Physical review letters*, vol. 85, no. 12, p. 2413, 2000.

[17] T.-L. Ho, "Vb shenoy binary mixtures of bose condensates of alkali atoms phys," *Rev. Lett*, vol. 77, p. 3276, 1996.

[18] R. Barankov, "Boundary of two mixed bose-einstein condensates," *Physical Review A*, vol. 66, no. 1, p. 013612, 2002.

[19] H. Pu and N. Bigelow, "Collective excitations, metastability, and nonlinear response of a trapped two-species bose-einstein condensate," *Physical review letters*, vol. 80, no. 6, p. 1134, 1998.

[20] S. K. Adhikari, "Coupled bose-einstein condensate: Collapse for attractive interaction," *Physical Review A*, vol. 63, no. 4, p. 043611, 2001.

[21] M. Cazalilla and A. Ho, "Instabilities in binary mixtures of one-dimensional quantum degenerate gases," *Physical review letters*, vol. 91, no. 15, p. 150403, 2003.

[22] A. Smerzi, S. Fantoni, S. Giovanazzi, and S. Shenoy, "Quantum coherent atomic tunneling between two trapped bose-einstein condensates," *Physical Review Letters*, vol. 79, no. 25, p. 4950, 1997.

[23] G.-H. Chen and Y.-S. Wu, "Quantum phase transition in a multicomponent bose-einstein condensate in optical lattices," *Physical Review A*, vol. 67, no. 1, p. 013606, 2003.

[24] J. Smyrnakis, S. Bargi, G. Kavoulakis, M. Magiropoulos, K. Kärkkäinen, and S. Reimann, "Mixtures of bose gases confined in a ring potential," *Physical review letters*, vol. 103, no. 10, p. 100404, 2009.

[25] A. Chikkatur, A. Görlitz, D. Stamper-Kurn, S. Inouye, S. Gupta, and W. Ketterle, "Suppression and enhancement of impurity scattering in a bose-einstein condensate," *Physical review letters*, vol. 85, no. 3, p. 483, 2000.

[26] M. Bruderer, W. Bao, and D. Jaksch, "Self-trapping of impurities in bose-einstein condensates: Strong attractive and repulsive coupling," *Europhysics Letters*, vol. 82, no. 3, p. 30004, 2008.

[27] D. M. Stamper-Kurn and M. Ueda, "Spinor bose gases: Explorations of symmetries, magnetism and quantum dynamics," *arXiv preprint arXiv:1205.1888*, 2012.

[28] M. Rizzi and A. Imambekov, "Pairing of one-dimensional bose-fermi mixtures with unequal masses," *Physical Review A—Atomic, Molecular, and Optical Physics*, vol. 77, no. 2, p. 023621, 2008.

[29] S. Akhanjee, "Quantum phase coherence in non-markovian and reaction-diffusive transport," *Physical Review B—Condensed Matter and Materials Physics*, vol. 82, no. 5, p. 054201, 2010.

[30] Y.-J. Hao, "Ground state density distribution of bose-fermi mixture in a one-dimensional harmonic trap," *Chinese Physics Letters*, vol. 28, no. 1, p. 010302, 2011.

[31] J. Čížek, "On the use of the cluster expansion and the technique of diagrams in calculations of correlation effects in atoms and molecules," *Advances in chemical physics*, vol. 14, pp. 35–89, 1969.

[32] M. Benarous, "Variational multi-time green's functions for nonequilibrium quantum fields," *Annals of Physics*, vol. 269, no. 2, pp. 107–128, 1998.

[33] R. Balian and M. Veneroni, "Static and dynamic variational principles for expectation values of observables," *Annals of Physics*, vol. 187, no. 1, pp. 29–78, 1988.

[34] M. Benarous and H. Flocard, "Time-dependent variational approach for boson systems," *Annals of Physics*, vol. 273, no. 2, pp. 242–266, 1999.

[35] A. Boudjemâa and M. Benarous, "Anomalous density for bose gases at finite temperature," *Physical Review A—Atomic, Molecular, and Optical Physics*, vol. 84, no. 4, p. 043633, 2011.

[36] M. Benarous, "Anomalous effects in a trapped bose-einstein condensate," *The European Physical Journal D*, vol. 67, no. 11, p. 243, 2013.

[37] A. Mehedi, M. Benarous, and A. Hocine, "Enhanced stability of self-bound droplets in quasi-one dimension via interspecies quantum fluctuations in ultracold bose–bose mixtures," *Journal of Low Temperature Physics*, pp. 1–13, 2024.

[38] M. Benarous, A. Hocine, and A. Mehedi, "Generalized stability conditions for binary bose mixtures," *arXiv preprint arXiv:2308.13608*, 2023.

[39] L. Pitaevskii and S. Stringari, *Bose-Einstein condensation and superfluidity*, vol. 164. Oxford University Press, 2016.

[40] W. D. Phillips, J. V. Prodan, and H. J. Metcalf, "Laser cooling and electromagnetic trapping of neutral atoms," *Journal of the Optical Society of America B*, vol. 2, no. 11, pp. 1751–1767, 1985.

[41] R. Balian and M. Vénéroni, "Fluctuations in a time-dependent mean-field approach," *Physics Letters B*, vol. 136, no. 5-6, pp. 301–306, 1984.

[42] J. E. Robinson, "Note on the bose-einstein integral functions," *Physical Review*, vol. 83, no. 3, p. 678, 1951.

[43] P. C. Hohenberg, "Existence of long-range order in one and two dimensions," *Physical Review*, vol. 158, no. 2, p. 383, 1967.

[44] V. Bagnato and D. Kleppner, "Bose-einstein condensation in low-dimensional traps," *Physical Review A*, vol. 44, no. 11, p. 7439, 1991.

[45] M. Zwierlein, C. Schunck, C. Stan, S. Raupach, and W. Ketterle, "Formation dynamics of a fermion pair condensate," *Physical review letters*, vol. 94, no. 18, p. 180401, 2005.

[46] A. Posazhennikova, "Colloquium: Weakly interacting, dilute bose gases in 2d," *Reviews of modern physics*, vol. 78, no. 4, pp. 1111–1134, 2006.

[47] K. Huang, *Quantum field theory: From operators to path integrals*. John Wiley & Sons, 2010.

[48] L. Schiff, "Quantum mechanics mcgraw-hill book co," *Inc., New York (195), Sec, vol.* 27, 1949.

[49] N. Bogoliubov, "Energy levels of the imperfect bose-einstein gas," *Bull. Moscow State Univ*, vol. 7, pp. 43–56, 1947.

[50] A. L. Fetter, "Nonuniform states of an imperfect bose gas," *Annals of physics*, vol. 70, no. 1, pp. 67–101, 1972.

[51] E. P. Gross, "Structure of a quantized vortex in boson systems," *Il Nuovo Cimento (1955-1965)*, vol. 20, no. 3, pp. 454–477, 1961.

[52] V. Ginzburg and L. Landau, "Zh. eksp. teor. fiz.," *Zh. Eksp. Teor. Fiz*, vol. 20, p. 1064, 1950.

[53] M. Edwards and K. Burnett, "Numerical solution of the nonlinear schrödinger equation for small samples of trapped neutral atoms," *Physical Review A*, vol. 51, no. 2, p. 1382, 1995.

[54] M. Edwards, R. Dodd, C. W. Clark, and K. Burnett, "Zero-temperature, mean-field theory of atomic bose-einstein condensates," *Journal of research of the National Institute of Standards and Technology*, vol. 101, no. 4, p. 553, 1996.

[55] C. Gardiner, "Particle-number-conserving bogoliubov method which demonstrates the validity of the time-dependent gross-pitaevskii equation for a highly condensed bose gas," *Physical Review A*, vol. 56, no. 2, p. 1414, 1997.

[56] C. Trallero-Giner, J. C. Drake-Perez, V. López-Richard, and J. L. Birman, "Formal analytical solutions for the gross–pitaevskii equation," *Physica D: Nonlinear Phenomena*, vol. 237, no. 18, pp. 2342–2352, 2008.

[57] M. Girardeau, "Comment on "particle-number-conserving bogoliubov method which demonstrates the validity of the time-dependent gross-pitaevskii equation for a highly condensed bose gas"," *Physical Review A*, vol. 58, no. 1, p. 775, 1998.

[58] P. T. Nam, N. Rougerie, and R. Seiringer, "Ground states of large bosonic systems: the gross–pitaevskii limit revisited," *Analysis & PDE*, vol. 9, no. 2, pp. 459–485, 2016.

[59] H. Veksler, S. Fishman, and W. Ketterle, "Simple model for interactions and corrections to the gross-pitaevskii equation," *Physical Review A*, vol. 90, no. 2, p. 023620, 2014.

[60] C. J. Pethick and H. Smith, *Bose–Einstein condensation in dilute gases*. Cambridge university press, 2008.

[61] S. Rajendran, P. Muruganandam, and M. Lakshmanan, "Bright and dark solitons in a quasi-1d bose–einstein condensates modelled by 1d gross–pitaevskii equation with time-dependent parameters," *Physica D: Nonlinear Phenomena*, vol. 239, no. 7, pp. 366–386, 2010.

[62] A. Mohamadou, E. Wamba, S. Y. Doka, T. B. Ekogo, and T. C. Kofane, "Generation of matter-wave solitons of the gross-pitaevskii equation with a time-dependent complicated potential," *Physical Review A—Atomic, Molecular, and Optical Physics*, vol. 84, no. 2, p. 023602, 2011.

[63] A. Griffin, "Conserving and gapless approximations for an inhomogeneous bose gas at finite temperatures," *Physical Review B*, vol. 53, no. 14, p. 9341, 1996.

[64] N. Proukakis and K. Burnett, "Generalized mean fields for trapped atomic bose-einstein condensates," *Journal of research of the National Institute of Standards and Technology*, vol. 101, no. 4, p. 457, 1996.

[65] T. Köhler and K. Burnett, "Microscopic quantum dynamics approach to the dilute condensed bose gas," *Physical Review A*, vol. 65, no. 3, p. 033601, 2002.

[66] S. A. Morgan, "A gapless theory of bose-einstein condensation in dilute gases at finite temperature," *Journal of Physics B: Atomic, Molecular and Optical Physics*, vol. 33, no. 19, p. 3847, 2000.

[67] E. Timmermans, P. Tommasini, and K. Huang, "Variational thomas-fermi theory of a nonuniform bose condensate at zero temperature," *Physical Review A*, vol. 55, no. 5, p. 3645, 1997.

[68] M. Benarous, "Bec from a time-dependent variational point of view," *Annals of Physics*, vol. 320, no. 1, pp. 226–236, 2005.

[69] R. Balian and M. Vénéroni, "Lyapunov stability and poisson structure of the thermal tdhf and rpa equations," *Annals of Physics*, vol. 195, no. 2, pp. 324–355, 1989.

[70] C. Gies, M. Lee, and D. Hutchinson, "Many-body t-matrix of a two-dimensional bose–einstein condensate within the hartree–fock–bogoliubov formalism," *Journal of Physics B: Atomic, Molecular and Optical Physics*, vol. 38, no. 11, p. 1797, 2005.

[71] D. Hutchinson, K. Burnett, R. Dodd, S. Morgan, M. Rusch, E. Zaremba, N. Proukakis, M. Edwards, and C. Clark, "Gapless mean-field theory of bose-einstein condensates," *Journal of Physics B: Atomic, Molecular and Optical Physics*, vol. 33, no. 19, p. 3825, 2000.

[72] S. Kouidri and M. Benarous, "Non-thomas–fermi behaviour of a finite-temperature bose–einstein condensate in the presence of a thermal cloud," *Journal of Physics B: Atomic, Molecular and Optical Physics*, vol. 44, no. 20, p. 205301, 2011.

[73] G. Bruun, Y. Castin, R. Dum, and K. Burnett, "Bcs theory for trapped ultracold fermions," *The European Physical Journal D-Atomic, Molecular, Optical and Plasma Physics*, vol. 7, pp. 433–439, 1999.

[74] A. Bulgac and Y. Yu, "Renormalization of the hartree-fock-bogoliubov equations in the case of a zero range pairing interaction," *Physical review letters*, vol. 88, no. 4, p. 042504, 2002.

[75] L. Pricoupenko, "Implicit ladder summation in the hartree-fock-bogoliubov approach," *Physical Review A—Atomic, Molecular, and Optical Physics*, vol. 84, no. 5, p. 053602, 2011.

[76] M. Olshanii and L. Pricoupenko, "Rigorous approach to the problem of ultraviolet divergencies in dilute bose gases," *Physical review letters*, vol. 88, no. 1, p. 010402, 2001.

[77] P. Schuck and X. Vinas, "Thomas-fermi approximation for bose-einstein condensates in traps," *Physical Review A*, vol. 61, no. 4, p. 043603, 2000.

[78] N. Hugenholtz and D. Pines, "Ground-state energy and excitation spectrum of a system of interacting bosons," *Physical Review*, vol. 116, no. 3, p. 489, 1959.

[79] H. Shi and A. Griffin, "Finite-temperature excitations in a dilute bose-condensed gas," *Physics Reports*, vol. 304, no. 1-2, pp. 1–87, 1998.

[80] P. Ring and P. Schuck, *The nuclear many-body problem*. Springer Science & Business Media, 2004.

[81] M. Günay, "Binary mixture of bose-einstein condensates in a double-well potential: Berry phase and two-mode entanglement," *Physical Review A*, vol. 101, no. 4, p. 043608, 2020.

[82] P. Tedrow and D. Lee, "Liquid-solid phase transition in he 3-he 4 mixtures," *Physical Review*, vol. 181, no. 1, p. 399, 1969.

[83] E. A. Cornell, J. R. Ensher, and C. E. Wieman, "Experiments in dilute atomic bose-einstein condensation," in *Bose-Einstein Condensation in Atomic Gases*, pp. 15–66, IOS Press, 1999.

[84] S. Papp, J. Pino, and C. Wieman, "Tunable miscibility in a dual-species bose-einstein condensate," *Physical review letters*, vol. 101, no. 4, p. 040402, 2008.

[85] P. Altin, N. Robins, D. Döring, J. Debs, R. Poldy, C. Figl, and J. Close, "R85b tunable-interaction bose–einstein condensate machine," *Review of Scientific Instruments*, vol. 81, no. 6, 2010.

[86] G. Thalhammer, G. Barontini, L. De Sarlo, J. Catani, F. Minardi, and M. Inguscio, "Double species bose-einstein condensate with tunable interspecies interactions," *Physical review letters*, vol. 100, no. 21, p. 210402, 2008.

[87] K. Pilch, A. Lange, A. Prantner, G. Kerner, F. Ferlaino, H.-C. Nägerl, and R. Grimm, "Observation of interspecies feshbach resonances in an ultracold rb-cs mixture," *Physical Review A—Atomic, Molecular, and Optical Physics*, vol. 79, no. 4, p. 042718, 2009.

[88] D. McCarron, H. Cho, D. Jenkin, M. Köppinger, and S. Cornish, "Dual-species bose-einstein condensate of rb 87 and cs 133," *Physical Review A—Atomic, Molecular, and Optical Physics*, vol. 84, no. 1, p. 011603, 2011.

[89] F. Baumer, F. Münchow, A. Görlitz, S. E. Maxwell, P. S. Julienne, and E. Tiesinga, "Spatial separation in a thermal mixture of ultracold yb 174 and rb 87 atoms," *Physical Review A—Atomic, Molecular, and Optical Physics*, vol. 83, no. 4, p. 040702, 2011.

[90] M. R. Matthews, B. P. Anderson, P. Haljan, D. Hall, C. Wieman, and E. A. Cornell, "Vortices in a bose-einstein condensate," *Physical Review Letters*, vol. 83, no. 13, p. 2498, 1999.

[91] H.-J. Miesner, D. Stamper-Kurn, J. Stenger, S. Inouye, A. Chikkatur, and W. Ketterle, "Observation of metastable states in spinor bose-einstein condensates," *Physical Review Letters*, vol. 82, no. 11, p. 2228, 1999.

[92] D. Stamper-Kurn, H.-J. Miesner, A. Chikkatur, S. Inouye, J. Stenger, and W. Ketterle, "Quantum tunneling across spin domains in a bose-einstein condensate," *Physical review letters*, vol. 83, no. 4, p. 661, 1999.

[93] S. Tojo, Y. Taguchi, Y. Masuyama, T. Hayashi, H. Saito, and T. Hirano, "Controlling phase separation of binary bose-einstein condensates via mixed-spin-channel feshbach resonance," *Physical Review A—Atomic, Molecular, and Optical Physics*, vol. 82, no. 3, p. 033609, 2010.

[94] T.-L. Ho and V. Shenoy, "Binary mixtures of bose condensates of alkali atoms," *Physical review letters*, vol. 77, no. 16, p. 3276, 1996.

[95] A. Alexandrov and V. V. Kabanov, "Excitations and phase segregation in a two-component bose-einstein condensate with an arbitrary interaction," *Journal of Physics: Condensed Matter*, vol. 14, no. 18, p. L327, 2002.

[96] P. Ao and S. Chui, "Binary bose-einstein condensate mixtures in weakly and strongly segregated phases," *Physical Review A*, vol. 58, no. 6, p. 4836, 1998.

[97] R. Ejnisman, H. Pu, Y. E. Young, N. P. Bigelow, and C. Law, "Studies of two-species bose-einstein condensation," *Optics express*, vol. 2, no. 8, pp. 330–337, 1998.

[98] R. Pattinson, T. Billam, S. Gardiner, D. McCarron, H. Cho, S. Cornish, N. Parker, and N. Proukakis, "Equilibrium solutions for immiscible two-species bose-einstein condensates in perturbed harmonic traps," *Physical Review A—Atomic, Molecular, and Optical Physics*, vol. 87, no. 1, p. 013625, 2013.

[99] H. Pu and N. Bigelow, "Properties of two-species bose condensates," *Physical review letters*, vol. 80, no. 6, p. 1130, 1998.

[100] S. Ronen, J. L. Bohn, L. E. Halmo, and M. Edwards, "Dynamical pattern formation during growth of a dual-species bose-einstein condensate," *Physical Review A—Atomic, Molecular, and Optical Physics*, vol. 78, no. 5, p. 053613, 2008.

[101] A. Sinatra and Y. Castin, "Binary mixtures of bose-einstein condensates: Phase dynamics and spatial dynamics," *The European Physical Journal D*, vol. 8, pp. 319–332, 2000.

[102] A. A. Svidzinsky and S.-T. Chui, "Symmetric-asymmetric transition in mixtures of bose-einstein condensates," *Physical Review A*, vol. 67, no. 5, p. 053608, 2003.

[103] E. Timmermans, "Phase separation of bose-einstein condensates," *Physical review letters*, vol. 81, no. 26, p. 5718, 1998.

[104] M. Trippenbach, K. Góral, K. Rzazewski, B. Malomed, and Y. Band, "Structure of binary bose-einstein condensates," *Journal of Physics B: Atomic, Molecular and Optical Physics*, vol. 33, no. 19, p. 4017, 2000.

[105] R. Graham and D. Walls, "Collective excitations of trapped binary mixtures of bose-einstein condensed gases," *Physical Review A*, vol. 57, no. 1, p. 484, 1998.

[106] T. Busch, J. Cirac, V. Pérez-García, and P. Zoller, "Stability and collective excitations of a two-component bose-einstein condensed gas: A moment approach," *Physical Review A*, vol. 56, no. 4, p. 2978, 1997.

[107] D. V. Skryabin, "Instabilities of vortices in a binary mixture of trapped bose-einstein condensates: Role of collective excitations with positive and negative energies," *Physical Review A*, vol. 63, no. 1, p. 013602, 2000.

[108] G. Lamporesi, "Two-component spin mixtures," *arXiv preprint arXiv:2304.03711*, 2023.

[109] W. Wang, V. Penna, and B. Capogrosso-Sansone, "Inter-species entanglement of bose–bose mixtures trapped in optical lattices," *New Journal of Physics*, vol. 18, no. 6, p. 063002, 2016.

[110] F. Lingua, A. Richaud, and V. Penna, "Residual entropy and critical behavior of two interacting boson species in a double well," *Entropy*, vol. 20, no. 2, p. 84, 2018.

[111] D. Hutchinson, R. Dodd, and K. Burnett, "Gapless finite-t theory of collective modes of a trapped gas," *Physical review letters*, vol. 81, no. 11, p. 2198, 1998.

[112] V. Chernyak, S. Choi, and S. Mukamel, "Generalized coherent state representation of bose-einstein condensates," *Physical Review A*, vol. 67, no. 5, p. 053604, 2003.

[113] S. Cormack and D. Hutchinson, "Finite-temperature dipolar ultracold bose gas with exchange interactions," *Physical Review A—Atomic, Molecular, and Optical Physics*, vol. 86, no. 5, p. 053619, 2012.

[114] H. Buljan, M. Segev, and A. Vardi, "Incoherent matter-wave solitons and pairing instability<? format?> in an attractively interacting bose-einstein condensate," *Physical review letters*, vol. 95, no. 18, p. 180401, 2005.

[115] I. Merhasin, B. A. Malomed, and Y. Band, "Partially incoherent gap solitons in bose-einstein condensates," *Physical Review A—Atomic, Molecular, and Optical Physics*, vol. 74, no. 3, p. 033614, 2006.

[116] O. E. Alon, A. I. Streltsov, and L. S. Cederbaum, "Multiconfigurational time-dependent hartree method for mixtures consisting of two types of identical particles," *Physical Review A—Atomic, Molecular, and Optical Physics*, vol. 76, no. 6, p. 062501, 2007.

[117] N. Guebli and A. Boudjemâa, "Effects of quantum fluctuations on the dynamics of dipolar bose polarons," *Journal of Physics B: Atomic, Molecular and Optical Physics*, vol. 52, no. 18, p. 185303, 2019.

[118] D. Hutchinson, E. Zaremba, and A. Griffin, "Finite temperature excitations of a trapped bose gas," *Physical review letters*, vol. 78, no. 10, p. 1842, 1997.

[119] F. Dalfovo, S. Giorgini, L. P. Pitaevskii, and S. Stringari, "Theory of bose-einstein condensation in trapped gases," *Reviews of modern physics*, vol. 71, no. 3, p. 463, 1999.

[120] C. D'Errico, A. Burchianti, M. Prevedelli, L. Salasnich, F. Ancilotto, M. Modugno, F. Minardi, and C. Fort, "Observation of quantum droplets in a heteronuclear bosonic mixture," *Physical Review Research*, vol. 1, no. 3, p. 033155, 2019.

[121] D. Petrov, "Quantum mechanical stabilization of a collapsing bose-bose mixture," *Physical review letters*, vol. 115, no. 15, p. 155302, 2015.

[122] M. Ota and G. E. Astrakharchik, "Beyond lee-huang-yang description of self-bound bose mixtures," *SciPost Physics*, vol. 9, no. 2, p. 020, 2020.

[123] M. Tylutki, G. E. Astrakharchik, B. A. Malomed, and D. S. Petrov, "Collective excitations of a one-dimensional quantum droplet," *Physical Review A*, vol. 101, no. 5, p. 051601, 2020.

[124] I. Englezos, S. I. Mistakidis, and P. Schmelcher, "Correlated dynamics of collective droplet excitations in a one-dimensional harmonic trap," *Physical Review A*, vol. 107, no. 2, p. 023320, 2023.

[125] D. Petrov and G. Astrakharchik, "Ultradilute low-dimensional liquids," *Physical review letters*, vol. 117, no. 10, p. 100401, 2016.

[126] S. Sinha, S. Biswas, L. Santos, and S. Sinha, "Impurities in quasi-one-dimensional droplets of binary bose mixtures," *Physical Review A*, vol. 108, no. 2, p. 023311, 2023.

[127] D. M. Larsen, "Binary mixtures of dilute bose gases with repulsive interactions at low temperature," *Annals of Physics (New York)(US)*, vol. 24, 1963.

[128] V. Mineev, "The theory of the solution of two near-ideal bose gases," *Zh. Eksp. Teor. Fiz*, vol. 67, no. 1, p. 263, 1974.

[129] F. Kh. ABDULLAEV, A. Gammal, A. M. Kamchatnov, and L. Tomio, "Dynamics of bright matter wave solitons in a bose–einstein condensate," *International Journal of Modern Physics B*, vol. 19, no. 22, pp. 3415–3473, 2005.

[130] Z.-H. Luo, W. Pang, B. Liu, Y.-Y. Li, and B. A. Malomed, "A new form of liquid matter: Quantum droplets," *Frontiers of Physics*, vol. 16, pp. 1–21, 2021.

[131] T. D. Lee, K. Huang, and C. N. Yang, "Eigenvalues and eigenfunctions of a bose system of hard spheres and its low-temperature properties," *Physical Review*, vol. 106, no. 6, p. 1135, 1957.

[132] K. E. Strecker, G. B. Partridge, A. G. Truscott, and R. G. Hulet, "Formation and propagation of matter-wave soliton trains," *Nature*, vol. 417, no. 6885, pp. 150–153, 2002.

[133] B. Malomed, "Multidimensional solitons, aip publishing (online), melville," *New York*, 2022.

[134] H. Kadau, M. Schmitt, M. Wenzel, C. Wink, T. Maier, I. Ferrier-Barbut, and T. Pfau, "Observing the rosensweig instability of a quantum ferrofluid," *Nature*, vol. 530, no. 7589, pp. 194–197, 2016.

[135] I. Ferrier-Barbut, H. Kadau, M. Schmitt, M. Wenzel, and T. Pfau, "Observation of quantum droplets in a strongly dipolar bose gas," *Physical review letters*, vol. 116, no. 21, p. 215301, 2016.

[136] C. Cabrera, L. Tanzi, J. Sanz, B. Naylor, P. Thomas, P. Cheiney, and L. Tarruell, "Quantum liquid droplets in a mixture of bose-einstein condensates," *Science*, vol. 359, no. 6373, pp. 301–304, 2018.

[137] P. Cheiney, C. Cabrera, J. Sanz, B. Naylor, L. Tanzi, and L. Tarruell, "Bright soliton to quantum droplet transition in a mixture of bose-einstein condensates," *Physical review letters*, vol. 120, no. 13, p. 135301, 2018.

[138] G. Semeghini, G. Ferioli, L. Masi, C. Mazzinghi, L. Wolswijk, F. Minardi, M. Modugno, G. Modugno, M. Inguscio, and M. Fattori, "Self-bound quantum droplets of atomic mixtures in free space," *Physical review letters*, vol. 120, no. 23, p. 235301, 2018.

[139] G. Ferioli, G. Semeghini, L. Masi, G. Giusti, G. Modugno, M. Inguscio, A. Gallemí, A. Recati, and M. Fattori, "Collisions of self-bound quantum droplets," *Physical review letters*, vol. 122, no. 9, p. 090401, 2019.

[140] P. Zin, M. Pylak, T. Wasak, M. Gajda, and Z. Idziaszek, "Quantum bose-bose droplets at a dimensional crossover," *Physical Review A*, vol. 98, no. 5, p. 051603, 2018.

[141] T. Ilg, J. Kumlin, L. Santos, D. S. Petrov, and H. P. Büchler, "Dimensional crossover for the beyond-mean-field correction in bose gases," *Physical Review A*, vol. 98, no. 5, p. 051604, 2018.

[142] L. Lavoine and T. Bourdel, "Beyond-mean-field crossover from one dimension to three dimensions in quantum droplets of binary mixtures," *Physical Review A*, vol. 103, no. 3, p. 033312, 2021.

[143] S. R. Otajonov, E. N. Tsoy, and F. K. Abdullaev, "Stationary and dynamical properties of one-dimensional quantum droplets," *Physics Letters A*, vol. 383, no. 34, p. 125980, 2019.

[144] G. Astrakharchik and B. A. Malomed, "Dynamics of one-dimensional quantum droplets," *Physical Review A*, vol. 98, no. 1, p. 013631, 2018.

[145] Y. V. Kartashov, V. M. Lashkin, M. Modugno, and L. Torner, "Spinor-induced instability of kinks, holes and quantum droplets," *New Journal of Physics*, vol. 24, no. 7, p. 073012, 2022.

[146] A. Debnath, A. Khan, and B. Malomed, "Interaction of one-dimensional quantum droplets with potential wells and barriers," *Communications in Nonlinear Science and Numerical Simulation*, vol. 126, p. 107457, 2023.

[147] A. Debnath and A. Khan, "Investigation of quantum droplets: An analytical approach," *Annalen der Physik*, vol. 533, no. 3, p. 2000549, 2021.

[148] A. Debnath, A. Khan, and S. Basu, "Dropleton-soliton crossover mediated via trap modulation," *Physics Letters A*, vol. 439, p. 128137, 2022.

[149] S. S. Adusumalli, K. Senapati, S. Singh, and A. Khan, "Quantum liquid in lower dimensions: From the perspective of surface tension," *Physics Letters A*, p. 129638, 2024.

[150] A. Debnath, A. Khan, and P. K. Panigrahi, "Dynamics of bright soliton under cubic-quartic interactions in quasi-one-dimensional geometry," *The European Physical Journal Plus*, vol. 138, no. 10, pp. 1–14, 2023.

Appendix A

Appendix

In this Appendix, we show a detailed derivation of the dynamics of a trapped ultracold bose-bose mixture, by using the time dependent variational principle of Balian-Veneroni

A.1 The Balian-Vénéroni variational principle

Balian and -Vénéroni (BV) [32–36]have introduced the action-like functional:

$$\mathcal{I}\{\mathcal{D}(t),\mathcal{A}(t)\} = \mathrm{Tr}\, A\mathcal{D}\,(t_1) - \int_{t_0}^{t_1} \mathrm{d}t\, \mathrm{Tr}\,\mathcal{A}\left(\frac{\mathrm{d}\mathcal{D}}{\mathrm{d}t} + \frac{i}{\hbar}[H,\mathcal{D}]\right) \tag{A.1}$$

The operators $\mathcal{D}(t)$ and $\mathcal{A}(t)$, which resemble a density operator and an observable, respectively, serve as the variational quantities. H represents the Hamiltonian of the system..

Once the variational spaces for $\mathcal{D}$ and $\mathcal{A}$ are defined, the stationary value of the action(2.1)gives the optimal estimate of $\mathrm{Tr}\, AD\,(t_1)$ for a given initial time t_0 and measurement time t_1.
The stationarity conditions with respect to variations of $\mathcal{A}$ and $\mathcal{D}$ read:

$$\begin{cases} \mathrm{Tr}\,\delta\mathcal{A}\left(\frac{\mathrm{d}\mathcal{D}}{\mathrm{d}t} + \frac{i}{\hbar}[H,\mathcal{D}]\right) = 0 \\ \mathrm{Tr}\,\delta\mathcal{D}\left(\frac{\mathrm{d}\mathcal{A}}{\mathrm{d}t} - \frac{i}{\hbar}[\mathcal{A},H]\right) = 0 \end{cases} \tag{A.2}$$

In order to treat binary mixtures, one has to introduce first a density operator for the global system $D = D_1 D_2$, where it should be noted that D_1 and D_2 define two disjoint Fock spaces.

In the exact scenario, the true density operator D of the system satisfies the Liouville-

von Neumann equation:

$$\frac{\mathrm{d}D}{\mathrm{d}t} + \frac{i}{\hbar}[H, D] = 0 \tag{A.3}$$

Let us consider the Fock space generated by n creation bose field operators $a_i^+$for the first and and $b_i^+$for the second $(i = 1 \ldots . n)$.Since we will be working with linear and quadratic forms that involve both the a_i^+'s and the b_i^+'s, along with their Hermitian conjugates, the a_i 's and b_i 's, it is convenient to introduce the $2n$-operators α and β, whose components α_i and β_i are:

$$\begin{pmatrix} \alpha_1 \\ \vdots \\ \alpha_n \\ \alpha_{n+1} \\ \vdots \\ \alpha_{2n}^+ \end{pmatrix} = \begin{pmatrix} a_1 \\ \vdots \\ a_n^1 \\ a_1^+ \\ \vdots \\ a_n^+ \end{pmatrix}, \begin{pmatrix} \beta_1 \\ \vdots \\ \beta_n \\ \beta_{n+1} \\ \vdots \\ \beta_{2n}^+ \end{pmatrix} = \begin{pmatrix} b_1 \\ \vdots \\ b_n \\ b_1^+ \\ \vdots \\ b_n^+ \end{pmatrix}. \tag{A.4}$$

In terms of the latter operators, the canonical boson commutation rules are expressed by the relations

$$[\alpha_i, \alpha_j] = [\beta_i, \beta_j] = \tau_{ij} \quad , \quad \tau = \begin{pmatrix} 0 & 1_n \\ -1_n & 0 \end{pmatrix}, \tag{A.5}$$

and

$$[\alpha_i, \beta_j] = 0 \tag{A.6}$$

where τ is the (4×4) symplectic matrix, in which enters 1_n is the $(n \times n)$ unity matrix.

A.2 The TDHFB equation

We will choose for $\mathcal{D}_1$ and $\mathcal{D}_2$ the most general exponential of quadratic form:

$$\begin{aligned} \mathcal{D}_1 &= e^{\nu_1} e^{\tilde{\lambda}_1 \tau \alpha} e^{\frac{1}{2}\tilde{\alpha}\tau \mathcal{S}_1 \alpha} \\ \mathcal{D}_2 &= e^{\nu_2} e^{\tilde{\lambda}_2 \tau \beta} e^{\frac{1}{2}\tilde{\beta}\mathcal{S}_2 \beta} \end{aligned} \tag{A.7}$$

where ν_i are a c-numbers, $\lambda_i(2n)$ component complex vectors and $\mathcal{S}_i(2n \times 2n)$ symplectic matrix.We furthermore define the centered operators $\bar{O} = O - \langle O \rangle_i$ where the expectation value with respect to the density operator $\mathcal{D}_i$ is defined as $\langle O \rangle_i = \operatorname{Tr} O\mathcal{D}_i / \operatorname{Tr} \mathcal{D}_i$, where $\operatorname{Tr} \mathcal{D}_i \equiv \mathcal{Z}_i$ represents the corresponding partition functions. These Ansätze belong to the class of generalized coherent states, These allow us to perform the calculation (since Wick's theorem applies) while preserving key aspects, such as the pairing between

particles.Note that, due to the time dependence of $\langle O\rangle_i$, the centered operator $\bar{O}$ is time-dependent even if O is not.

It turns out that instead of the set (ν_i, λ_i and $\mathcal{S}_i$), it is more convenient to use as variational parameters the partition function $\mathcal{Z}_i$, the "one-boson" expectation values

$$\begin{aligned} \langle\alpha_i\rangle_1 &= \operatorname{Tr}\alpha_i\mathcal{D}_1/\operatorname{Tr}\mathcal{D}_1, \\ \langle\beta_i\rangle_2 &= \operatorname{Tr}\beta_i\mathcal{D}_2/\operatorname{Tr}\mathcal{D}_2, \end{aligned} \tag{A.8}$$

and the single particle density matrix

$$\begin{aligned} (\mathcal{R}_{ij})_1 &= \tau_{jk}\left\langle\bar{\alpha}_k\bar{\alpha}_i\right\rangle_1, \\ (\mathcal{R}_{ij})_2 &= \tau_{jk}\left\langle\bar{\beta}_k\bar{\beta}_i\right\rangle_2 \end{aligned} \tag{A.9}$$

The trial observables $\mathcal{A}_i(t)$ are selected among the one-body operators. We therefore take

$$\begin{aligned} \mathcal{A}_1(t) &= \nu'_1(t) + \lambda'_1(t)\tau\alpha + \frac{1}{2}\tilde{\alpha}\tau\mathcal{S}'_1(t)\alpha, \\ \mathcal{A}_2(t) &= \nu'_2 + \lambda'_2(t)\tau\beta + \frac{1}{2}\tilde{\beta}\tau\mathcal{S}'_2(t)\beta \end{aligned} \tag{A.10}$$

where ν'_i, λ'_i and $\mathcal{S}'_i$ have the same properties as ν_i, λ_i and $\mathcal{S}_i$.
In order to obtain the BV reduced fonctional (A.1), corresponding to (A.10), we need the quantities $\operatorname{Tr}\mathcal{A}d\mathcal{D}/dt$ and $\operatorname{Tr}\mathcal{A}[H,\mathcal{D}]$. The evaluation of the former is done more easily by calculating first $\operatorname{Tr}\mathcal{A}\mathcal{D}$; using Wick's theorem, we obtain

$$\operatorname{Tr}\mathcal{A}\mathcal{D} = \operatorname{Tr}\left(\mathcal{A}_1+\mathcal{A}_2\right)\mathcal{D}_1\mathcal{D}_2 = \mathcal{Z}_1\mathcal{Z}_2\left(\langle\mathcal{A}_1\rangle\right) + \langle\mathcal{A}_2\rangle) = \operatorname{Tr}\mathcal{D}\left(\langle\mathcal{A}_1\rangle + \langle\mathcal{A}_2\rangle\right) \tag{A.11}$$

Then straightforwardly,

$$\operatorname{Tr}\mathcal{A}\frac{\mathrm{d}\mathcal{D}}{\mathrm{d}t} = \left.\frac{\mathrm{d}}{\mathrm{d}t}\operatorname{Tr}\mathcal{A}\mathcal{D}\right|_{\mathcal{A}} \tag{A.12}$$

where the subscript $\mathcal{A}$ means that in the derivation with respect to t, we keep fixed the variational parameters of the observables $\mathcal{A}_1$ and $\mathcal{A}_2$ appearing in (A.10). A strightforward calculation yields:

$$\operatorname{Tr}\mathcal{A}\frac{\mathrm{d}\mathcal{D}}{\mathrm{d}t}=\frac{\mathrm{d}\mathcal{Z}}{\mathrm{d}t}\left(\langle\mathcal{A}_1\rangle+\langle\mathcal{A}_2\rangle\right)+\mathcal{Z}\left\{\tilde{L}_1\tau\frac{\mathrm{d}\langle\alpha\rangle}{\mathrm{d}t}+\tilde{L}_2\tau\frac{\mathrm{d}\langle\beta\rangle}{\mathrm{d}t}-\frac{1}{2}\operatorname{tr}\mathcal{S}_1'\frac{\mathrm{d}\mathcal{R}_1}{\mathrm{d}t}-\frac{1}{2}\operatorname{tr}\mathcal{S}_2'\frac{\mathrm{d}\mathcal{R}_2}{\mathrm{d}t}\right. \tag{A.13}$$

In the previous expression $\mathcal{Z}=\mathcal{Z}_1\mathcal{Z}_2$ is the total partition function, $L_1=\lambda'_1-\mathcal{S}_1'\langle\alpha\rangle$ and $L_2=\lambda'_2-\mathcal{S}_2'\langle\alpha\rangle$. The second term $\operatorname{Tr}\mathcal{A}[H,\mathcal{D}]$ that appears in (A.1) may be evaluated by the following trick. We first decompose the hamiltoian in three parts: $H=H_1+H_2+H_{12}$, where $H_1\,(H_2)$ is the hamiltonian for the first (second) species and H_{12} is the inter-species hamiltonian, depends on both operators. Then,

$$\operatorname{Tr}\mathcal{A}[H,\mathcal{D}]=\mathcal{Z}\left\langle[\mathcal{A}_1,H_1+H_{12}]\right\rangle+\left\langle[\mathcal{A}_2,H_2+H_{12}]\right\rangle \tag{A.14}$$

But we can show [141] in general that

$$\left\langle[\mathcal{A}_1,H_1]\right\rangle=\tilde{L}_1'\tau\mathcal{V}_1-\frac{1}{2}\operatorname{tr}\mathcal{S}_1'\left[\mathcal{R}_1,\mathcal{H}_1\right] \tag{A.15}$$

where

$$\begin{cases}\mathcal{V}_1=\tau\frac{\partial\mathcal{E}_1}{\partial\langle\alpha\rangle_1}\\ \mathcal{H}_1=-2\frac{\partial\mathcal{E}_1}{\partial\mathcal{R}_1}\end{cases} \tag{A.16}$$

where $\mathcal{E}_1=\langle H_1\rangle$ is the energy of the first space.Evidently,simliar expressions hold for the second species.

Analogous calculations may be conduced for the inter-species hamiltonian with a quite natural result

$$\left\langle[\mathcal{A}_1,H_{12}]\right\rangle=\tilde{L}\tau\mathcal{V}_{12}-\frac{1}{2}\operatorname{tr}\mathcal{S}'\left[\mathcal{R},\mathcal{H}_{12}\right] \tag{A.17}$$

with

$$\begin{cases}\mathcal{V}_{12}=\tau\frac{\partial\mathcal{E}_{12}}{\partial\langle\alpha\rangle_1}\\ \mathcal{H}_{12}=-2\frac{\partial\mathcal{E}_{12}}{\partial\mathcal{R}_1}\end{cases} \tag{A.18}$$

and $\mathcal{E}_{12}=\langle H_{12}\rangle$ is the inter-species energy computed with respect to the total density operator and we use the convention of derivation $\left(\frac{\partial}{\partial\mathcal{R}}\right)_{ij}=\frac{\partial}{\partial\mathcal{R}_{ji}}$. Upon defining the equivalent expressions

$$\begin{cases}\mathcal{V}_{21}=\tau\frac{\partial\mathcal{E}_{12}}{\partial\langle\beta\rangle_{\lambda_2}},\\ \mathcal{H}_{21}=-2\frac{\partial\mathcal{E}_{12}}{\partial\mathcal{R}_2},\end{cases} \tag{A.19}$$

We then obtain the final expression for the integrand (A.1):

$$\begin{aligned}
&\frac{1}{\mathcal{Z}}\frac{\mathrm{d}\mathcal{Z}}{\mathrm{d}t}\left(\langle\mathcal{A}_1\rangle+\langle\mathcal{A}_2\rangle\right)\\
&+\tilde{L}_1\tau\left(\frac{\mathrm{d}\langle\alpha\rangle}{\mathrm{d}t}+\frac{i}{\hbar}\left(\mathcal{V}_1+\mathcal{V}_{12}\right)\right)-\frac{1}{2}\operatorname{tr}\mathcal{S}_1'\left(\frac{\mathrm{d}\mathcal{R}_1}{\mathrm{d}t}+\frac{i}{\hbar}\left[\mathcal{R}_1,\mathcal{H}_1+\mathcal{H}_{12}\right]\right)\\
&+\tilde{L}_2\tau\left(\frac{\mathrm{d}\langle\beta\rangle}{\mathrm{d}t}+\frac{i}{\hbar}\left(\mathcal{V}_2+\mathcal{V}_{21}\right)\right)-\frac{1}{2}\operatorname{tr}\mathcal{S}_2'\left(\frac{\mathrm{d}\mathcal{R}_2}{\mathrm{d}t}+\frac{i}{\hbar}\left[\mathcal{R}_2,\mathcal{H}_2+\mathcal{H}_{21}\right]\right)
\end{aligned}\tag{A.20}$$

The stationarity conditions of this expression with respect to the variations of $\mathcal{A}$ are equivalent to those of their variational parameters $\nu_1'\left(\nu_2'\right), L_1'\left(L_2'\right)$ and $\mathcal{S}_1'\left(\mathcal{S}_2'\right)$. Because the observable (A.10) is linear in the parameter $\nu_{1,2}'$, the first conditions yield directly $\mathrm{d}\mathcal{Z}/\mathrm{d}t=0$: the total partition function is a constant of the motion. This is an exact result !!

Furthermore, varying (A.20) with respect to L'_{12} and $\mathcal{S}_{12}'$, yields the time-dependent Hartree-Fock-Bogoliubov equations for the mixture (the dot denotes time derivative):

$$\begin{cases} i\hbar\langle\dot{\alpha}\rangle=\mathcal{V}_1+\mathcal{V}_{12}\\ i\hbar\dot{\mathcal{R}}_1=\left[\mathcal{R}_1,\mathcal{H}_1+\mathcal{H}_{12}\right]\end{cases}\tag{A.21}$$

$$\begin{cases} i\hbar\langle\dot{\beta}\rangle=\mathcal{V}_2+\mathcal{V}_{21}\\ i\hbar\dot{\mathcal{R}}_2=\left[\mathcal{R}_2,\mathcal{H}_2+\mathcal{H}_{21}\right]\end{cases}\tag{A.22}$$

As evident from their very definitions, the coupling between the dynamics of the two species will occur via the "generalized mean field" or Hatree-Fock hamiltonians(A.18-A.19).

Evidently,the equations (A.21-A.22) conserve the total energy $\mathcal{E}=\mathcal{E}_1+\mathcal{E}_2+\mathcal{E}_{12}$ and the trace of any function of $\mathcal{R}$. Furthermore, the unitary evolution of the single particle density matrix shows that if $\mathcal{R}_i\left(\mathcal{R}_i+1\right)=0$ at some initial time, then it will remain so during evolution whatever the interactions[139, 141].This is an indication that there re no correlations between the species .